UNIVERSITY OF CALIFORNIA, SAN DIEGO

Decoding the ionic basis of neuronal diversity in the medial vestibular nucleus

A dissertation submitted in partial satisfaction of the

requirements for the degree Doctor of Philosophy

in

Neurosciences

by

Aryn Hilary Gittis

Committee in charge:

Sascha du Lac, Chair
Marla B. Feller
Jeffry S. Isaacson
Paul A. Slesinger
Nicholas C. Spitzer

2008

The Dissertation of Aryn Hilary Gittis is approved, and it is acceptable in quality and form for publication on microfilm:

Chair

University of California, San Diego
2008

This thesis is dedicated to my parents, Margaret and Alan Gittis

for their unconditional love and support

and

to my husband, DJ Brasier

the love of my life.

Table of Contents

List of Figures and Tables

Acknowledgements

Figure 1.1 is a revised version of the figure that appeared in Gittis AH, du Lac S. Curr Opin Neurobiol. 2006. Intrinsic and synaptic plasticity in the vestibular system. Aug;16(4):385-90. It is included with the permission of all the authors on the final publication.

Chapter 2 is a revised version of Nelson AB, Gittis AH, du Lac S. Neuron 2005 Decreases in CaMKII activity trigger persistent potentiation of intrinsic excitability in spontaneously firing vestibular nucleus neurons. May 19; 46(4):623-31. The portions present here are included with the permission of all the authors on the final publication.

Chapter 3 is a reprint of the material as it appears in Gittis AH, du Lac S. J Neurophysiol. 2007 Firing properties of GABAergic versus non-GABAergic vestibular nucleus neurons conferred by a differential balance of potassium currents. Jun;97(6):3986-96. It is included with the permission of all the authors on the final publication.

Chapter 4 is original work submitted as Gittis AH, du Lac S. J Neurophysiol Similar Properties of Transient, Persistent, and Resurgent Na Currents in GABAergic and non-GABAergic MVN neurons. in press. It is included with the permission of all the authors on the final publication.

Chapter 5 is original work in preparation as Gittis AH, Larson SD, Mogadam S, du Lac S. Functional regulation of ionic currents during firing establishes distinct firing properties of GABAergic and non-GABAergic neurons in the medial vestibular nuclei and is included with permission from all the

manuscript's authors. The dissertation author was the primary author on this paper.

Vita and Publications

2001 B.A, Neurosciences, Brandeis University, summa cum laude

2005 M.S., Neurosciences, University of California, San Diego

2008 Ph.D., Neurosciences, University of California, San Diego

Publications

Strachan GD, Morgan KL, Otis LL, Caltagarone J, Gittis A, Bowser R, Jordan-Sciutto KL. (2004) Fetal Alz-50 clone 1 interacts with the human orthologue of the Kelch-like Ech-associated protein. *Biochemistry*. 43(38):12113-22.

Nelson AB, Gittis AH, du Lac S. (2005) Decreases in CaMKII activity trigger persistent potentiation of intrinsic excitability in spontaneously firing vestibular nucleus neurons. *Neuron* 46, 623-631.

Gittis AH, du Lac S (2006) Intrinsic and Synaptic Plasticity in the Vestibular System. *Current Opinions Neurobiology* 16, 1-6.

Gittis AH, du Lac S (2007) Firing Properties of GABAergic versus Non-GABAergic Vestibular Nucleus Neurons Conferred by a Differential Balance of Potassium Currents. *J. Neurophys* 97, 3986

Gittis AH, du Lac S (2008) Similar Properties of Transient, Persistent, and Resurgent Na Currents in GABAergic and non-GABAergic MVN neurons. In press.

Awards

2000 HHMI Summer Undergraduate Research Fellowship
2000 Barry M. Goldwater Scholarship
2001 Pfizer Summer Undergraduate Research Fellowship
2001 Elected member of Phi Beta Kappa
2001 Fulbright Fellowship (France)
2007 Achievement Rewards for College Scientists (ARCS)

ABSTRACT OF THE DISSERTATION

Decoding the ionic basis of neuronal diversity in the medial vestibular nucleus

by

Aryn Hilary Gittis

Doctor of Philosophy in Neurosciences

University of California, San Diego 2008

Professor Sascha du Lac, Chair

Somatic excitability plays a key role in the patterning of action potential generation by shaping the integration of synaptic information with recent neuronal activity, however its importance has been neglected in a number of systems. An exception is in spontaneously firing neurons of the vestibular system, where intrinsic excitability is central to adaptive plasticity and diversifies the firing properties of distinct cell types in the medial vestibular nuclei (MVN). Experiments revealed that MVN neurons express sodium currents with similar biophysical properties but exhibit different ratios of potassium currents that likely underlie cell type diversity. Recordings of ionic currents during firing demonstrated that high expression of Ca^{2+}-dependent potassium currents decreases neuronal excitability and limits sodium current availability while Kv3-type potassium currents mediate rapid action potential repolarization and protect sodium current availability at high firing rates, creating a broad spectrum of neuronal firing properties in the MVN.

I. Introduction

Intrinsic excitability determines the responsiveness of neurons to their inputs in a functioning network. It is regulated by the expression patterns of ionic currents, whose wide diversity reflects the extensive degree of molecular tuning which optimizes neuronal function (Hille, 2006). The well studied networks of neurons in the neocortex and the hippocampus are largely populated by cells that fire at low rates, making an understanding of how synaptic inputs alter the probability of an action potential important. By contrast, in networks of spontaneously firing cells, information is encoded not in the integration of inputs to fire a single spike but rather by changing rates of action potentials.

The vestibular system provides an ideal model for studying intrinsic excitability because it is a simple system where the activity of neurons is directly related to animal behavior (du Lac et al., 1995). The system processes information with extreme temporal precision, making the rate of action potential firing important. Changes in intrinsic excitability could therefore have profound effects on the dynamics of network function and several studies show that plasticity of intrinsic excitability has direct behavioral relevance for the system (Darlington and Smith, 2000; Darlington et al., 2002; Straka et al., 2005; Gittis and du Lac, 2006). The vestibular nuclei consist of a heterogeneous population of excitatory and inhibitory neurons that are differentially regulated during plasticity (Beraneck et al., 2003; Beraneck et al., 2004). Understanding how changes in intrinsic excitability are distributed throughout the network requires an understanding of the ionic currents regulating excitability in these different cell

types. In this dissertation, I examine the ionic basis of intrinsic excitability in distinct cell types in the MVN with different functions in vestibular circuitry. In the following sections, I will summarize the scientific context motivating the experiments presented in Chapters 2-5.

Vestibular circuitry

The vestibular system transforms sensory information about head and image motion into temporally and spatially precise motor commands that move the eyes in a compensatory manner to stabilize objects on the retina, the biological equivalent of an image stabilizer on a camera. Behaviors mediated by this system are the vestibulo-ocular reflex (VOR) which drives compensatory eye movements in the opposite direction of head motion and the optokinetic reflex (OKR), in which the eyes move to track full field image motion (Faulstich et al., 2006). The neuronal backbone of this rapid sensory -> motor converter is a simple circuit consisting of three components: (1) sensory neurons in the inner ear canals that convert head or image motion into neuronal firing patterns (2) neurons in the vestibular nuclei that process the information and (3) motor neurons that convert the neuronal firing pattern to muscle contractions that move the eyes (Fig. 1). This basic neural circuitry is highly conserved, from goldfish to humans and is subject to multiple forms of plasticity to maintain proper functioning over the lifetime of an organism (du Lac et al., 1995; Gittis and du Lac, 2006).

Plasticity of the VOR

The vestibular nuclei are optimally positioned in the vestibular circuit to integrate information from accessory areas required for plasticity. Inhibitory inputs from Purkinje cells in the floccular lob of the cerebellum are a primary example (Langer et al., 1985; Sekirnjak et al., 2003). These inputs are required to initiate plasticity of the vestibulo-ocular reflex (VOR) (Lisberger et al., 1984; Blazquez et al., 2004; De Zeeuw and Yeo, 2005). Purkinje neurons, themselves are sites of convergence for information about head and image motion, conveyed by parallel fibers from granule cells and climbing fibers from the inferior olive, respectively (Fig. 1). When there is a discrepancy between head and image motion, Purkinje cells provide the necessary error signal to initiate VOR plasticity (Frens et al., 2001). Disrupting Purkinje cell activity or their inputs to vestibular nucleus neurons blocks adaptive plasticity of the VOR but does not strongly affect baseline VOR performance (De Zeeuw et al., 1998; Shutoh et al., 2003; Carter and McElligott, 2005; Shutoh et al., 2006).

The importance of the cerebellum in initiating adaptive VOR plasticity is firmly established, but the site of long-term storage of oculomotor memories is still an issue of debate. Two independent studies found that during memory consolidation, long-term memory storage shifts from the cerebellum to the vestibular nuclei (Kassardjian et al., 2005; Shutoh et al., 2006). Another form of vestibular learning occurs when loss of peripheral vestibular function acutely reduces neuronal activity in the ipsilateral vestibular nucleus, creating severe

postural symptoms and almost completely abolishing VOR and OKR behaviors. Although peripheral vestibular function is never restored, recovery of VOR and OKR behaviors are nearly complete within 1-2 weeks. This recovery is termed vestibular compensation. Although vestibular compensation is dependent on the cerebellum (Johnston et al., 2002), electrophysiological recordings suggest that it is driven by changes in the intrinsic excitability of vestibular nucleus neurons (Smith and Curthoys, 1989; Darlington et al., 2002) that can persist for up to 1 month (Beraneck et al., 2003; Beraneck et al., 2004). The cellular basis of this plasticity is not know but some hypotheses include reduced sensitivity to inhibitory neurotransmitters (Vibert et al., 2000; Yamanaka et al., 2000; Johnston et al., 2001) or changes in ionic currents that regulate membrane excitability (Beraneck et al., 2003; Beraneck et al., 2004).

Cellular mechanisms of plasticity

Studies probing more deeply into the cellular basis of plasticity in vestibular nucleus neurons have uncovered mechanism of both synaptic and intrinsic plasticity (Fig. 1). Synaptic plasticity (both LTP and LTD) has been identified at the synapses from the vestibular nerve (axons of primary sensory neurons) onto vestibular nucleus neurons (Capocchi et al., 1992; Grassi et al., 1995; Grassi et al., 1998; Grassi and Pettorossi, 2001; Grassi et al., 2002; Grassi et al., 2004; Grassi et al., 2005). The directionality of this plasticity is likely to be cell-type specific, as demonstrated by the observation that vestibular nerve stimulation paired with somatic hyperpolarization (simulating coincidence

detection of head motion and error signals from Purkinje cells) induced LTD of vestibular nerve inputs onto GABAergic interneurons but LTP onto non-GABAergic neurons (L. .McElvain, unpublished).

Vestibular nucleus neurons also show robust plasticity of intrinsic excitability, trigged by inhibitory synaptic stimulation or direct membrane hyperpolarization (Nelson et al., 2003). These stimuli reduce intracellular calcium levels, triggering a persistent increase in spontaneous firing rates and sensitivity to depolarizing inputs, termed firing rate potentiation (FRP) (Nelson et al., 2003). FRP is induced by decreases in CaMKII activity, triggered by decreases in intracellular calcium levels that ultimately cause a reduction of currents through BK-type K channels (Nelson et al., 2003; Nelson et al., 2005). BK currents regulate neuronal excitability by contributing to the early after-hyperpolarization (AHP) (Smith et al., 2002) and increases in excitability following FRP induction were occluded by iberiotoxin, a specific blocker of BK currents (Nelson et al., 2003).

The notion that this plasticity could be triggered by decreases rather than increases in CaMKII activity represents a novel role for this already multifaceted kinase. Although decades of research have formulated a comprehensive description of how CaMKII activity is regulated by complex phosphorylation patterns (Schulman, 1993), little is known about how the kinase behaves in spontaneously firing neurons. This question is addressed through a combination of biochemical and electrophysiological experiments in Chapter 2. The results show that CaMKII activity in MVN neurons is distinct from that previously

characterized in hippocampal and cortical neurons. MVN neurons expressed predominantly β-isoforms of CaMKII which were maximally activated by spontaneous activity at baseline. Additionally, changes in neuronal excitability were accompanied by *decreases* in phosphorylation on residue T287, rather than increases which are required for plasticity in hippocampal and cortical neurons (Silva et al., 1992b; Silva et al., 1992a; Glazewski et al., 1996; Glazewski et al., 2000; Frankland et al., 2001). These results demonstrate that learning rules in spontaneously firing neurons can differ substantially from those previously established in non-spontaneously firing neurons and emphasizes the importance of conducting studies on a variety of cell types throughout the brain.

Identifying distinct cell types with unique roles in vestibular circuitry

Targeting inhibitory and excitatory neurons in the vestibular circuit has been historically challenging due to a lack of morphological distinctions or laminar organization in the vestibular nuclei. The rules governing plasticity vary across cell types, demonstrated by variability in the expression of FRP (Nelson et al., 2003), changes in excitability during behavioral plasticity (Beraneck et al., 2003; Beraneck et al., 2004), or the direction of synaptic plasticity observed across neurons (Grassi and Pettorossi, 2001; McIlvain, unpublished). The firing properties of MVN neurons form a continuous distribution with no obvious divisions between classes of neurons (du Lac and Lisberger, 1995; Sekirnjak and du Lac, 2002), although several groups have historically divide the population into Type A and Type B neurons on the basis of their intrinsic firing properties

(Serafin et al., 1991b; Johnston et al., 1994). However, this classification scheme is insufficient to track changes in intrinsic excitability during plasticity (Beraneck et al., 2003; Nelson et al., 2003; Beraneck et al., 2004).

The development of transgenic technology has revolutionized the ability to reliably target specific populations of neurons in the vestibular circuit to understand their roles in basic information processing and plasticity. Neurons that receive direct input from the cerebellum can be identified using a mouse line that drives GFP expression specifically in Purkinje cells, under control of the L7 (Pcp2) promotor (Sekirnjak et al., 2003). More recently 2 mouse lines were discovered that divide the MVN into physiologically distinct populations with different transmitter phenotypes (Bagnall et al., 2007). The GIN line of transgenic mice (Oliva et al., 2000) labels a subset of GAD-67 expressing neurons in the MVN with intrinsic firing properties similar to Type A neurons while the YFP-16 line of transgenic mice (Feng et al., 2000) labels a subset of glycinergic and glutamatergic neurons in the MVN with intrinsic properties similar to Type B neurons (Takazawa et al., 2004; Bagnall et al., 2007).

The majority of projections from the vestibular nuclei are either glutamatergic or glycinergic (McCrea et al., 1980; Spencer et al., 1989; Graf et al., 1997; Graf et al., 2002), but some GABAergic projections have also been observed (Holstein, 2000). Based on these studies and the distribution of GIN and YFP-16 neurons in the dorsal and ventral portions of the MVN, respectively, GIN neurons represent local inhibitory, GABAergic neurons and YFP-16 neurons represent non-GABAergic projection neurons in the circuit (Bagnall et al., 2007).

Experiments in Chapters 3-5 take advantage of these recent advances in our ability to target GABAergic and non-GABAergic neurons in the vestibular nuclei with unique roles in vestibular circuitry. The results demonstrate that ionic currents are specifically tuned in these classes of neurons to provide non-GABAergic neurons with greater temporal precision and GABAergic neurons with greater sensitivity to fluctuations in Ca levels, which might lower their threshold for plasticity.

Ionic mechanisms regulating intrinsic excitability of MVN neurons

The firing properties of MVN neurons are well tuned to meet the rapid and accurate signaling requirements of the vestibular system. MVN neurons fire spontaneously both *in vitro* and *in vivo* at rates ranging between 5-50 Hz (Cullen and Roy, 2004). During head rotation, their firing rates modulate over a 100 – 200 Hz range (Cullen and Roy, 2004) and in slice preparations they can be driven to fire action potentials as high as 100 – 600 Hz for 1 s with DC depolarization (Smith et al., 2002; Bagnall et al., 2007). One of the most interesting properties of MVN neurons is their ability to linearly modulate their firing rates in response to changes in input current, acting as linear filters across their dynamic range. This ensures that information will be propagated faithfully through the nucleus without distortions that could compromise the tight relationship between head and image motion.

Classes of ionic currents that regulate excitability in MVN neurons have been hypothesized through pharmacologically-induced changes in firing

properties(Serafin et al., 1991a; Johnston et al., 1994; Smith et al., 2002) or computational models (Quadroni and Knopfel, 1994; Av-Ron and Vidal, 1999). The slope of a neuron's linear input-output curve (gain) is affected by apamin-sensitive SK currents and iberiotoxin-sensitive BK currents (Smith et al., 2002) but changes in intrinsic excitability during FRP are driven specifically by changes in BK currents (Nelson et al., 2003; Nelson et al., 2005).

Grouping neurons as either Type A or Type B on the basis of their intrinsic firing properties led to the hypothesis that different classes of MVN neurons express distinct currents. In Type A neurons, the presence of an A-like rectification (a delay in the rebound firing normally observed after acute hyperpolarization) was attributed to the selective expression of a hyperpolarization-activated K current (Serafin et al., 1991b). In Type B neurons, the presence of plateau potentials was attributed to the selective expression of a persistent Na current (Serafin et al., 1991a). However, a computer model was able to reproduce differences in firing properties of Type A and Type B neurons by simply changing the relative conductance of a fast K current (Quadroni and Knopfel, 1994), creating controversy as to the precise mechanisms underlying cell-type diversity in firing properties.

Insights into the ionic mechanisms of intrinsic excitability in MVN neurons can also be made from recordings of fast firing neurons in other brain regions, including deep cerebellar nucleus (DCN) neurons (Raman et al., 2000; Aman and Raman, 2007), cerebellar Purkinje cells (Raman and Bean, 1997, 1999), fast firing neurons from the cortex or hippocampus (Martina and Jonas,

1997; Massengill et al., 1997; Martina et al., 1998), subthalamic nucleus neurons (Bevan and Wilson, 1999; Do and Bean, 2003), basal ganglia (Baranauskas et al., 1999; Baranauskas et al., 2003), and auditory cortex (Leao et al., 2005; Song et al., 2005; Song and Kaczmarek, 2006). These studies reveal the presence of several ionic mechanisms that are conserved in fast firing neurons across the brain. These include the expression of Kv3-type K currents, identified by their high sensitivity to TEA [1 mM] (Perney et al., 1992; Weiser et al., 1994; Martina and Jonas, 1997; Massengill et al., 1997; Erisir et al., 1999; Hernandez-Pineda et al., 1999) and the expression of Na channels with unique biophysical properties that minimize accumulation of inactivation (Martina and Jonas, 1997; Raman and Bean, 1997; Raman et al., 2000; Do and Bean, 2003; Afshari et al., 2004; Mercer et al., 2007).

In Chapters 3-4, I use voltage clamp recordings to make the first direct measurements of ionic currents expressed in MVN neurons. These experiments, carried in YFP-16 and GIN lines of transgenic mice to identify specific cell types, show that all MVN neurons express the same ionic currents, but that the ratios of these currents vary 4 – 5- fold across neurons. All MVN neurons express Kv3 and Na currents, consistent with their classification as fast firing neurons. Na currents were similar in all MVN neurons, but Kv3 currents varied systematically with intrinsic firing properties and distinguished GABAergic from non-GABAergic neurons.

Regulation of currents in MVN neurons

The contribution of ionic currents to intrinsic excitability depends not only on the level of expression, but also on how their activity is regulated by rapid changes in membrane voltage and the influence of other currents during firing (Ma and Koester, 1996; Marder, 1998; Bean, 2007). In some neurons, voltage-dependent interactions of ionic currents shift a neuron's firing pattern between bursting, tonic, and silent modes (Llinas, 1988; Turrigiano et al., 1994; Womack and Khodakhah, 2004). Adaptive changes in intrinsic excitability are often mediated by concerted changes in multiple currents to maintain a critical balance required for appropriate neural output (Alkon, 1984; Turrigiano et al., 1995; Desai et al., 1999; Swensen and Bean, 2005).

These coordinated changes in current expression create both stability and flexibility in neural systems. For example, the firing properties of identified neurons in the lobster somatogastric ganglion are nearly identical from animal to animal, despite 2 - 4 fold variations in current expression (Schulz et al., 2006). The stability of firing properties is achieved through the coordination of expression of multiple ionic currents (Goldman et al., 2001; Schulz et al., 2006). At the other extreme, variability in action potential waveforms required to differentiate individual EOD frequencies of electric fish is achieved through the coordinated expression of Na and K currents with co-varying kinetics (McAnelly and Zakon, 2000).

Although all neurons in the medial vestibular nuclei (MVN) exhibit tonic,

spontaneous firing and respond to depolarizing inputs with linear increases in firing rate (du Lac and Lisberger, 1995; Ris et al., 2001; Smith et al., 2002), there is considerable variability in the more specific details of their intrinsic firing properties, including differences in action potential waveforms, rebound burst firing, spike adaptation, and maximum firing rates that set the dynamic range of a neuron (Serafin et al., 1991b; Sekirnjak and du Lac, 2002; Bagnall et al., 2007). This raises the question of how ionic current expression in MVN neurons is coordinated to create diversity yet stability in their firing properties. This question is the focus of experiments in Chapter 5 which reveal differences in the functional regulation of ionic currents between GABAergic and non-GABAergic MVN neurons during firing. In non-GABAergic neurons, Kv3 currents engage a novel mechanism of Na current protection at high firing, allowing them to function over broader firing ranges than GABAergic neurons. This provides projection neurons with the ability to operate with greater temporal precision than the local inhibitory neurons, which may have important functional implications for the network.

Acknowledgements

Figure 1.1 is a revised version of the figure that appeared in Gittis AH, du Lac S. Curr Opin Neurobiol. 2006. Intrinsic and synaptic plasticity in the vestibular system. Aug;16(4):385-90. It is included with the permission of all the authors on the final publication.

References

Afshari FS, Ptak K, Khaliq ZM, Grieco TM, Slater NT, McCrimmon DR, Raman IM (2004) Resurgent Na currents in four classes of neurons of the cerebellum. J Neurophysiol.

Alkon DL (1984) Calcium-mediated reduction of ionic currents: a biophysical memory trace. Science 226:1037-1045.

Aman TK, Raman IM (2007) Subunit dependence of Na channel slow inactivation and open channel block in cerebellar neurons. Biophys J 92:1938-1951.

Av-Ron E, Vidal PP (1999) Intrinsic membrane properties and dynamics of medial vestibular neurons: a simulation. Biol Cybern 80:383-392.

Bagnall MW, Stevens RJ, du Lac S (2007) Transgenic mouse lines subdivide medial vestibular nucleus neurons into discrete, neurochemically distinct populations. J Neurosci 27:2318-2330.

Baranauskas G, Tkatch T, Surmeier DJ (1999) Delayed rectifier currents in rat globus pallidus neurons are attributable to Kv2.1 and Kv3.1/3.2 K(+) channels. J Neurosci 19:6394-6404.

Baranauskas G, Tkatch T, Nagata K, Yeh JZ, Surmeier DJ (2003) Kv3.4 subunits enhance the repolarizing efficiency of Kv3.1 channels in fast-spiking neurons. Nat Neurosci 6:258-266.

Bean BP (2007) The action potential in mammalian central neurons. Nat Rev Neurosci 8:451-465.

Beraneck M, Idoux E, Uno A, Vidal PP, Moore LE, Vibert N (2004) Unilateral labyrinthectomy modifies the membrane properties of contralesional vestibular neurons. J Neurophysiol 92:1668-1684.

Beraneck M, Hachemaoui M, Idoux E, Ris L, Uno A, Godaux E, Vidal PP, Moore LE, Vibert N (2003) Long-term plasticity of ipsilesional medial vestibular nucleus neurons after unilateral labyrinthectomy. J Neurophysiol 90:184-203.

Bevan MD, Wilson CJ (1999) Mechanisms underlying spontaneous oscillation and rhythmic firing in rat subthalamic neurons. J Neurosci 19:7617-7628.

Blazquez PM, Hirata Y, Highstein SM (2004) The vestibulo-ocular reflex as a model system for motor learning: what is the role of the cerebellum? Cerebellum 3:188-192.

Capocchi G, Della Torre G, Grassi S, Pettorossi VE, Zampolini M (1992) NMDA receptor-mediated long term modulation of electrically evoked field potentials in the rat medial vestibular nuclei. Exp Brain Res 90:546-550.

Carter TL, McElligott JG (2005) Cerebellar AMPA/KA receptor antagonism by CNQX inhibits vestibuloocular reflex adaptation. Exp Brain Res 166:157-169.

Cullen KE, Roy JE (2004) Signal processing in the vestibular system during active versus passive head movements. J Neurophysiol 91:1919-1933.

Darlington CL, Smith PF (2000) Molecular mechanisms of recovery from vestibular damage in mammals: recent advances. Prog Neurobiol 62:313-325.

Darlington CL, Dutia MB, Smith PF (2002) The contribution of the intrinsic excitability of vestibular nucleus neurons to recovery from vestibular damage. Eur J Neurosci 15:1719-1727.

De Zeeuw CI, Yeo CH (2005) Time and tide in cerebellar memory formation. Curr Opin Neurobiol 15:667-674.

De Zeeuw CI, Hansel C, Bian F, Koekkoek SK, van Alphen AM, Linden DJ, Oberdick J (1998) Expression of a protein kinase C inhibitor in Purkinje cells blocks cerebellar LTD and adaptation of the vestibulo-ocular reflex. Neuron 20:495-508.

Desai NS, Rutherford LC, Turrigiano GG (1999) Plasticity in the intrinsic excitability of cortical pyramidal neurons. Nat Neurosci 2:515-520.

Do MT, Bean BP (2003) Subthreshold sodium currents and pacemaking of subthalamic neurons: modulation by slow inactivation. Neuron 39:109-120.

du Lac S, Lisberger SG (1995) Membrane and firing properties of avian medial vestibular nucleus neurons in vitro. J Comp Physiol [A] 176:641-651.

du Lac S, Raymond JL, Sejnowski TJ, Lisberger SG (1995) Learning and memory in the vestibulo-ocular reflex. Annu Rev Neurosci 18:409-441.

Erisir A, Lau D, Rudy B, Leonard CS (1999) Function of specific K(+) channels in sustained high-frequency firing of fast-spiking neocortical interneurons. J Neurophysiol 82:2476-2489.

Faulstich M, van Alphen AM, Luo C, du Lac S, De Zeeuw CI (2006) Oculomotor Plasticity During Vestibular Compensation Does Not Depend on Cerebellar LTD. J Neurophysiol 96:1187-1195.

Feng G, Mellor RH, Bernstein M, Keller-Peck C, Nguyen QT, Wallace M, Nerbonne JM, Lichtman JW, Sanes JR (2000) Imaging neuronal subsets in transgenic mice expressing multiple spectral variants of GFP. Neuron 28:41-51.

Frankland PW, O'Brien C, Ohno M, Kirkwood A, Silva AJ (2001) Alpha-CaMKII-dependent plasticity in the cortex is required for permanent memory. Nature 411:309-313.

Frens MA, Mathoera AL, van der Steen J (2001) Floccular complex spike response to transparent retinal slip. Neuron 30:795-801.

Gittis AH, du Lac S (2006) Intrinsic and synaptic plasticity in the vestibular system. Curr Opin Neurobiol 16:385-390.

Glazewski S, Chen CM, Silva A, Fox K (1996) Requirement for alpha-CaMKII in experience-dependent plasticity of the barrel cortex. Science 272:421-423.

Glazewski S, Giese KP, Silva A, Fox K (2000) The role of alpha-CaMKII autophosphorylation in neocortical experience-dependent plasticity. Nat Neurosci 3:911-918.

Goldman MS, Golowasch J, Marder E, Abbott LF (2001) Global structure, robustness, and modulation of neuronal models. J Neurosci 21:5229-5238.

Graf W, Spencer R, Baker H, Baker R (1997) Excitatory and inhibitory vestibular pathways to the extraocular motor nuclei in goldfish. J Neurophysiol 77:2765-2779.

Graf W, Gerrits N, Yatim-Dhiba N, Ugolini G (2002) Mapping the oculomotor system: the power of transneuronal labelling with rabies virus. Eur J Neurosci 15:1557-1562.

Grassi S, Pettorossi VE (2001) Synaptic plasticity in the medial vestibular nuclei: role of glutamate receptors and retrograde messengers in rat brainstem slices. Prog Neurobiol 64:527-553.

Grassi S, Malfagia C, Pettorossi VE (1998) Effects of metabotropic glutamate receptor block on the synaptic transmission and plasticity in the rat medial vestibular nuclei. Neuroscience 87:159-169.

Grassi S, Frondaroli A, Pettorossi VE (2002) Different metabotropic glutamate receptors play opposite roles in synaptic plasticity of the rat medial vestibular nuclei. J Physiol 543:795-806.

Grassi S, Frondaroli A, Pettorossi VE (2005) Role of group II metabotropic glutamate receptors 2/3 and group I metabotropic glutamate receptor 5 in developing rat medial vestibular nuclei. Neuroreport 16:1303-1307.

Grassi S, Dieni C, Frondaroli A, Pettorossi VE (2004) Influence of visual experience on developmental shift from long-term depression to long-term potentiation in the rat medial vestibular nuclei. J Physiol 560:767-777.

Grassi S, Della Torre G, Capocchi G, Zampolini M, Pettorossi VE (1995) The role of GABA in NMDA-dependent long term depression (LTD) of rat medial vestibular nuclei. Brain Res 699:183-191.

Hernandez-Pineda R, Chow A, Amarillo Y, Moreno H, Saganich M, Vega-Saenz de Miera EC, Hernandez-Cruz A, Rudy B (1999) Kv3.1-Kv3.2 channels underlie a high-voltage-activating component of the delayed rectifier K+ current in projecting neurons from the globus pallidus. J Neurophysiol 82:1512-1528.

Hille B (2001) Ion channels of excitable membranes, 3rd ed. Massachusetts: Sinauer Associcates, Inc.

Holstein GR (2000) Inhibitory amino acid transmitters in the vestibular nuclei. In: Neurochemistry of the vestibular system (Beitz AJ, Anderson JH, eds), pp 143-162. Florida: CRC Press.

Johnston AR, MacLeod NK, Dutia MB (1994) Ionic conductances contributing to spike repolarization and after-potentials in rat medial vestibular nucleus neurones. J Physiol 481 (Pt 1):61-77.

Johnston AR, Him A, Dutia MB (2001) Differential regulation of GABA(A) and GABA(B) receptors during vestibular compensation. Neuroreport 12:597-600.

Johnston AR, Seckl JR, Dutia MB (2002) Role of the flocculus in mediating vestibular nucleus neuron plasticity during vestibular compensation in the rat. J Physiol 545:903-911.

Kassardjian CD, Tan YF, Chung JY, Heskin R, Peterson MJ, Broussard DM (2005) The site of a motor memory shifts with consolidation. J Neurosci 25:7979-7985.

Langer T, Fuchs AF, Chubb MC, Scudder CA, Lisberger SG (1985) Floccular efferents in the rhesus macaque as revealed by autoradiography and horseradish peroxidase. J Comp Neurol 235:26-37.

Leao RM, Kushmerick C, Pinaud R, Renden R, Li GL, Taschenberger H, Spirou G, Levinson SR, von Gersdorff H (2005) Presynaptic Na+ channels: locus, development, and recovery from inactivation at a high-fidelity synapse. J Neurosci 25:3724-3738.

Lisberger SG, Miles FA, Zee DS (1984) Signals used to compute errors in monkey vestibuloocular reflex: possible role of flocculus. J Neurophysiol 52:1140-1153.

Llinas RR (1988) The intrinsic electrophysiological properties of mammalian neurons: insights into central nervous system function. Science 242:1654-1664.

Ma M, Koester J (1996) The role of K+ currents in frequency-dependent spike broadening in Aplysia R20 neurons: a dynamic-clamp analysis. J Neurosci 16:4089-4101.

Marder E (1998) From biophysics to models of network function. Annu Rev Neurosci 21:25-45.

Martina M, Jonas P (1997) Functional differences in Na+ channel gating between fast-spiking interneurones and principal neurones of rat hippocampus. J Physiol 505 (Pt 3):593-603.

Martina M, Schultz JH, Ehmke H, Monyer H, Jonas P (1998) Functional and molecular differences between voltage-gated K+ channels of fast-spiking interneurons and pyramidal neurons of rat hippocampus. J Neurosci 18:8111-8125.

Massengill JL, Smith MA, Son DI, O'Dowd DK (1997) Differential expression of K4-AP currents and Kv3.1 potassium channel transcripts in cortical neurons that develop distinct firing phenotypes. J Neurosci 17:3136-3147.

McAnelly ML, Zakon HH (2000) Coregulation of voltage-dependent kinetics of Na(+) and K(+) currents in electric organ. J Neurosci 20:3408-3414.

McCrea RA, Yoshida K, Berthoz A, Baker R (1980) Eye movement related activity and morphology of second order vestibular neurons terminating in the cat abducens nucleus. Exp Brain Res 40:468-473.

Mercer JN, Chan CS, Tkatch T, Held J, Surmeier DJ (2007) Nav1.6 sodium channels are critical to pacemaking and fast spiking in globus pallidus neurons. J Neurosci 27:13552-13566.

Nelson AB, Gittis AH, du Lac S (2005) Decreases in CaMKII activity trigger persistent potentiation of intrinsic excitability in spontaneously firing vestibular nucleus neurons. Neuron 46:623-631.

Nelson AB, Krispel CM, Sekirnjak C, du Lac S (2003) Long-lasting increases in intrinsic excitability triggered by inhibition. Neuron 40:609-620.

Oliva AA, Jr., Jiang M, Lam T, Smith KL, Swann JW (2000) Novel hippocampal interneuronal subtypes identified using transgenic mice that express green fluorescent protein in GABAergic interneurons. J Neurosci 20:3354-3368.

Perney TM, Marshall J, Martin KA, Hockfield S, Kaczmarek LK (1992) Expression of the mRNAs for the Kv3.1 potassium channel gene in the adult and developing rat brain. J Neurophysiol 68:756-766.

Quadroni R, Knopfel T (1994) Compartmental models of type A and type B guinea pig medial vestibular neurons. J Neurophysiol 72:1911-1924.

Raman IM, Bean BP (1997) Resurgent sodium current and action potential formation in dissociated cerebellar Purkinje neurons. J Neurosci 17:4517-4526.

Raman IM, Bean BP (1999) Ionic currents underlying spontaneous action potentials in isolated cerebellar Purkinje neurons. J Neurosci 19:1663-1674.

Raman IM, Gustafson AE, Padgett D (2000) Ionic currents and spontaneous firing in neurons isolated from the cerebellar nuclei. J Neurosci 20:9004-9016.

Ris L, Hachemaoui M, Vibert N, Godaux E, Vidal PP, Moore LE (2001) Resonance of spike discharge modulation in neurons of the guinea pig medial vestibular nucleus. J Neurophysiol 86:703-716.

Schulz DJ, Goaillard JM, Marder E (2006) Variable channel expression in identified single and electrically coupled neurons in different animals. Nat Neurosci 9:356-362.

Schulman H , Hanson PI (1993) Multifunctional Ca2+/calmodulin-dependent protein kinase II. Neurochem res 18: 65-77.

Sekirnjak C, du Lac S (2002) Intrinsic firing dynamics of vestibular nucleus neurons. J Neurosci 22:2083-2095.

Sekirnjak C, Vissel B, Bollinger J, Faulstich M, du Lac S (2003) Purkinje cell synapses target physiologically unique brainstem neurons. J Neurosci 23:6392-6398.

Serafin M, de Waele C, Khateb A, Vidal PP, Muhlethaler M (1991a) Medial vestibular nucleus in the guinea-pig. II. Ionic basis of the intrinsic membrane properties in brainstem slices. Exp Brain Res 84:426-433.

Serafin M, de Waele C, Khateb A, Vidal PP, Muhlethaler M (1991b) Medial vestibular nucleus in the guinea-pig. I. Intrinsic membrane properties in brainstem slices. Exp Brain Res 84:417-425.

Shutoh F, Ohki M, Kitazwa H, Itohara S, Nagao S (2006) Memory trace of motor learning shifts transsynaptically from cerebellar cortex to nuclei for consolidation. Neuroscience.

Shutoh F, Katoh A, Ohki M, Itohara S, Tonegawa S, Nagao S (2003) Role of protein kinase C family in the cerebellum-dependent adaptive learning of horizontal optokinetic response eye movements in mice. Eur J Neurosci 18:134-142.

Silva AJ, Stevens CF, Tonegawa S, Wang Y (1992a) Deficient hippocampal long-term potentiation in alpha-calcium-calmodulin kinase II mutant mice. Science 257:201-206.

Silva AJ, Paylor R, Wehner JM, Tonegawa S (1992b) Impaired spatial learning in alpha-calcium-calmodulin kinase II mutant mice. Science 257:206-211.

Smith MR, Nelson AB, Du Lac S (2002) Regulation of firing response gain by calcium-dependent mechanisms in vestibular nucleus neurons. J Neurophysiol 87:2031-2042.

Smith PF, Curthoys IS (1989) Mechanisms of recovery following unilateral labyrinthectomy: a review. Brain Res Brain Res Rev 14:155-180.

Song P, Kaczmarek LK (2006) Modulation of Kv3.1b potassium channel phosphorylation in auditory neurons by conventional and novel protein kinase C isozymes. J Biol Chem 281:15582-15591.

Song P, Yang Y, Barnes-Davies M, Bhattacharjee A, Hamann M, Forsythe ID, Oliver DL, Kaczmarek LK (2005) Acoustic environment determines phosphorylation state of the Kv3.1 potassium channel in auditory neurons. Nat Neurosci 8:1335-1342.

Spencer RF, Wenthold RJ, Baker R (1989) Evidence for glycine as an inhibitory neurotransmitter of vestibular, reticular, and prepositus hypoglossi neurons that project to the cat abducens nucleus. J Neurosci 9:2718-2736.

Straka H, Vibert N, Vidal PP, Moore LE, Dutia MB (2005) Intrinsic membrane properties of vertebrate vestibular neurons: function, development and plasticity. Prog Neurobiol 76:349-392.

Swensen AM, Bean BP (2005) Robustness of burst firing in dissociated purkinje neurons with acute or long-term reductions in sodium conductance. J Neurosci 25:3509-3520.

Takazawa T, Saito Y, Tsuzuki K, Ozawa S (2004) Membrane and firing properties of glutamatergic and GABAergic neurons in the rat medial vestibular nucleus. J Neurophysiol 92:3106-3120.

Turrigiano G, Abbott LF, Marder E (1994) Activity-dependent changes in the intrinsic properties of cultured neurons. Science 264:974-977.

Turrigiano G, LeMasson G, Marder E (1995) Selective regulation of current densities underlies spontaneous changes in the activity of cultured neurons. J Neurosci 15:3640-3652.

Vibert N, Beraneck M, Bantikyan A, Vidal PP (2000) Vestibular compensation modifies the sensitivity of vestibular neurones to inhibitory amino acids. Neuroreport 11:1921-1927.

Weiser M, Vega-Saenz de Miera E, Kentros C, Moreno H, Franzen L, Hillman D, Baker H, Rudy B (1994) Differential expression of Shaw-related K+ channels in the rat central nervous system. J Neurosci 14:949-972.

Womack MD, Khodakhah K (2004) Dendritic control of spontaneous bursting in cerebellar Purkinje cells. J Neurosci 24:3511-3521.

Yamanaka T, Him A, Cameron SA, Dutia MB (2000) Rapid compensatory changes in GABA receptor efficacy in rat vestibular neurones after unilateral labyrinthectomy. J Physiol 523 Pt 2:413-424.

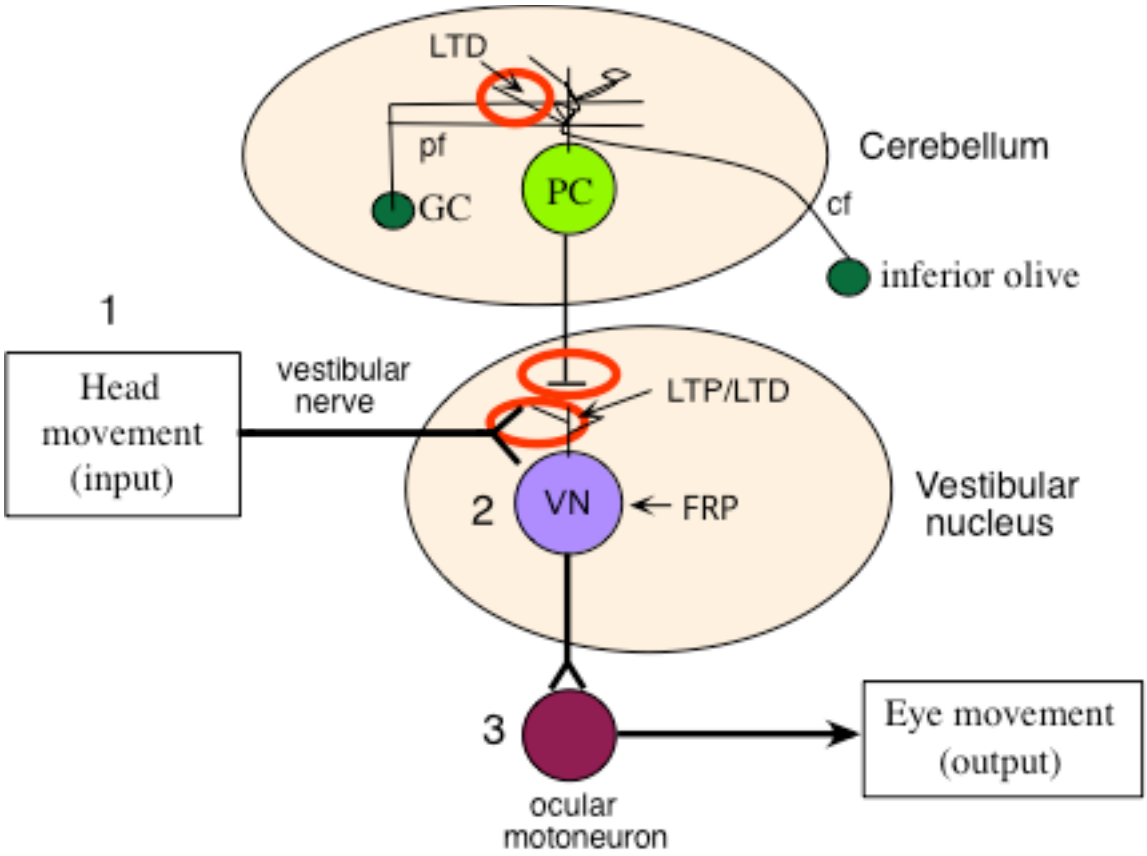

Fig. 1.1 : Sites of plasticity in the vestibular circuitry. The basic neural connections underlying the vestibulo-ocular reflex (VOR) are indicated with a thick black line and labeled 1-3. Head movement information is carried from sensory neurons in the inner ears to the vestibular nucleus via the vestibular nerve. These neurons then excite ocular motoneurons to drive compensatory eye movements. VOR plasticity involves a cerebellar circuit in which Purkinje cells serve as the site of integration about head and image motion, carried by parallel fibers from granule cells and climbing fibers from neurons in the inferior olive, respectively. LTD at the parallel fiber synapse onto Purkinje cells (circled in red) could underlie early stages of vestibular learning. Additional sites of synaptic plasticity that contribute to consolidation and long-term storage of vestibular memories lie within the vestibular nuclei (circled in red). High frequency stimulation of the vestibular nerve induces LTP or LTD at its synapses onto vestibular nucleus neurons. Synaptic plasticity might also occur at the projections from Purkinje cells onto vestibular nucleus neurons. Additionally, vestibular nucleus neurons exhibit a form of intrinsic plasticity, termed firing rate potentiation (FRP). Abbreviations: FRP, firing rate potentiation; GC, granule cell; LTD, long-term synaptic depression; LTP, long-term synaptic potentiation; PC, Purkinje cell; pf, parallel fibers; cf, climbing fibers; VN, vestibular nucleus neuron.

II. CaMKII regulates intrinsic excitability of MVN neurons

Abstract

Ca^{2+}/CaM-dependent protein kinase II (CaMKII) is traditionally described as a biological switch that is turned on by increases in intracellular calcium to mediate plasticity. A more recent study in spontaneously firing neurons demonstrated that this switch works in both directions and that turning CaMKII off can also mediate a form plasticity called firing rate potentiation (FRP). High levels of CaMKII activity keep baseline excitability of MVN neurons low. Blocking CaMKII in spontaneously firing neurons increased neuronal excitability and adding constiutively active CaMKII to non-spontaneously firing neurons decreased neuronal excitability. Consistent with the role of CaMKII as a modulator of BK currents during FRP, blocking CaMKII activity slightly reduced the amplitude of the whole cell Ca^{2+}-sensitive K^+ currents measured in acutely dissociated MVN neurons, over half of which is attributable to current through BK channels. However, the reduction of BK currents by CaMKII was small, suggesting that there may be other changes that accompany the downregulation of BK currents to increase neuronal excitability during FRP. Western blots probing the phosphorylation state of residue T287 in ß-CaMKII, the dominant isoform in MVN neurons, suggested that reductions in CaMKII activity during FRP persisted for up to 30 minutes after induction. However, the presence of synaptic blockers, kyneurinic acid and picrotoxin, blocked changes in phosphorylation at this residue

without blocking the induction and maintenance of FRP, raising the possibility that reductions phosphorylation on T287 are not necessarily related to FRP.

Introduction

Cellular mechanisms of long term plasticity have been extensively studied in cortical and hippocampal neurons and learning rules established in these neurons are frequently extended to other cell types. Although plasticity is certainly analogous in some of these cell types, generalizations should not extend too broadly given the similar properties of hippocampal and cortical neurons. Both cell types are relatively silent under baseline conditions and plasticity is induced by depolarizing stimuli that increase internal Ca^{2+} concentrations. In contrast, long term plasticity in medial vestibular nucleus (MVN) neurons that are spontaneously active, is triggered by decreases in intracellular Ca^{2+} concentrations. This demonstrates that the canonical rules for plasticity can differ substantially in spontaneously firing neurons and suggests that spontaneously firing neurons utilize novel molecular mechanisms for long term plasticity.

Ca^{2+}/calmodulin-dependent protein kianse II (CaMKII) is a ubiquitous protein with elegantly complex biochemistry that can encode a 'memory' of neuronal activity. CaMKII is activated by Ca^{2+}/CaM and subsequently autophosphorylates on residue T287, which keeps the kinase active even after Ca^{2+} levels have returned to baseline (Schulman and Hanson, 1993; Lisman, 1994; Hudmon and Schulman, 2002; Lisman et al., 2002). High frequency stimulation of hippocampal neurons activates CaMKII, a necessary step for the

induction of long-term potentiation (LTP) (Fukunaga et al., 1995; Barria et al., 1997). In the MVN, where neurons are spontaneously active at 5-50 Hz in the absence of synaptic input, decreases, rather than increases in CaMKII induce a form of plasticity called firing rate potentiation (FRP) (Nelson et al., 2003; Nelson et al., 2005).

In MVN neurons, FRP leads to a long term increase in intrinsic excitability, characterized by increases in spontaneous firing rates and increases in a neuron's firing rate sensitivity to depolarizing inputs, referred to as neuronal gain (Nelson et al., 2003). These changes in neuronal excitability were occluded by application of iberiotoxin (ibtx), which blocks BK-type Ca^{2+}-activated K^{+} (KCa) currents. BK currents contribute to action potential repolarization and are particularly prominent during the early phase of the afterhyperpolariztion (AHP) (Smith et al., 2002). Downregulation of these K^{+} currents during FRP, therefore, increases neuronal excitability. Under baseline conditions, Ca^{2+} influx due to the spontaneous activity of MVN neurons, was sufficient to activate CaMKII. It was only when Ca^{2+} levels dropped that CaMKII could be turned off, directly or indirectly decreasing BK currents.

The contribution of CaMKII during FRP defined a novel role for the kinase in neuronal plasticity and raised questions about normal function and regulation in spontaneously firing neurons. In this paper, we address the following questions: (1) How does constitutively active CaMKII regulate the initial excitability of MVN neurons (2) To what extent does it affect the amplitude

of the whole cell BK current, and (3) Is CaMKII activity permanently decreased following FRP or does its activity return to baseline levels?

Methods

Electrophysiology: Slices from mice aged 17-24 days old were placed in a submersion chamber perfused with carbogenated ACSF at 31-33°C, supplemented with kynurenic acid (2 mM) and picrotoxin (100 μM) to block ionotropic glutamatergic and GABAergic neurotransmission, respectively. Neurons in the MVN were visualized with differential interference contrast optics under infrared illumination. Neurons were patched in the whole-cell, current-clamp mode using an Axoclamp 2B amplifier. Membrane potential was sampled at 3 kHz for continuous measurement of firing rate; 20-40 kHz sampling was used for all other measurements. Pipet and access resistances were bridge-balanced throughout each experiment, and voltage offsets were corrected after removing the electrode from the neuron. Membrane potential traces were corrected by subtracting a liquid junction potential of -14 mV. Electrodes contained an internal solution of (in mM) 140 K gluconate, 10 HEPES, 8 NaCl, 0.1 EGTA, 2 MgATP, 0.3 Na_2GTP.

Western blots: The medial vestibular nucleus (MVN) was dissected from mouse brainstem slices, prepared as above, and homogenized in buffer containing: 10mM Tris-HCl pH 6.8, 2.5% SDS, 2mM EDTA, 5 mM β-glycerophosphate, 0.5 μg/mL aprotinin, 10 μg/mL leupeptin, and 100 μM PMSF (Sigma). Samples were separated on a 7.5% SDS PAGE and transferred to

nitrocellulose membrane (BioRad). The membrane was blocked with 5% nonfat milk and blotted with antibody. Anti-αCaMKII (Chemicon) was used at a concentration of 1:1000, anti-βCaMKII (Zymed) at 1:200, Anti-phospho-CaMKII (Novus) at 1:1000. Protein was visualized using an HRP-conjugated goat anti-mouse or anti-rabbit antibody with a chemiluminescent reaction (kit, Amersham Biosciences).

Histology: Immunohistochemistry was performed on slices prepared as above. The tissue was fixed overnight at 4°C in 4% paraformaldehyde then treated in 30% sucrose at room temperature for 1 hour before re-sectioning. The tissue was re-sectioned into 30μm sections, blocked in phosphate-buffered saline containing: 2% normal goat serum, 1% BSA, 0.3% Triton-X-100 and incubated in primary antibody overnight at 4°C. Anti-phospho-CaMKII was used at a concentration of 1:2500; anti-NeuN was used at 1:200. Goat anti-rabbit secondary, conjugated to Cy3 (1:200, Chemicon) and goat anti-mouse secondary, conjugated to Alexa-fluor 488 (1:500, Molecular Probes), were used to visualize each primary antibody.

Results

CaMKII activity contributes to baseline neuronal excitability

The finding that FRP requires decreases in CaMKII activity suggests that high CaMKII activity at baseline negatively regulates the excitability of MVN neurons.

Consistent with this hypothesis, decreasing CaMKII activity in spontaneously firing MVN neurons increased their excitability (Fig. 1A-B). Application of the CaMKII inhibitor, KN-62, in the extracellular solution increased the slope of a neuron's input-output curve (neuronal gain) by 42% ± 10% ($p = 0.0008$, $n = 16$) and inclusion of a peptide inhibitor, CaMKIIi290-309, in the pipet increased neuronal gain by 36% ± 14% ($p = 0.008$, $n = 10$) .

In another experiment, a truncated version of CaMKII was constitutively activated *in vitro* (see methods) then introduced to neurons through the recording pipet. Because it took 9-10 minutes for active CaMKII to have an effect, baseline neuronal excitability could be measured within 1 min of break-in. Changes in excitability in neurons patched with activate CaMKII were compared with control data from neurons patched with heat inactivated CaMKII. Introducing constitutively active CaMKII to spontaneously firing MVN neurons had no effect on intrinsic excitability, suggesting CaMKII was already maximally active in these neurons (Fig. 1B). Alternatively, when constiutively active CaMKII was introduced to silent MVN neurons, which should have very low basal Ca^{2+} levels, it caused a decrease in neuronal excitability (-12 ± 9 %, $n = 11$, $p = 0.001$). These results indicate that CaMKII activity negatively regulates excitability in MVN neurons.

CaMKII inhibition decreases KCa currents

CaMKII is thought to exert its influence on neuronal excitability in the MVN through regulation of BK-type K channels. To determine the extent to

which BK currents were reduced by decreases in CaMKII activity, the amplitude of KCa currents were compared in acutely dissociated neurons, patched with either control internal or with internal containing CaMKIIi290-309. Acutely dissociated neurons were used because the accurate voltage control of this prep allows for more accurate measurements of whole cell current amplitudes than in slice preparations. To further reduce variability in current amplitudes, recordings were restricted to GABAergic MVN neurons which tend to have large BK currents (Gittis and du Lac, 2007).

Currents were elicited with 300 ms voltage steps between -55 and +15 mV and KCa currents were isolated by subtraction after extracellular $CaCl_2$ [2 mM] was replaced with $MgCl_2$ [2 mM] (Fig. 2A). Over half of this current is likely to be through BK channels (Gittis and du Lac, 2007). Robust KCa currents were still observed in the presence of CaMKIIi290-309. KCa currents under both conditions showed typical kinetics with a fast, transient phase followed by a slower, non-inactivating phase. The peak amplitudes of the currents (measured at +15 mV) tended to be smaller in neurons containing CaMKIIi290-309 (5.4 ± 2.9 nA, $n = 21$ vs 4.0 ± 1.6 nA, $n = 8$, $p = 0.26$).

Figure 2B shows average IV curves for the family of KCa currents recorded in control neurons and those patched with CaMKIIi290-309. Inhibiting CaMKII activity did not change the voltage-dependence of the current. In both conditions, KCa currents activated between -45 and -35 mV with sigmoidal relationships to voltage, reflecting the influence of Ca^{2+} on the gating properties of the channel.

These data suggest that inhibiting CaMKII decreases the whole cell KCa current by about 25%, with no changes in its voltage dependence or kinetics of activation. Although the decrease in current amplitude was not significant, this parameter varied 5-fold across cells, making small effects on amplitude hard to distinguish from the noise.

β-CaMKII is the dominant isoform in MVN neurons

To understand the molecular expression and regulation of CaMKII in the MVN, tissue homogenates from mouse MVN were immunblotted with antibodies against the α- and β- subunits of CaMKII, the predominant neuronal isoforms (Miller and Kennedy, 1985). As shown in Fig. 3A, both α-CaMKII and β-CaMKII were detected in the MVN. A doublet in the β-CaMKII position (58 kDa and 60 kDa) suggests the presence of multiple splice variants of β-CaMKII in the MVN. A single band at 58 kDa was observed in a forebrain sample prepared and run in parallel with the MVN samples (data not shown).

Consistent with the electrophysiological evidence for constitutively active CaMKII, signal was detected under basal conditions with an antibody against phosphorylation at T287, the residue associated with persistent CaMKII activity. Fig. 3 A shows strong expression of this phospho-CaMKII in the MVN, particularly prominent at the molecular weight corresponding to β-CaMKII.

The high level of phosphorylated β-CaMKII in MVN neurons was confirmed by immunolabeling. The majority of MVN neurons contained β-CaMKII but not α-CaMKII (Fig. 3B-C). For comparison, images were taken

from the proximal cerebellum in which α-CaMKII labeling in Purkinje cells was strong. Staining for phosphorylated CaMKII was strong in both MVN and Purkinje neurons which have high basal levels of activity, but not in granule cells which have lower spontaneous activity (Fig. 3D). The phospho-CaMKII signal colocalized with β-CaMKII in the MVN and α-CaMKII in the cerebellum (Fig. 3E).

Changes in CaMKII phosphorylation

To determine whether decreases in CaMKII activity during FRP correspond

with changes in the phosphorylation state of the kinase, tissue samples were probed with the phospho-T287 antibody following the global induction of FRP, either by incubating slices in Ringer's + 1.5 mM glycine to silence firing or by replacing extracellular $CaCl_2$ with $MgCl_2$ which increases firing but reduces intracellular Ca^{2+} levels (Nelson et al., 2003). Both protocols produced modest increases in neuronal excitability, measured as increases in spontaneous firing rate (10 ± 54% in 1.5 mM glycine, n = 8; 29 ± 19% in 0 Ca^{2+}, n = 8), gain (14 ± 10% in 1.5 mM glycine; 13 ± 8% in 0 Ca^{2+}), and decreases in the AHP (-15 ± 8% in 1.5 mM glycine; -14 ± 7% in 0 Ca^{2+}).

Protein samples were collected at 2 time points after FRP induction: (1) immediately after the 10 min. incubation in 0 Ca^{2+} / glycine solutions and (2) after a 30 minute recovery period in Ringer's solution. As shown in Fig. 4A, the signal for phospho-CaMKII at the predicted molecular weight for β-CaMKII decreased

immediately following treatment with either 0 Ca^{2+} or 1.5 mM glycine. This decrease in phosphorylated CaMKII does not simply reflect changes in the firing rate of the neurons because in the presence of 0 Ca2+, neurons increase their firing rate but in the presence of 1.5 mM glycine, neurons are silenced. Furthermore, these changes in CaMKII phosphorylation persisted 30 minutes after FRP induction, when the spontaneous firing rates of neurons are higher than before. This suggests that FRP is associated with persistent decreases in CaMKII activity as assessed by phosphorylation at T287.

Further support for persistent changes in CaMKII phosphorylation following FRP induction came from immunostaining of slices treated with 0 Ca^{2+}, either immediately following treatment or 30 minutes later. The number of β-CaMKII-expressing neurons in the MVN that were positive for phosphoT287 decreased from 78% (216 / 267) to 58% (131/224) ($p = 0.02$) immediately after FRP induction and remained at 60% (136/227) ($p = 0.04$) 30 minutes later (Fig. 4B).

Although this data indicated a decrease of CaMKII phosphorylation during FRP induction and maintenance, the experiments were not done in the presence of the synaptic blockers, kyneurinic acid [uM] and picrotoxin [uM] which are always present during electrophysiological experiments of FRP. Puzzlingly, when the global induction experiment was repeated in the presence of these synaptic blockers, decreases in CaMKII phosphorylation at T287 were no longer observed (Fig. 4C). Phosphorylation of β-CaMKII was still strong under control conditions, but showed no evidence of decreasing intensity either

immediately after or 30 minutes following treatment with 0 Ca^{2+} or 1.5 mM glycine. This finding derailed the project.

Discussion

The results of this study demonstrate that β-CaMKII is the predominant isoform in the MVN and that basal Ca^{2+} levels in spontaneously firing MVN neurons maximally activate CaMKII. Activated CaMKII acts as a negative regulator of excitability, revealed by decreased excitability after its activation in non-spontaneously firing neurons and increased excitability after its inhibition in spontaneously firing neurons. Transient reduction of intracellular Ca^{2+} levels, consistent with those required to induce FRP, persistently decreased CaMKII phosphorylation on T287. However, the synaptic blockers kyneurinic acid and pictrotoxin blocked reductions in T287 phosphorylation without blocking FRP, raising the possibility that these two processes are dissociable.

Role of β-CaMKII in MVN neurons

CaMKII is a ubiquitous protein and its two major isoforms, α and β, associate into heteromeric holoenzyme complexes composed of 10-12 CaMKII molecules linked through an association domain. The ratio of α : β isoforms varies across brain regions and although the isoforms exhibit a great deal of structural similarity, their binding partners and biochemical properties differ in significant ways. Only the β isoform contains an f-actin binding domain which is important for targeting and anchoring the holoenzyme complex to synapses (Shen

et al., 1998). Additionally, the β isoform has a higher affinity for Ca^{2+}/CaM which makes it more sensitive to low calcium levels (Brocke et al., 1999) and more responsive to brief Ca^{2+} spikes (De Koninck and Schulman, 1998). MVN neurons have strong endogenous Ca^{2+} buffers that likely restrict Ca^{2+} influx to temporally and spatially precise windows during action potentials (I. van Welie, personal communication). β-CaMKII isoforms might provide a necessary sensitivity to these rapid Ca^{2+} fluctuations. The sensitivity of β-CaMKII isoforms to Ca^{2+} spikes can be further refined by alternative splicing (Bayer et al., 2002), and western blots suggest the presence of at least two splice variants of β-CaMKII.

Mechanisms of CaMKII regulation during FRP

Are persistent decreases in CaMKII activity required for the maintenance of FRP or does its activity decrease only transiently during FRP induction? Phosphorylation at T287 was reduced immediately after FRP induction by 2 different methods: (1) replacing extracellular $CaCl_2$ with $MgCl_2$ and (2) silencing neurons with 1.5 mM glycine. MVN samples harvested after a 30 minute recovery period in Ringer's solution still showed reduced levels of T287 phosphorylation, suggesting that CaMKII activity is locked into a lower activity state after FRP induction. However, decreases in T287 phosphorylation were not observed when FRP was induced in the presence of the synaptic blockers, kyneurinic acid and picrotoxin. It is not clear why this should change the effect of the FRP induction protocol on CaMKII phosphorylation. Synaptic activity is not

required to induce FRP (Nelson et al., 2003) and should already be blocked by the induction protocols. Nevertheless, the different results in the presence or absence of synaptic blockers were reproducible and raised concerns about whether the decreases observed in T287 were necessary for FRP.

The finding that CaMKII might not change its phosphorylation state on T287 during FRP was suprising given strong electrophysiological evidence that FRP induction requires decreases in CaMKII activity (Nelson et al., 2005). However, phosphorylation at T287 is not a direct correlate of CaMKII activity and there are other ways that the kinase could be regulated. One possibility is autophosphorylation at the inhibitory residue T305/306, triggered by abrupt reductions in Ca^{2+} levels (Kuret and Schulman, 1985; Hashimoto et al., 1987; Colbran and Soderling, 1990; Patton et al., 1990; Hanson and Schulman, 1992; Lu et al., 2007). Phosphorylation at this residue disrupts the ability of CaMKII to bind Ca^{2+}/CaM, and changes its subcellular distribution, distancing it from calcium sources and molecular targets at the membrane (Elgersma et al., 2002; Fox, 2003; Griffith, 2004; Lu et al., 2007; Shen and Meyer, 1999; Schulman, 2004). We performed a series of experiments using a phospho-specific T305/306 antibody to look for changes in phosphorylation after FRP induction, but the results of this study were inconclusive. We also performed activity assays to directly measure CaMKII activity after FRP induction, but these, too, were inconclusive.

CaMKII regulation of BK currents

An important molecular target of CaMKII in MVN neurons are BK channels, which are likely down-regulated during FRP to increase neuronal excitability (Smith et al., 2002; Nelson et al., 2003; Nelson et al., 2005). BK currents recorded from acutely dissociated MVN neurons were slightly smaller in the presence of CaMKII inhibitors, but not dramatically so. This supports the hypothesis that CaMKII inhibits BK currents to induce FRP, but suggests that either (1) only a small percentage of BK currents are affected during FRP or (2) CaMKII inhibitors have differential effects on somatic vs. dendritic BK currents.

In support of the first explanation, the effect of CaMKII inhibitors on BK currents in slice was only measured for the small fraction of BK currents activated by a brief depolarization to mimic an action potential (Nelson et al., 2005). This represents a tiny percentage of the total BK current in the cell, consistent with the notion that changes to a small number of BK channels might be sufficient to induce FRP.

Support for the second possibility comes from the fact that the dissociated preparation is limited to the study of somatic currents. A significant portion of the somatic KCa current in MVN neurons is BK (Gittis and du Lac, 2007), but it is unknown how much additional BK current is found on the dendrites. The observation that BK blockers reduce the magnitude of the AHP much more in slice than in dissociated neurons suggests that contribution from dendritic BK currents in slice might be large (Gittis, unpublished observations). This raises the possibility that during FRP, there are large reductions in dendritic BK currents but

only small reductions in somatic BK currents. Further experiments would be required to distinguish between these 2 possibilities.

Acknowledgements

Chapter 2 is a revised version of Nelson AB, Gittis AH, du Lac S. Neuron 2005 Decreases in CaMKII activity trigger persistent potentiation of intrinsic excitability in spontaneously firing vestibular nucleus neurons. May 19; 46(4):623-31. The portions present here are included with the permission of all the authors on the final publication.

References

Barria A, Muller D, Derkach V, Griffith LC, Soderling TR (1997) Regulatory phosphorylation of AMPA-type glutamate receptors by CaM-KII during long-term potentiation. Science 276:2042-2045.

Bayer KU, De Koninck P, Schulman H (2002) Alternative splicing modulates the frequency-dependent response of CaMKII to Ca(2+) oscillations. Embo J 21:3590-3597.

Brocke L, Chiang LW, Wagner PD, Schulman H (1999) Functional implications of the subunit composition of neuronal CaM kinase II. J Biol Chem 274:22713-22722.

Colbran RJ, Soderling TR (1990) Calcium/calmodulin-independent autophosphorylation sites of calcium/calmodulin-dependent protein kinase II. Studies on the effect of phosphorylation of threonine 305/306 and serine 314 on calmodulin binding using synthetic peptides. J Biol Chem 265:11213-11219.

De Koninck P, Schulman H (1998) Sensitivity of CaM kinase II to the frequency of Ca2+ oscillations. Science 279:227-230.

Elgersma Y, Fedorov NB, Ikonen S, Choi ES, Elgersma M, Carvalho OM, Giese KP, Silva AJ (2002) Inhibitory autophosphorylation of CaMKII controls PSD association, plasticity, and learning. Neuron 36:493-505.

Fox K (2003) Synaptic plasticity: the subcellular location of CaMKII controls plasticity. Curr Biol 13:R143-145.

Fukunaga K, Muller D, Miyamoto E (1995) Increased phosphorylation of Ca2+/calmodulin-dependent protein kinase II and its endogenous substrates in the induction of long-term potentiation. J Biol Chem 270:6119-6124.

Gittis AH, du Lac S (2007) Firing properties of GABAergic versus non-GABAergic vestibular nucleus neurons conferred by a differential balance of potassium currents. J Neurophysiol 97:3986-3996.

Griffith LC (2004) Regulation of calcium/calmodulin-dependent protein kinase II activation by intramolecular and intermolecular interactions. J Neurosci 24:8394-8398.

Hanson PI, Schulman H (1992) Inhibitory autophosphorylation of multifunctional Ca2+/calmodulin-dependent protein kinase analyzed by site-directed mutagenesis. J Biol Chem 267:17216-17224.

Hashimoto Y, Schworer CM, Colbran RJ, Soderling TR (1987) Autophosphorylation of Ca2+/calmodulin-dependent protein kinase II. Effects on total and Ca2+-independent activities and kinetic parameters. J Biol Chem 262:8051-8055.

Hudmon A, Schulman H (2002) Structure-function of the multifunctional Ca2+/calmodulin-dependent protein kinase II. Biochem J 364:593-611.

Kuret J, Schulman H (1985) Mechanism of autophosphorylation of the multifunctional Ca2+/calmodulin-dependent protein kinase. J Biol Chem 260:6427-6433.

Lisman J (1994) The CaM kinase II hypothesis for the storage of synaptic memory. Trends Neurosci 17:406-412.

Lisman J, Schulman H, Cline H (2002) The molecular basis of CaMKII function in synaptic and behavioural memory. Nat Rev Neurosci 3:175-190.

Lu CS, Hodge JJ, Mehren J, Sun XX, Griffith LC (2003) Regulation of the Ca2+/CaM-responsive pool of CaMKII by scaffold-dependent autophosphorylation. Neuron 40, 6:1185-97.

Miller SG, Kennedy MB (1985) Distinct forebrain and cerebellar isozymes of type II Ca2+/calmodulin-dependent protein kinase associate differently with the postsynaptic density fraction. J Biol Chem 260:9039-9046.

Nelson AB, Gittis AH, du Lac S (2005) Decreases in CaMKII activity trigger persistent potentiation of intrinsic excitability in spontaneously firing vestibular nucleus neurons. Neuron 46:623-631.

Nelson AB, Krispel CM, Sekirnjak C, du Lac S (2003) Long-lasting increases in intrinsic excitability triggered by inhibition. Neuron 40:609-620.

Patton BL, Miller SG, Kennedy MB (1990) Activation of type II calcium/calmodulin-dependent protein kinase by Ca2+/calmodulin is inhibited by autophosphorylation of threonine within the calmodulin-binding domain. J Biol Chem 265:11204-11212.

Schulman H (2004) Activity-dependent regulation of calcium/calmodulin-dependent protein kinase II localization. J Neurosci 24:8399-8403.

Schulman H, Hanson PI (1993) Multifunctional Ca2+/calmodulin-dependent protein kinase. Neurochem Res 18:65-77.

Shen K, Meyer T (1999) Dynamic control of CaMKII translocation and localization in hippocampal neurons by NMDA receptor stimulation. Science 284:162-166.

Shen K, Teruel MN, Subramanian K, Meyer T (1998) CaMKIIbeta functions as an F-actin targeting module that localizes CaMKIIalpha/beta heterooligomers to dendritic spines. Neuron 21:593-606.

Smith MR, Nelson AB, Du Lac S (2002) Regulation of firing response gain by calcium-dependent mechanisms in vestibular nucleus neurons. J Neurophysiol 87:2031-2042.

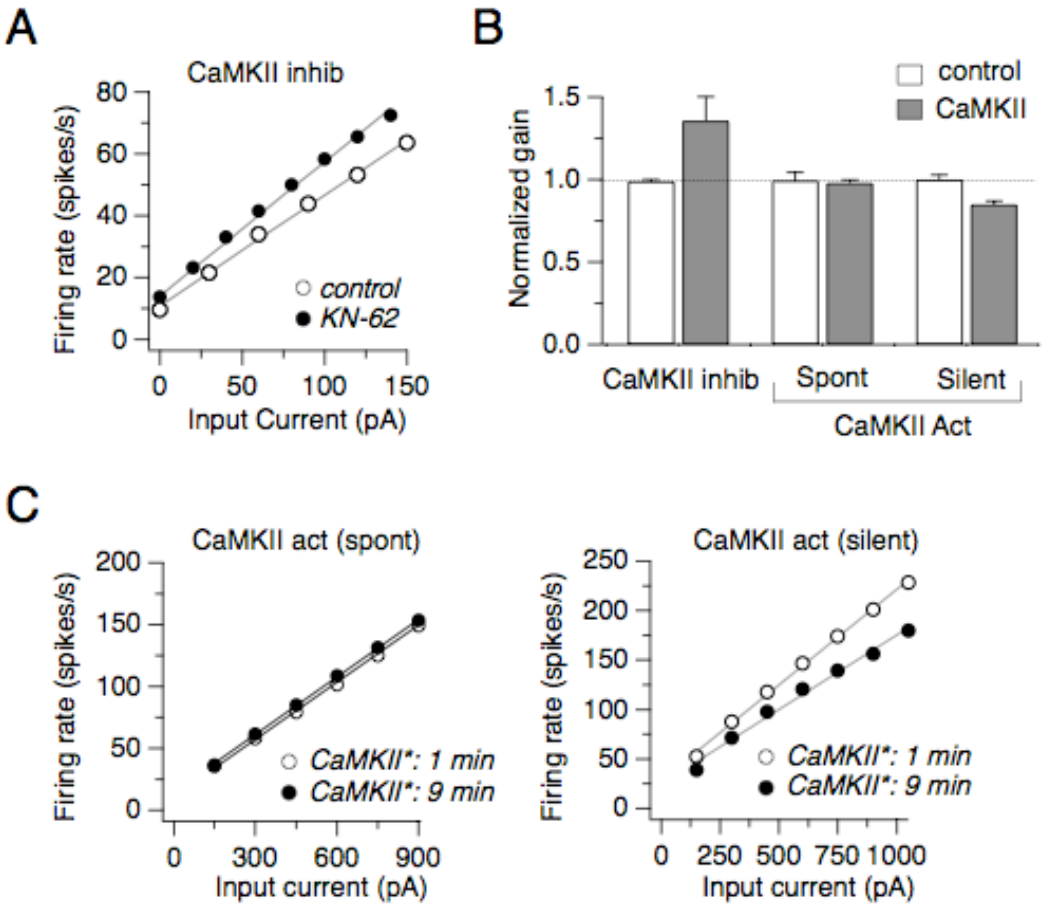

Fig 2.1: CaMKII activity negatively regulates baseline excitability of MVN neurons. **A.** Linear input-output curve (gain) of a representative neuron, before and after inhibition of CaMKII activity with KN-62. The gain of the neuron increased from x to x. **B.** Changes in neuronal gain recorded across the population of MVN neurons after decreasing CaMKII activity with the peptide inhibitor, CaMKIIi290-305 (CaMKII Inhib) or increasing CaMKII activity with a constitutively active form of the kinase (CaMKII Act). Changes in gain over the first 10 minutes were normalized to changes in gain over the first 10 minutes in control neurons, patched with regular internal or internal containing a heat-inactivated version of the constitutively active kinase. The effect of constitutively active CaMKII was different in spontaneously firing vs. silent neurons. It had no effect on the gain of spontaneously firing neurons but significantly decreased the gain of silent neurons **C.** Representative spontaneously firing neuron in which adding constitutively active CaMKII had no effect on gain. **D.** Representative silent neuron showing decrease in gain induced by the addition of constitutively active CaMKII.

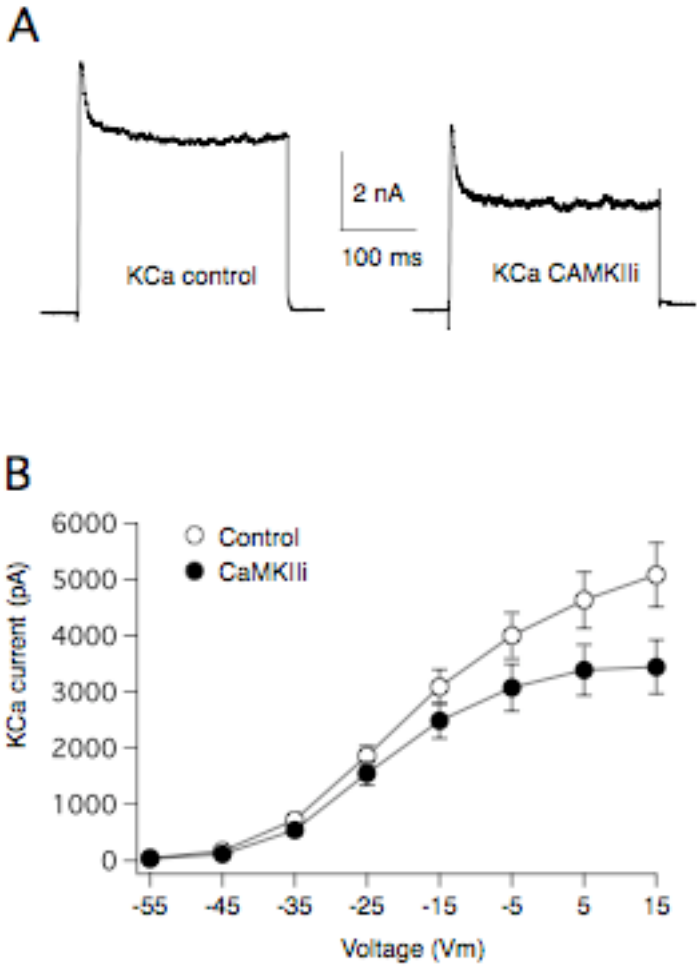

Fig 2.2: Decreases in CaMKII activity reduce KCa currents in acutely dissociated neurons. **A.** Whole cell KCa currents measured by digital subtraction after replacing extracellular calcium with magnesium. Currents were elicited with a 300 ms voltage step from -65 mV to + 15 mV. Recordings were made with standard internal (left) or internal containing the CaMKII peptide inhibitor CaMKIIi290-305 (right). No changes in current kinetics were observed in the presence of CaMKIIi290-305. **B.** Average IV curves of KCa currents measured in the presence or absence of CaMKIIi290-309. Inhibiting CaMKII had no effect on the voltage-dependence of KCa currents which activated between -45 and -35 mV and were sigmoidally related to voltage. The amplitude of KCa currents were reduced by inhibiting CaMKII activity from 5.4 ± 2.9 nA (n = 21) to 4.0 ± 1.6 nA, (n = 8; p = 0.26)

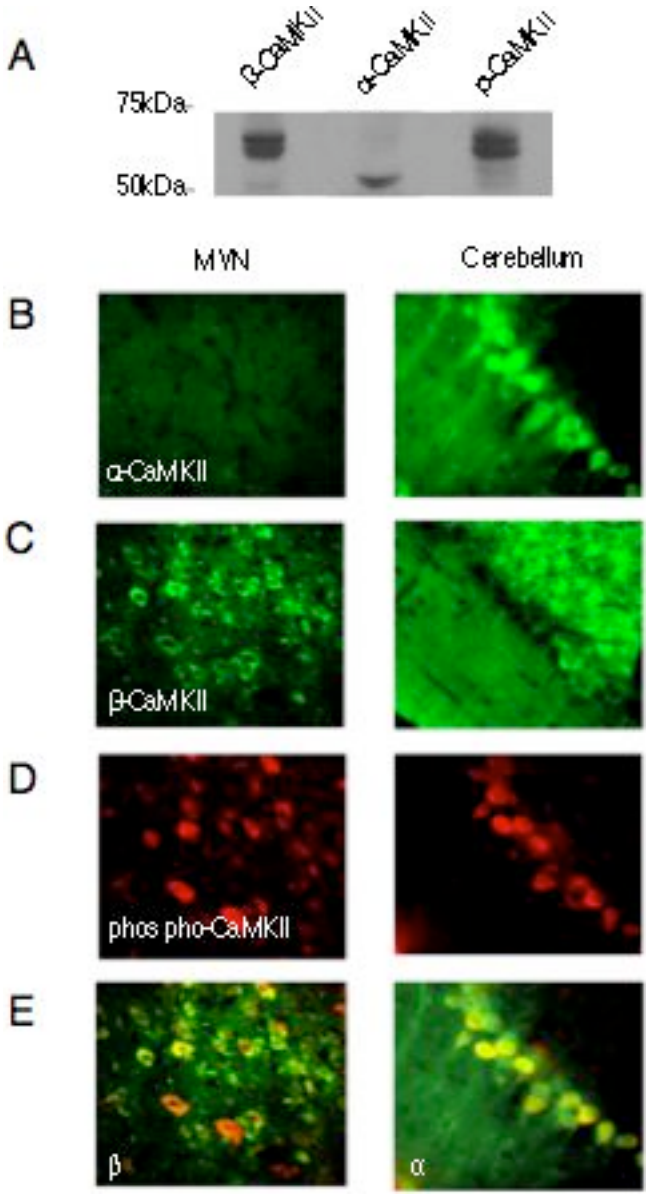

Fig 2.3: β-CaMKII is constitutively phosphorylated on residue T287 in MVN neurons. **A.** Homogenates of medial vestibular nuclei (MVN), immunoblotted with anti-βCaMKII (left), anti-αCaMKII (center), and anti-phospho-T287 CaMKII (right). Both αCaMKII (55kDa) and βCaMKII (58 and 60kDa) were detected in the MVN but only βCaMKII was phosphorylated on T287. **B.** Results of immunostains with anti-αCaMKII in the MVN (left) and cerebellum (right). Purkinje cells in the cerebellum were labeled. **C.** Results of immunostains with anti-βCaMKII in the MVN (left) and cerebellum (right). Neurons in the MVN and cerebellar granule cells were labeled. **D.** Results of immunostain with anti-phospho-T287 in the MVN (left) and cerebellum (right). **E.** Overlay of images from C & D (left) and B & D (right).

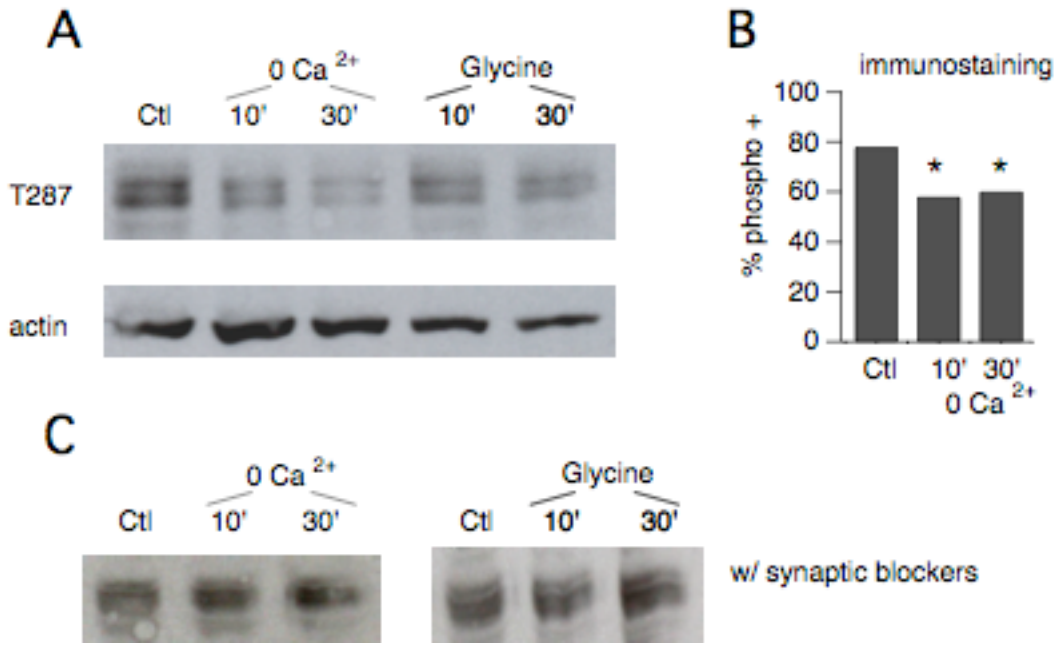

Fig 2.4: Changes in phosphorylation of βCaMKII on T287 after FRP induction. **A.** *Top*: Western blot of tissue homogenates from medial vestibular nuclei (MVN), probed with a phospho-specific antibody against T287. Molecular weights of 58 kDa and 60 kDa were consistent with phosphorylation of βCaMKII isoforms. Homogenates were harvested from slices incubated in control ACSF (Ctl), 0 Ca^{2+} ACSF (0 Ca^{2+}), or ACSF + 1.5 mM glycine (Glycine). Homogenates were collected immediately after a 10 min FRP induction period (10'), or after a 30 min recovery period in ACSF (30'). *Bottom*: Actin loading control. **B.** Percentage of neurons in the MVN labeled with an anti- βCaMKII antibody that were also labeled with the phospho-T287 antibody in control slices (Ctl) or in slices that had been treated with 0 Ca^{2+} ACSF to induce FRP. The percentage of phospho-labeled neurons dropped from 78 % in control slices to 58% immediately after FRP induction (10') and remained at 60 % after a 30 min recovery period in ACSF (30'). **C.** Same experiment as described in A, but ACSF contained the synaptic blockers kyneurinic acid and picrotoxin. Under these conditions, no changes were observed in T287 phosphorylation.

III. Firing properties of GABAergic vs. non-GABAergic vestibular nucleus neurons conferred by a differential balance of potassium currents

Abstract

Neural circuits are composed of diverse cell types whose firing properties reflect their intrinsic ionic currents. GABAergic and non-GABAergic neurons in the medial vestibular nuclei, identified in GIN and YFP-16 lines of transgenic mice, respectively, exhibit different firing properties in brain slices. The intrinsic ionic currents of these cell types were investigated in acutely dissociated neurons from 3-4 week-old mice, where differences in spontaneous firing and action potential parameters observed in slice preparations are preserved. Both GIN and YFP-16 neurons express a combination of four major outward currents: Ca^{2+}-dependent K^+ currents (I_{KCa}), 1 mM TEA-sensitive delayed rectifier K^+ currents (I_{1TEA}), 10 mM TEA-sensitive delayed rectifier K^+ currents (I_{10TEA}), and A-type K^+ currents (I_A). The balance of these currents varied across cells, with GIN neurons tending to express proportionately more I_{KCa} and I_A and YFP-16 neurons tending to express proportionately more I_{1TEA} and I_{10TEA}. Correlations in charge densities suggested that several currents were coregulated. Variations in the kinetics and density of I_{1TEA} could account for differences in repolarization rates observed both within and between cell types. These data indicate that diversity in the firing properties of GABAergic and non-GABAergic vestibular nucleus neurons arises from graded differences in the balance and kinetics of ionic currents.

Diverse classes of neurons have evolved to perform specific functions in complex circuits, requiring specialization of their ability to process inputs into meaningful patterns of firing. The ability of a neuron to processes and transmit information depends on its intrinsic ionic currents. An emerging question is how these currents are regulated to produce the appropriate pattern of output. Recent studies in invertebrates have shown that the level of channel expression can vary considerably within the same cell from animal to animal, but the output pattern is kept constant through correlated channel expression that maintains a target balance of currents that are unique to a particular cell type (Prinz et al. 2004; Schulz et al. 2006).

Spontaneously firing neurons in the medial vestibular nuclei (MVN) respond linearly over a wide dynamic range and are capable of sustaining firing rates of hundreds of spikes/s (Sekirnjak and du Lac 2002; 2006; Sekirnjak et al. 2003; Smith et al. 2002). Action potential and firing properties form a continuum across MVN neurons (du Lac et al. 1995; Sekirnjak and du Lac 2002; Straka et al. 2005). Initial studies subdivided the continuum into two broad types defined by canonical properties of action potentials at the extremes (Johnston et al. 1994; Serafin et al. 1991). Subsequent studies combining electrophysiological recordings with anatomical (Sekirnjak and du Lac 2006; Sekirnjak et al. 2003) or molecular (Takazawa et al. 2004) analyses revealed a diversity of cell types with graded differences in firing properties. Experience-dependent changes in intrinsic excitability of MVN neurons can be evoked by synaptic inhibition

(Nelson et al. 2003) or by unilateral labyrinthectomy, the vestibular equivalent of monocular deprivation (Beraneck et al. 2003; Beraneck et al. 2004; Cameron and Dutia 1997; Guilding and Dutia 2005; Him and Dutia 2001). Progress in dissecting the mechanisms and functional consequences of such intrinsic plasticity, however, has been hampered by a lack of knowledge about the ionic currents expressed in specific cell types.

Recently, two lines of transgenic mice have been identified that label different classes of MVN neurons: GIN mice (Oliva et al. 2000) express GFP in GABAergic neurons, and YFP-16 mice (Feng et al. 2000) express YFP in non-GABAergic, glutamatergic and glycinergic neurons (Bagnall et al. 2007). YFP-16 neurons have narrower action potentials and can sustain higher firing rates than GIN neurons. These differences in firing properties could be achieved via a number of alternative mechanisms, including expression of distinct ionic currents, as observed in regular spiking pyramidal cells vs. fast-spiking interneurons in the cortex (Martina et al. 1998), differences in dendritic morphology (Mainen and Sejnowski 1996), or variations in the ratio of current expression, as in somatogastric ganglion neurons (Schulz et al. 2006).

To investigate mechanisms that underlie differences in firing properties between GIN and YFP-16 neurons, somatic whole cell currents were measured in an acutely dissociated cell preparation that preserves both spontaneous firing and differences in action potential properties between the two cell classes. The results suggest that graded differences in the balance of ionic currents underlie the

continuous variations in firing properties of GABAergic and non-GABAergic vestibular nucleus neurons.

Materials and Methods

Cell preparation: 350-400 μM coronal slices through the rostral 2/3 of the MVN were prepared as described in Sekirnjak et al., 2003 from 24-39-day-old mice (average = 29 ± 4 d), either c57bl6 wild-type, GIN (Oliva et al. 2000), or YFP-16 (Feng et al. 2000) lines of mice both in c57bl6 backgrounds. Neurons were enzymatically dissociated at 30ºC for 10 minutes in a solution of 9.4 mg/mL MEM powder (Gibco), 10 mM Hepes, 0.2 mM cysteine, and 40 U/mL papain (Worthington), pH 7.2. The vestibular nuclei were dissected out in a similar ice cold solution in which papain was replaced by 1 μg/mL BSA and 1 μg/mL Trypsin inhibitor. The nuclei were triturated with fire polished Pasteur pipets of decreasing diameter in 500 μL of Tyrode's solution (see *Electrophysiological Recording*) and plated on the glass slide of the recording chamber. The cells were allowed to settle for 10 minutes, then were continuously perused with oxygenated Tyrode's solution for the duration of the recording (2-3 hours).

Electrophysiological recording: Whole cell patch recordings were made at room temperature under continuous perfusion with oxygenated Tyrode's solution (in mM: 150 NaCl, 3.5 KCa, 2 $CaCl_2$, 1 $MgCl_2$, 10 Hepes, 10 glucose). Borosilicate pipettes (2-4 MΩ) were filled with a $KMeSO_4$-based intracellular solution (in mM: 140 $KMeSO_4$, 8 NaCl, 10 Hepes, 0.02 EGTA, 2 Mg_2-ATP, 0.3 Na_2-GTP, and 14 Tris-creatine PO_4). The measured liquid junction potential was

+15 mV and was corrected off-line. Data were collected and analyzed using IGOR software with a MultiClamp 700B amplifier (Axon Instruments) and an ITC-16 interface (Instrutech).

Action potentials recorded in current clamp mode were filtered at 10 kHz and digitized at 40 kHz. Action potential width, rate of repolarization, afterhyperpolarization (AHP), and afterdepolarization (ADP) were calculated from the average action potential shape over a 5 s window during which the cell was made to fire at 5 ± 2 spikes/s with DC current injection. For experiments in which the action potential was measured in different drug conditions, the firing rate of the neuron was maintained at ~5 spikes/s by adjusting the level of DC current injection as needed. Cells included for analysis had action potential heights greater than 50 mV (avg = 71.8 ± 7.9 mV) and could fire spontaneously. Action potential threshold was defined as the voltage at which the rate of change exceeded 10 V/s. Action potential height was calculated as the change in voltage from threshold to the peak of the action potential. Action potential width was measured half way between action potential threshold and peak.

The rate of repolarization was measured as the greatest rate of change (minimum derivative V/s) during the falling phase of the action potential. The amplitude of the AHP was measured as the peak drop in membrane voltage (Vm) below action potential threshold. The ADP was calculated as the maximum derivative of Vm within 3 ms of action potential repolarization below threshold.

After action potentials were collected in current clamp, the amplifier was switched into voltage clamp mode. Recordings of whole cell currents were made

in voltage clamp mode with a 6 kHz filter, and digitized at 20 kHz. Whole cell capacitance was compensated through the amplifier and series resistance (R_{series}) was compensated at 70%. The average series resistance read off the dial was 9 ± 3 MΩ and cells were excluded if they had a series resistance > 20 MΩ. The capacitance was measured by integrating the area of the transient following a step from -65 mV to -95 mV with whole cell capacitance and series resistance compensation turned off.

To evaluate stability in currents during the recording, the waveform of each component current was added together and compared to the outward current measured in TTX at the beginning of the experiment at nominal +15 mV. The error between the summed wave and measured wave was calculated by dividing the integral of the summed wave by the integral of the measured wave. The average error was 2 % and cells with greater than 3% error were excluded.

Corrections for voltage errors: MVN neurons had large whole cell outward currents, often reaching 10 nA or more in response to a +15 mV command potential. The actual voltage experienced by the cell deviated from the command voltage of the amplifier by the product of the amplitude of the evoked current and the uncompensated series resistance, which averaged 2 ± 1 MΩ. In response to the highest nominal voltage command used in this study (+15 mV), the average evoked current was 10 ± 3 nA, so the actual voltage used to evoke I_{total} and I_{Kca} deviated from the command voltage by 20 ± 6 mV. As drugs were applied and currents got smaller, this voltage error got smaller; the voltage error for I_{1TEA} was 11 ± 6 mV and for I_{10TEA} and I_A was less than 5 mV. I_{total} and R_{series}

did not differ significantly between GIN and YFP-16 neurons, enabling comparison of the balance of currents in response to the same nominal (+15 mV) voltage step.

Boltzmann fits for I_{total}, I_{KCa}, and I_{1TEA} were corrected for errors in voltage due to uncompensated R_{series}, resulting in shifts of 3 mV on average in $v_{1/2}$ and 3 mV on average in the slope. The remaining currents, I_A and I_{10TEA} were small enough that the voltage error was typically less than 5 mV different from the command voltage and therefore, no corrections were made to their Boltzmann fits.

Pharmacology: GIN and YFP-16 neurons were targeted for recording using fluorescence. After formation of a gigohm seal, the cell was lifted off the bottom of the recording chamber and positioned directly in front of a small piece of tubing through which pharmacological solutions were delivered to isolate ionic current components of the TTX-insensitive current in the cell (I_{total}). Solutions were rapidly exchanged using a gravity-driven, VC-6 perfusion valve control system (Warner) and were applied in the following order:

(1) Tyrode's

(2) Tyrode's + 300 nM TTX

(3) 0 Ca^{2+} Tyrodes (Tyrode's in which 2 mM $CaCl_2$ was replaced with 1.7 mM

$MgCl_2$ and 0.3mM $CdCl_2$) + 300 nM TTX

(4) 0 Ca^{2+} Tyrode's + 300 nM TTX + 1 mM TEA

(5) 0 Ca^{2+} Tyrode's + 300 nM TTX + 10 mM TEA.

(6) In some neurons, a sixth solution was applied containing 0 Ca^{2+} Tyrode's +

300 nM TTX + 10 mM TEA + 5 mM 4-AP.

The transient Na current (I_{NaT}) was measured by subtracting the currents between solutions (1) and (2). The Ca^{2+}-dependent K^+ current (I_{KCa}) was measured as the difference current between solution (2) and (3). The 1 mM TEA-sensitive current was measured as the difference current between solution (3) and (4), and the 10mM TEA-sensitive current was measured as the difference current between solution (4) and (5). I_A was insensitive to 10 mM TEA and was isolated as the difference current inactivated by a pre-depolarizing step to -45 mV compared to a pre-hyperpolarizing step to -75 mV. This divided the 10 mM TEA-insensitive current into I_A and a small current that could not be resolved further, termed I_{other} that made up < 5% I_{total}. The A current isolated in this manner was similar in amplitude and kinetics to the 4-AP-sensitive current.

In some cells, I_{KCa} was further divided into I_{BK} and I_{SK}. In these cells, the following solutions were applied:

(1) Tyrode's

(2) Tyrode's + 300 nM TTX

(3/4) Tyrode's + 120 nM IBTX

(3/4) Tyrode's + 100 nM apamin

(5) 0 Ca^{2+} Tyrode's + 300 nM TTX.

IBTX was slower to block current compared to other drugs used in this study, so IBTX was applied to the cell for ~2 min while looping the voltage

protocol 3 times. The current remaining during the last voltage protocol was subtracted from I_{total} measured in TTX to calculate I_{BK}. A similar protocol was used to measure I_{SK}. In some cells, both IBTX and apamin were applied. In all of these cells, 0.3 mM $CdCl_2$ blocked outward current that had not been previously blocked by IBTX or apamin.

The solutions for measuring Ca^{2+} currents were adapted from Swensen and Bean, 2005. The solution consisted of (in mM): 50 NaCl, 3.5 KCl, 2 $CaCl_2$, 1 $MgCl_2$, 10 Hepes, 100 TEA-Cl, 300 nM TTX, 10 glucose + 5 4-AP, and 100 nM apamin. Ca^{2+} currents were isolated by subtraction following application of a similar solution in which 2 mM $CaCl_2$ was replaced by 2 mM $MgCl_2$.

TTX, and IBTX were purchased from Tocris. TEA, $CdCl_2$, 4-AP, and apamin were from Sigma. Stock solutions were diluted in water and stored at 4ºC, except 4-AP, IBTX, and apamin which were stored at -20ºC.

Calculations and statistics: To control for the different soma sizes of MVN neurons, current magnitudes were compared across cells in terms of current density. Current density was calculated by dividing the current amplitude (pA) by the cell capacitance (pF).

Because the data was not normally distributed, statistical differences were tested with the non-parametric Wilcoxon test for unpaired data with the exception of changes in action potential shape following $CdCl_2$ or 1 mM TEA application where a Wilcoxon test for paired data was used. The strength of a correlation was measured with the Pearson correlation (r) and was tested for significance against

the critical values on a two-tailed test. Errors reported in text are standard deviations.

Results

Firing properties of dissociated MVN neurons

Acutely dissociated MVN neurons were isolated from mice, age 24-39 days-old (average = 29 ± 4 d). At this age, the intrinsic firing dynamics of MVN neurons are mature (Dutia et al. 1995; Johnston and Dutia 1996; Murphy and Du Lac 2001). Soma sizes ranged from 15-30 μm along the long axis, with short, proximal processes (<30 μm) (Fig. 1A). The neurons had an average input resistance (R_{input}) of 1662 ± 602 MΩ and capacitance of 7.9 ± 2.3 pF (n = 129).

Dissociated MVN neurons exhibited intrinsic pacemaking capabilities and fired regular, spontaneous action potentials (Fig. 1B & C). All recordings were done at room temperature because recordings from dissociated cells were unstable at more physiological temperatures. Compared to neurons recorded from slice at room temperature, dissociated MVN neurons had taller action potentials (71.8 ± 7.9 mV vs. 68.4 ± 7.4 mV; $p = 0.008$), wider action potentials (0.80 ± 0.19 ms, n = 124 vs. 0.64 ± 0.26 ms, n = 72; $p < 0.0001$) and more hyperpolarization between action potentials, measured as deeper afterhyperpolarizations (AHPs) (33.6 ± 4.5 mV, n = 124 vs. 22.5 ± 3.1 mV, n = 50; $p < 0.0001$), suggesting that these properties are influenced by dendritic conductances which are absent in the dissociated preparation. Despite these differences, dissociated MVN neurons

exhibited similar spontaneous firing rates (12 ± 6 spikes/s, n = 129) as neurons in slice (13 ± 9 spikes/s, n = 32; p = 0.86).

To specifically target different cell types in this study, recordings were made from fluorescently labeled neurons from GIN (Oliva et al. 2000) and YFP-16 lines of transgenic mice (Feng et al. 2000), which in the MVN label GABAergic and non-GABAergic neurons, respectively (Bagnall et al. 2007) YFP-16 and GIN neurons fired spontaneous action potentials, with YFP-16 neurons exhibiting somewhat higher firing rates than GIN neurons (Table 1). R_{input}, capacitance, and R_{series} did not differ significantly between GIN and YFP-16 neurons, indicating that cell size and recording quality were equivalent (Table 1).

Action potentials were similar in the two cell types but tended to be faster in YFP-16 than in GIN neurons. Examples of action potentials from dissociated GIN and YFP-16 neurons are shown in Fig. 1D. In both cell types, the action potential is followed by an afterhyperpolarization (AHP), which was smaller on average in YFP-16 neurons (Table 1). The trajectory of the interspike membrane potential varied considerably across neurons (Fig. 1D). An afterdepolarization (ADP) that separated the AHP into two components was apparent in some neurons of both types but was larger on average in YFP-16 neurons (Table 1). The parameter that best distinguished the two populations was action potential width, which was significantly narrower in YFP-16 vs. GIN neurons as a consequence of faster rise and fall rates (Table 1). As is evident in Fig. 1E, action potential width and the magnitude of the AHP vary continuously across MVN

neurons, with YFP-16 neurons tending to populate one end of the spectrum and GIN neurons tending to populate the other, but with no clean division between the two populations. Variations in action potential parameters observed in YFP-16 and GIN neurons spanned the range of those observed in unidentified neurons, confirming that the population of MVN neurons is well represented by neurons recorded in the two transgenic mouse lines (Bagnall et al. 2007).

Inward and outward whole cell currents

The preservation of the intrinsic differences in action potentials between GIN and YFP-16 neurons in the dissociated preparation implies differences in the underlying somatic currents. To identify these differences, whole cell somatic currents were elicited from dissociated neurons with 150 ms voltage steps from -55 to +15 mV from a holding potential of -65 mV, and pharmacology was used to isolate multiple currents within each neuron.

The transient Na current (I_{NaT}) was defined as the large, fast inward current isolated by subtraction after application of 300 nM TTX (Fig. 2A). The voltage at which I_{NaT} reached its peak varied across cells, but tended to occur between -45 and -35 mV and was not significantly different between GIN (-36 ± 8.9 mV, n = 35) and YFP-16 neurons (-36 ± 8.8 mV, n = 39). Although I_{NaT} density, measured at -35 mV, tended to be larger in YFP-16 neurons, this difference was not significant, $p = 0.10$ (Fig. 2B).

The 'total outward' current (I_{total}) refers to the combination of currents that were insensitive to 300 nM TTX (Fig. 2C). Although I_{total} includes small inward

currents through Ca^{2+} channels, I_{Ca} density was only 35.4 ± 7.2 pA/pF in GIN neurons (n = 9) and 33.0 ± 11.5 pA/pF in YFP-16 neurons (n = 5), about 1/40 the size of I_{total}, suggesting that the majority of I_{total} was the result of outward current through K^+ channels. Therefore, I_{total} was a reasonable estimate of the total TTX-insensitive K^+ current in the cell.

I_{total} had a similar time course between GIN and YFP-16 neurons and a similar rate of activation, calculated as the peak derivative over the rising phase of the current (GIN = 6090 ± 2553 pA/ms, n = 19; YFP-16 = 6640 ± 2728 pA/ms, n = 20). The density of I_{total} varied by > 2.5-fold across cells but did not differ significantly between GIN and YFP-16 neurons, p = 0.29 (Fig. 2D). The voltage-dependence of I_{total} was measured by its voltage of half maximal activation ($v_{1/2}$) and the steepness of its voltage-dependence (k), measured by fitting the normalized conductance graph with a Boltzmann fit. The $v_{1/2}$ and slope (k) values of I_{total} in GIN and YFP-16 neurons were similar (Table 2), suggesting that differences in firing properties between the two cell types arise from differences either in specific current subtypes or in the balance of currents.

Ca^{2+}-dependent K^+ currents

The Ca^{2+}-dependent K^+ current (I_{KCa}) was measured by subtraction after replacing extracellular Ca^{2+} with a mixture of Mg^{2+} (1.7 mM) and Cd^{2+} (0.3 mM). I_{KCa} varied in timecourse and magnitude across the population of recorded neurons. In most neurons, I_{KCa} had a prominent transient component that decayed within the first 10 ms, revealing a steady-state sustained component (Fig. $3A_1$).

The rate of activation of I_{KCa}, described as the maximum derivative during the rising phase of the current was not different between the cell types (3541± 1825 pA/ms (GIN) vs. 3030 ± 1240 pA/ms (YFP-16), p = 0.38). Although both components of I_{KCa} tended to be larger in GIN neurons, the current density was not significantly different between cell types (Fig. 3B-C).

At least two types of currents contribute to I_{Kca} in MVN neurons: BK and SK (Smith et al. 2002); (du Lac 1996; Johnston et al. 1994). These currents can be distinguished using the specific blockers, iberiotoxin (IBTX) for BK currents, and apamin for SK currents (Coetzee et al. 1999; Smith et al. 2002). BK currents displayed the same time course as I_{KCa}, with a fast transient and slower sustained component (Fig. $3A_2$). SK currents were smaller and did not inactivate during the 150 ms step (Fig. $3A_3$).

The relative contribution of I_{BK} and I_{SK} to I_{KCa} varied considerably across neurons but did not differ between GIN and YFP-16 neurons. In GIN neurons, 63 ± 18 % of I_{KCa} was sensitive to IBTX and 11 ± 14 % was sensitive to apamin; in YFP-16 neurons, 62 ± 15% of I_{KCa} was sensitive to IBTX and 20 ± 23% was sensitive to apamin (Fig. 3D). Although over half of I_{KCa} in MVN neurons tended to be IBTX-sensitive, this proportion ranged from 38-85% in GIN neurons and from 34-73% in YFP-16 neurons. This high variability could reflect differences in channel expression or in the relative insensitivity to IBTX conferred by some BK channel ß-subunits (Brenner et al. 2005; Meera et al. 2000). The remaining Ca^{2+}-sensitive K^+ current could reflect a combination of BK and SK insensitive to IBTX and apamin (Brenner et al. 2005; Coetzee et al. 1999; Meera et al. 2000)

but suggests there is likely to be a third type of I_{KCa} in MVN neurons, as has been described in other cell types (Joiner et al. 1998; Limon et al. 2005; Sah and Faber 2002; Vergara et al. 1998). Taken together, these results suggest that BK is the dominant somatic current that contributes to I_{KCa} in MVN neurons.

Boltzmann fits revealed differences in the gating properties of I_{KCa} current between GIN and YFP-16 neurons. The $v_{1/2}$ was more hyperpolarized in YFP-16 neurons than GIN neurons ($p = 0.006$) and showed a steeper voltage dependence compared to GIN neurons ($p = 0.0002$) (Table 2). This could reflect differences in the channel subunits contributing to I_{KCa} or differences in Ca^{2+} currents. Since the Ca^{2+} concentration influences the probability of opening of BK and SK channels, the voltage-dependent properties of I_{KCa} should be related to the voltage-dependence of I_{Ca}. The Ca^{2+} current reached its peak voltage at -15 mV in 3/5 YFP-16 neurons and at -5 mV in 7/9 GIN neurons, consistent with the lower $v_{1/2}$ of YFP-16 neurons compared to that of GIN neurons.

TEA-sensitive K^+ currents

A subset of K^+ currents can be identified based on their high sensitivity to tetraethylammonium (TEA, 1 mM) , including BK-, Kv1-, and Kv3-currents (Coetzee et al. 1999). In dissociated MVN neurons, in the presence of $CdCl_2$ (which blocks I_{BK}), 1 mM TEA blocked a non-inactivating current with a depolarized $v_{1/2}$ that activated between -25 and -15 mV (Fig. 4B, Table 2). In 14/14 cells, this current was insensitive to 50 nM dendrotoxin, a specific blocker of non-inactivating, Kv1-containing channels (Gamkrelidze et al. 1998; Grissmer

et al. 1994; Khavandgar et al. 2005). Based on its voltage-dependence and pharmacology, the 1 mM TEA-sensitive current in MVN neurons likely represents current through Kv3-containing channels (Coetzee et al. 1999).

In most cells, I_{1TEA} did not inactivate during the 150 ms step (Fig. 4A), but its rate of activation was faster in YFP-16 neurons, $p = 0.01$ (Fig. 4D). In 2/20 YFP-16 neurons, an additional I_{1TEA} component was seen that activated rapidly, then decayed within the first 50 ms, similar to the kinetics observed for Kv3.4-containing channels (Baranauskas et al. 2003). The density of the sustained component of I_{1TEA} was greater in YFP-16 than GIN neurons, $p = 0.04$ (Fig. 4C). Despite these differences in the activation rate, neither the $v_{1/2}$ or k values of I_{1TEA} differed in YFP-16 vs. GIN neurons, indicating that the current had similar voltage-dependent properties in both cell types (Table 2).

The second component of the delayed rectifier current in MVN neurons was measured by subtraction following application of 10 mM TEA (I_{10TEA}) (Fig. 4E). YFP-16 neurons expressed a greater density of I_{10TEA} than GIN neurons, $p = 0.05$ (Fig. 4F), but the current did not exhibit different activation rates (351 ± 189 pA/ms, n = 20, YFP-16 vs. 283 ± 167 pA/ms, n = 19, GIN) or different voltage dependences (Table 2) between the cell types. The depolarized activation voltage of I_{10TEA} (between -25 and -15 mV) and depolarized $v_{1/2}$ are consistent with values reported for Kv2-containing channels (Coetzee et al. 1999; Kerschensteiner and Stocker 1999; Murakoshi et al. 1997; Murakoshi and Trimmer 1999).

TEA-insensitive K^+ currents

The remaining current in MVN neurons was insensitive to 0.3 mM $CdCl_2$ and 10 mM TEA. A portion of this current inactivated rapidly upon depolarization, was blocked by 5 mM 4-AP (n = 25), and had the classic fast inactivation kinetics of an A current (I_A). Because of the unique voltage-dependent properties of I_A, it was possible to isolate the current without pharmacology. I_A was maximally activated with a 500 ms pre-hyperpolarizing step to -75 mV then inactivated with a pre-depolarizing step to -45 mV. The current obtained by subtraction between these two protocols was I_A (Fig. 5A) and the remaining current, not blocked by depolarization to -45 mV, was referred to as I_{other}.

I_A density did not differ significantly between GIN and YFP-16 neurons, p = 0.25 (Fig. 5B) and there were no differences in its activation kinetics (234 ± 144 pA/ms, GIN vs. 282 ± 132 pA/ms YFP-16), p = 0.12, inactivation kinetics (18.5 ± 2.8 ms, n = 18, GIN vs. 16.3 ± 3.8 ms, n = 19, YFP-16), p = 0.07, or voltage dependence (Table 2) between the cell types.

I_{other} was insensitive to $CdCl_2$, TEA, 4-AP, did not inactivate upon depolarization and contributed about 5% to I_{total} (Fig. 5C-D). The expression of this current was not significantly different between GIN and YFP-16 neurons, p = 0.22, and given its small size and lack of specific identification, it was not analyzed further in this study

Balance of outward currents differs between GIN and YFP-16 neurons

GIN and YFP-16 neurons express the same outward currents yet exhibit different action potential and firing properties. The analyses thus far have only considered the absolute levels of current density expression and demonstrate that YFP-16 neurons express more I_{1TEA} and I_{10TEA} than GIN neurons. However, these analyses do not address the relative expression levels of currents within neurons, which might better distinguish cell types than the absolute expression level of any individual current.

To determine whether the relative expression levels of outward currents differed between GIN and YFP-16 neurons, the ratios of I_{KCa}, I_{1TEA}, I_{10TEA}, and I_A were compared across the two populations. The balance of currents in each neuron was quantified by normalizing each isolated outward current by I_{total}, obtained at nominal +15 mV (see Methods). Currents were quantified using the integral rather than the peak over the first 30 ms, to compare currents with different time courses. Qualitatively similar results were also observed over the first 10 ms and the first 50 ms.

The balance of currents varied considerably within and between cell types (Fig. 6). Overall, I_{KCa} and I_{1TEA} dominated, however some neurons had a prominent contribution from I_A. I_{10TEA} was a small fraction of I_{total} in all neurons. Although there was a high degree of variability, the expression pattern of currents differed significantly in GIN neurons compared to YFP-16 neurons. GIN neurons had proportionately more I_{KCa} ($p = 0.006$) and I_A ($p = 0.03$) while YFP-16 neurons had proportionately more I_{1TEA} ($p = 0.004$) and I_{10TEA} ($p = 0.04$) (Fig.

6A). GIN and YFP-16 neurons were best distinguished by the ratio of I_{KCa} : I_{1TEA}. In 84% (16/19) of GIN neurons, the I_{KCa} : I_{1TEA} ratio was greater than 1.6 (0.55-3.6, avg. = 2.3 ± 0.9) and in 86% (18/21) of YFP-16 neurons, the I_{KCa} : I_{1TEA} ratio was less than 1.6 (0.07-4.1, avg. = 1.2 ± 1.0).

The differences in the balance of currents across cells likely stems from correlated current expression, as evidenced by correlations in the charge densities of several pairs of currents. The strongest correlations were between I_{KCa} and I_A in YFP-16 neurons (Fig. 7A) and between I_{1TEA} and I_{10TEA} in GIN neurons (Fig. 7B). Weaker correlations were also observed for I_{KCa} and I_A in GIN neurons and I_{1TEA} and I_{10TEA} in YFP-16 neurons (Fig. 7A-B). Correlations in GIN but not YFP-16 neurons were also observed between I_{KCa} and I_{1TEA} (Fig. 7C) and between I_{KCa} and I_{10TEA} (Fig. 7D). These results suggest that although the density of current varies across MVN neurons, currents are coregulated to achieve a target balance.

Density and kinetics of I_{1TEA} underlie differences in the rate of action potential repolarization

How does the differential balance of currents in GIN vs. YFP-16 neurons relate to differences in action potential and firing properties of these two cell classes? The AHP in MVN neurons influences firing response gain and depends predominantly on Ca^{2+}-dependent K^+ currents (Johnston et al. 1994; Smith et al. 2002) (Fig. 9A & B) , with additional contributions from 4-AP and TEA-sensitive currents (Johnston et al. 1994). The relatively larger contribution of I_{KCa} and I_A to

outward currents in GIN vs. YFP-16 neurons is consistent with relatively larger AHP in GIN neurons. Across individual neurons, however, neither the amplitude nor density of I_{KCa} (or any of the other outward current measured in this study) correlated with the magnitude or integral of the AHP (data not shown). The lack of correlations with individual outward currents are consistent with the AHP waveform depending on voltage dependent interactions of multiple currents, including potentially critical contributions from sodium currents (Akemann and Knopfel 2006; Swensen and Bean 2005).

The predominant differences between action potentials in GIN and YFP-16 neurons are in the rates of rise and repolarization (Table 1), which are correlated in both cell types (GIN: $r^2 = 0.72$, $p<0.0001$, $n=35$; YFP-16: $r^2 = 0.5$, $p<0.0001$, $n=39$) and underlie differences in the ability of YFP-16 and GIN neurons to sustain high firing rates (Bagnall et al. 2007). The current that differed most between GIN and YFP-16 neurons was I_{1TEA}, likely corresponding to current through Kv3-type channels which promote fast firing in neurons in other parts of the brain (Rudy and McBain 2001). In MVN neurons, the peak rate of rise of I_{1TEA} (in response to +15 mV step) correlated with action potential repolarization rates in both GIN ($r^2 = 0.85$) and YFP-16 neurons ($r^2 = 0.28$) (Fig. 8). These data indicate that variations in I_{1TEA} currents may account for differences in action potential repolarization rate both within and between cell types.

To directly test the contributions of potassium currents to action potentials, neurons were allowed to fire in current clamp and action potentials

were compared in control solution and in the presence of pharmacological blockers of the two dominant currents, I_{KCa} and I_{1TEA}. As exemplified in Figs. 9A and B, blocking I_{KCa} with $CdCl_2$ (0.3 mM) had no effect on the width of the action potential or rate of repolarization (Fig. 9C) but significantly reduced the magnitude of the AHP in both GIN (by 7.2 ± 2.8 mV; n = 7; p = 0.004) and YFP-16 neurons (by 6.7 ± 2.2 mV; n = 7; p = 0.008). In contrast, blockade of I_{1TEA} with 1mM TEA broadened the action potential, increasing action potential width in both GIN (by 0.5 ± 0.3 ms, n = 7; p = 0.03) and YFP-16 neurons (by 0.4 ± 0.2, n = 7; p = 0.008). The increase in action potential width was due specifically to slower repolarization (Fig. 9D), as TEA had no effect on action potential rise rates (Fig. 9F). Interestingly, the effects of TEA on repolarization rate were well correlated with initial repolarization rate (Fig. 9E). Furthermore, 1 mM TEA abolished the differences in repolarization rates of YFP-16 and GIN neurons (p = 0.26). Taken together, these results demonstrate that differences in density and kinetics of I_{1TEA} account for differences in repolarization rates between GIN and YFP-16 neurons, and that I_{1TEA} affects repolarization rates in a graded manner across MVN neurons.

Discussion

In this study, recordings from dissociated vestibular nucleus neurons from transgenic mouse lines indicate that heterogeneity in the firing properties of MVN neurons reflects variations in the balance of potassium currents. GABAergic neurons recorded in GIN mice tended to have wider action potentials, deeper

AHPs, and lower spontaneous firing rates than did non-GABAergic neurons recorded in YFP-16 mice. GABAergic and non-GABAergic neurons expressed the same four major potassium currents, but GABAergic neurons expressed relatively more I_{KCa} and I_A and relatively less I_{1TEA} and I_{10TEA} than non-did GABAergic neurons. Variations in the expression of $I_{1TEA,}$ which likely corresponds to current carried through Kv3 channels, accounted for differences in action potential repolarization rates both within and between the two classes of neurons. Shifts in the balance of currents in vestibular nucleus neurons could mediate activity-dependent changes in intrinsic excitability which have been observed in response to acute synaptic inhibition (Nelson et al. 2003) or after loss of peripheral vestibular function (Beraneck et al. 2003; Beraneck et al. 2004; Cameron and Dutia 1997; Guilding and Dutia 2005; Him and Dutia 2001).

Intrinsic firing properties are preserved in dissociated MVN neurons

Although acutely dissociated MVN neurons had slower action potential kinetics and deeper AHPs than those recorded in slice at room temperature (Bagnall et al. 2007) differences in spontaneous firing rates and action potential waveforms observed in slice between GIN and YFP-16 neurons were largely preserved in the dissociated preparation. Together with the observation that YFP-16 neurons have more dendrites and lower input resistances than GIN neurons in slice (Bagnall et al. 2007) but not in dissociated neurons, these results indicate that dendritic currents contribute to action potential repolarization, but that the predominant currents underlying the differences in the firing properties of GIN

and YFP-16 MVN neurons are located on the soma and proximal processes (and are not greatly altered by enzymatic or mechanical stress during the dissociation processes). In support of this, the voltage-dependence of the currents, measured by the $v_{1/2}$ and slopes of the Boltzmann fits were within the range of reported values for each current, with the exception of I_A whose voltage of activation and $v_{1/2}$ was slightly depolarized compared to more commonly reported values (Bekkers 2000; Molineux et al. 2005; Sacco and Tempia 2002; Song et al. 1998) but see also (Martina et al. 1998). This could reflect the presence of $CdCl_2$ in the perfusion solution, which has been shown to shift the voltage-dependence of I_A (Song et al. 1998).

Variations in I_{1TEA} density and kinetics underlie differences in action potential repolarization rates

A previous model of firing mechanisms in MVN neurons indicated that differences between action potential waveforms across neurons could be attributed predominantly to differences in the kinetics of a fast voltage-gated K^+ current (Quadroni and Knopfel 1994). Consistent with the predictions of this model, YFP-16 neurons expressed more I_{1TEA} and I_{10TEA} than did GIN neurons. Variations in I_{1TEA} accounted entirely for differences in action potential repolarization rates between and within cell types. Based on its depolarized voltage of activation, Boltzmann parameters, and insensitivity to $CdCl_2$ and dendrotoxin, the 1 mM TEA-sensitive current in MVN neurons likely flows through Kv3-containing channels.

Kv3 currents are expressed in neurons specialized for high frequency firing (Akemann and Knopfel 2006; Erisir et al. 1999; Hernandez-Pineda et al. 1999; Martina et al. 1998; Massengill et al. 1997; McDonald and Mascagni 2006; McKay and Turner 2004; Perney et al. 1992; Rudy and McBain 2001; Song et al. 2005; Weiser et al. 1995) and their voltage-dependence and fast decay kinetics are precisely tuned to facilitate the rapid repolarization of action potentials (Erisir et al. 1999; Raman and Bean 1999). In the cortex, the presence of I_{Kv3} distinguishes fast-spiking GABAergic interneurons from excitatory pyramidal cells (Martina et al. 1998; Massengill et al. 1997). In the cerebellar and vestibular nuclei, in contrast, both GABAergic and non-GABAergic neurons are capable of sustaining very fast firing rates (Bagnall et al. 2007; Uusisaari et al. 2007), indicating a role for Kv3 in both cell types in these nuclei. Each of the 4 major Kv3 family subunits are expressed in MVN neurons (Weiser et al. 1995; Weiser et al. 1994). Differences in kinetics across MVN neurons might arise from the expression of different subunits (Baranauskas et al. 2003; Lewis et al. 2004; McCrossan et al. 2003; Murakoshi et al. 1997; Murakoshi and Trimmer 1999),regulation of mRNA transcript levels (Schulz et al. 2006), or different phosphorylation states (Song et al. 2005).

Although I_{Kca}, was expressed strongly in MVN neurons and exhibited rapid activation during voltage steps, action potential repolarization was dominated by $I_{1TEA.}$ Results from MVN neuronal recordings in brain slices similarly indicate a prominent role for I_{Kca} in generation of the AHP but not in action potential repolarization (Smith et al. 2002). Analysis of currents

regulating burst firing in Purkinje neurons showed that calcium influx occurs during the falling phase of the action potential, and that the peak of I_{KCa} is delayed compared to the peak of TEA-sensitive repolarizing currents (Swensen and Bean 2003), consistent with pharmacological results in MVN neurons. Thus, although voltage step protocols can provide valuable information about current expression levels, assessing how specific currents interact to shape neuronal excitability is facilitated by the use of more natural stimuli, such as action potential waveforms (Raman and Bean 1999; Swensen and Bean 2003).

Coregulation of currents in MVN neurons

Given that firing properties are shaped by a the interplay of intrinsic currents, neurons must be able to actively monitor and adjust the balance of currents accordingly. In support of such a mechanism in MVN neurons, correlations were observed in charge densities of several currents. In both GIN and YFP-16 neurons, significant positive correlations existed between I_{1TEA} and I_{10TEA} and between I_{KCa} and I_A. Additional correlations between I_{KCa} and I_{1TEA} and between I_{KCa} and I_{10TEA} were observed in GIN neurons but not in YFP-16 neurons. These data suggest that outward currents are functionally coregulated in MVN neurons but that the rules for this coregulation differ across cell types.

Non-inactivating Na^+ currents are likely to play a prominent role in shaping the firing properties of MVN neurons, as is the case for cerebellar neurons (Khaliq et al. 2003; Raman and Bean 1997; Raman et al. 2000). Although no correlations were observed in MVN neurons between transient I_{NaT}

and I_{1TEA} kinetics or densities, action potential rise and fall rates were well-matched (Fig. 9D), suggesting an interaction between Na^+ and K^+ currents that might only be revealed during natural spiking behavior (Akemann and Knopfel 2006; Swensen and Bean 2005). Coregulation of Na^+ and K^+ currents have been observed in neurons of the electric fish, where the kinetics of the currents co-vary as a function of the neuronal output properties (McAnelly and Zakon 2000). Coregulation of currents might occur at the transcriptional level (MacLean et al. 2005; Schulz et al. 2006), by post-translational modifications (Park et al. 2006; Song et al. 2005) or by functional interactions via voltage dependence of the currents themselves (Akemann and Knopfel 2006; Swensen and Bean 2005).

Implications for plasticity

MVN neurons express a novel form of intrinsic plasticity, termed firing rate potentiation (FRP), which produces increases in spontaneous and evoked firing rates via decreases in the AHP (Nelson et al. 2003). FRP is accompanied by a decreased sensitivity to IBTX and is occluded by blockade of CaMKII, which reduces BK currents (Nelson et al. 2005). Most neurons in the MVN have the capacity to express FRP, but its expression varies across neurons (Nelson et al. 2005; Nelson et al. 2003). This finding is better understood in light of the variability of I_{KCa} expression across the population of MVN neurons. The presence of other currents, such as I_A, might compensate functionally for the loss of BK currents in some neurons.

The finding that GABAergic and non-GABAergic neurons possess the same major outward currents is significant because it suggest that both cell types express currents required for a broad range of firing properties. Long-term changes in the ratio of 'Type A' and 'Type B' neurons in the MVN, which appear to correspond to GIN and YFP-16 neurons in slice, respectively (Bagnall et al. 2007), have been reported during recovery from unilateral labyrinthectomy (Beraneck et al. 2003; Beraneck et al. 2004). The data from the present study would suggest that a GIN neuron with a 'Type A' action potential shape could adopt a 'Type B' action potential shape if there were a shift in the I_{KCa} : I_{1TEA} ratio, induced either by a down-regulation of BK currents, which occurs during FRP, or an increase in the kinetics or expression of I_{1TEA}. Rapid shifts in the balance of currents, and by extension in firing properties, could be induced by phosphorylation-dependent changes in current kinetics or channel conductances, as has been shown for each of the predominant potassium currents expressed in MVN neurons (Jerng et al. 2004; Koh et al. 1999; Liu and Kaczmarek 1998; Nelson et al. 2005; Park et al. 2006; Sansom et al. 2000; Sergeant et al. 2005; Smith et al. 2002; Song et al. 2005). Regulation of the firing properties of neurons on a fast time scale might be especially important in systems with high levels of activity, such as the vestibular system in which neurons fire at rates of hundreds of action potentials/s *in vivo*. Activity-dependent shifts in the balance of currents would provide rapid, online regulation of firing properties, maintaining the balance of activity across the network.

Acknowledgments

Chapter 3 is a reprint of the material as it appears in Gittis AH, du Lac S. J Neurophysiol. 2007 Firing properties of GABAergic versus non-GABAergic vestibular nucleus neurons conferred by a differential balance of potassium currents. Jun;97(6):3986-96. It is included with the permission of all the authors on the final publication.

References

Akemann W, and Knopfel T. Interaction of Kv3 potassium channels and resurgent sodium current influences the rate of spontaneous firing of Purkinje neurons. *J Neurosci* 26: 4602-4612, 2006.

Bagnall MW, Stevens RJ, and du Lac S. Transgenic mouse lines subdivide medial vestibular nucleus neurons into discrete, neurochemically distinct populations. *J Neurosci* 27: 2318-2330, 2007.

Baranauskas G, Tkatch T, Nagata K, Yeh JZ, and Surmeier DJ. Kv3.4 subunits enhance the repolarizing efficiency of Kv3.1 channels in fast-spiking neurons. *Nat Neurosci* 6: 258-266, 2003.

Bekkers JM. Properties of voltage-gated potassium currents in nucleated patches from large layer 5 cortical pyramidal neurons of the rat. *J Physiol* 525 Pt 3: 593-609, 2000.

Beraneck M, Hachemaoui M, Idoux E, Ris L, Uno A, Godaux E, Vidal PP, Moore LE, and Vibert N. Long-term plasticity of ipsilesional medial vestibular nucleus neurons after unilateral labyrinthectomy. *Journal of neurophysiology* 90: 184-203, 2003.

Beraneck M, Idoux E, Uno A, Vidal PP, Moore LE, and Vibert N. Unilateral labyrinthectomy modifies the membrane properties of contralesional vestibular neurons. *Journal of neurophysiology* 92: 1668-1684, 2004.

Brenner R, Chen QH, Vilaythong A, Toney GM, Noebels JL, and Aldrich RW. BK channel beta4 subunit reduces dentate gyrus excitability and protects against temporal lobe seizures. *Nat Neurosci* 8: 1752-1759, 2005.

Cameron SA, and Dutia MB. Cellular basis of vestibular compensation: changes in intrinsic excitability of MVN neurones. *Neuroreport* 8: 2595-2599, 1997.

Coetzee WA, Amarillo Y, Chiu J, Chow A, Lau D, McCormack T, Moreno H, Nadal MS, Ozaita A, Pountney D, Saganich M, Vega-Saenz de Miera E, and Rudy B. Molecular diversity of K+ channels. *Ann N Y Acad Sci* 868: 233-285, 1999.

du Lac S. Candidate cellular mechanisms of vestibulo-ocular reflex plasticity. *Ann N Y Acad Sci* 781: 489-498, 1996.

du Lac S, Raymond JL, Sejnowski TJ, and Lisberger SG. Learning and memory in the vestibulo-ocular reflex. *Annu Rev Neurosci* 18: 409-441, 1995.

Dutia MB, Lotto RB, and Johnston AR. Post-natal development of tonic activity and membrane excitability in mouse medial vestibular nucleus neurones. *Acta Otolaryngol Suppl* 520 Pt 1: 101-104, 1995.

Erisir A, Lau D, Rudy B, and Leonard CS. Function of specific K(+) channels in sustained high-frequency firing of fast-spiking neocortical interneurons. *Journal of neurophysiology* 82: 2476-2489, 1999.

Feng G, Mellor RH, Bernstein M, Keller-Peck C, Nguyen QT, Wallace M, Nerbonne JM, Lichtman JW, and Sanes JR. Imaging neuronal subsets in transgenic mice expressing multiple spectral variants of GFP. *Neuron* 28: 41-51, 2000.

Gamkrelidze G, Giaume C, and Peusner KD. The differential expression of low-threshold sustained potassium current contributes to the distinct firing patterns in embryonic central vestibular neurons. *J Neurosci* 18: 1449-1464, 1998.

Grissmer S, Nguyen AN, Aiyar J, Hanson DC, Mather RJ, Gutman GA, Karmilowicz MJ, Auperin DD, and Chandy KG. Pharmacological characterization of five cloned voltage-gated K+ channels, types Kv1.1, 1.2, 1.3, 1.5, and 3.1, stably expressed in mammalian cell lines. *Mol Pharmacol* 45: 1227-1234, 1994.

Guilding C, and Dutia MB. Early and late changes in vestibular neuronal excitability after deafferentation. *Neuroreport* 16: 1415-1418, 2005.

Hernandez-Pineda R, Chow A, Amarillo Y, Moreno H, Saganich M, Vega-Saenz de Miera EC, Hernandez-Cruz A, and Rudy B. Kv3.1-Kv3.2 channels underlie a high-voltage-activating component of the delayed rectifier K+ current in projecting neurons from the globus pallidus. *Journal of neurophysiology* 82: 1512-1528, 1999.

Him A, and Dutia MB. Intrinsic excitability changes in vestibular nucleus neurons after unilateral deafferentation. *Brain Res* 908: 58-66, 2001.

Jerng HH, Pfaffinger PJ, and Covarrubias M. Molecular physiology and modulation of somatodendritic A-type potassium channels. *Mol Cell Neurosci* 27: 343-369, 2004.

Johnston AR, and Dutia MB. Postnatal development of spontaneous tonic activity in mouse medial vestibular nucleus neurones. *Neurosci Lett* 219: 17-20, 1996.

Johnston AR, MacLeod NK, and Dutia MB. Ionic conductances contributing to spike repolarization and after-potentials in rat medial vestibular nucleus neurones. *J Physiol* 481 (Pt 1): 61-77, 1994.

Joiner WJ, Tang MD, Wang LY, Dworetzky SI, Boissard CG, Gan L, Gribkoff VK, and Kaczmarek LK. Formation of intermediate-conductance calcium-activated potassium channels by interaction of Slack and Slo subunits. *Nat Neurosci* 1: 462-469, 1998.

Kerschensteiner D, and Stocker M. Heteromeric assembly of Kv2.1 with Kv9.3: effect on the state dependence of inactivation. *Biophys J* 77: 248-257, 1999.

Khaliq ZM, Gouwens NW, and Raman IM. The contribution of resurgent sodium current to high-frequency firing in Purkinje neurons: an experimental and modeling study. *J Neurosci* 23: 4899-4912, 2003.

Khavandgar S, Walter JT, Sageser K, and Khodakhah K. Kv1 channels selectively
prevent dendritic hyperexcitability in rat Purkinje cells. *J Physiol* 569: 545-557, 2005.

Koh SD, Perrino BA, Hatton WJ, Kenyon JL, and Sanders KM. Novel regulation of the A-type K+ current in murine proximal colon by calcium-calmodulin-dependent protein kinase II. *J Physiol* 517 (Pt 1): 75-84, 1999.

Lewis A, McCrossan ZA, and Abbott GW. MinK, MiRP1, and MiRP2 diversify Kv3.1 and Kv3.2 potassium channel gating. *J Biol Chem* 279: 7884-7892, 2004.

Limon A, Perez C, Vega R, and Soto E. Ca2+-activated K+-current density is correlated with soma size in rat vestibular-afferent neurons in culture. *Journal of neurophysiology* 94: 3751-3761, 2005.

Liu SJ, and Kaczmarek LK. The expression of two splice variants of the Kv3.1 potassium channel gene is regulated by different signaling pathways. *J Neurosci* 18: 2881-2890, 1998.

MacLean JN, Zhang Y, Goeritz ML, Casey R, Oliva R, Guckenheimer J, and Harris-Warrick RM. Activity-independent coregulation of IA and Ih in rhythmically active neurons. *Journal of neurophysiology* 94: 3601-3617, 2005.

Mainen ZF, and Sejnowski TJ. Influence of dendritic structure on firing pattern in model neocortical neurons. *Nature* 382: 363-366, 1996.

Martina M, Schultz JH, Ehmke H, Monyer H, and Jonas P. Functional and molecular differences between voltage-gated K+ channels of fast-spiking interneurons and pyramidal neurons of rat hippocampus. *J Neurosci* 18: 8111-8125, 1998.

Massengill JL, Smith MA, Son DI, and O'Dowd DK. Differential expression of K4-AP currents and Kv3.1 potassium channel transcripts in cortical neurons that develop distinct firing phenotypes. *J Neurosci* 17: 3136-3147, 1997.

McAnelly ML, and Zakon HH. Coregulation of voltage-dependent kinetics of Na(+) and K(+) currents in electric organ. *J Neurosci* 20: 3408-3414, 2000.

McCrossan ZA, Lewis A, Panaghie G, Jordan PN, Christini DJ, Lerner DJ, and Abbott GW. MinK-related peptide 2 modulates Kv2.1 and Kv3.1 potassium channels in mammalian brain. *J Neurosci* 23: 8077-8091, 2003.

McDonald AJ, and Mascagni F. Differential expression of Kv3.1b and Kv3.2 potassium channel subunits in interneurons of the basolateral amygdala. *Neuroscience* 138: 537-547, 2006.

McKay BE, and Turner RW. Kv3 K+ channels enable burst output in rat cerebellar Purkinje cells. *Eur J Neurosci* 20: 729-739, 2004.

Meera P, Wallner M, and Toro L. A neuronal beta subunit (KCNMB4) makes the large conductance, voltage- and Ca2+-activated K+ channel resistant to charybdotoxin and iberiotoxin. *Proc Natl Acad Sci U S A* 97: 5562-5567, 2000.

Molineux ML, Fernandez FR, Mehaffey WH, and Turner RW. A-type and T-type currents interact to produce a novel spike latency-voltage relationship in cerebellar stellate cells. *J Neurosci* 25: 10863-10873, 2005.

Murakoshi H, Shi G, Scannevin RH, and Trimmer JS. Phosphorylation of the Kv2.1 K+ channel alters voltage-dependent activation. *Mol Pharmacol* 52: 821-828, 1997.

Murakoshi H, and Trimmer JS. Identification of the Kv2.1 K+ channel as a major component of the delayed rectifier K+ current in rat hippocampal neurons. *J Neurosci* 19: 1728-1735, 1999.

Murphy GJ, and du Lac S. Postnatal development of spike generation in rat medial vestibular nucleus neurons. *Journal of neurophysiology* 85: 1899-1906, 2001.

Nelson AB, Gittis AH, and du Lac S. Decreases in CaMKII activity trigger persistent potentiation of intrinsic excitability in spontaneously firing vestibular nucleus neurons. *Neuron* 46: 623-631, 2005.

Nelson AB, Krispel CM, Sekirnjak C, and du Lac S. Long-lasting increases in intrinsic excitability triggered by inhibition. *Neuron* 40: 609-620, 2003.

Oliva AA, Jr., Jiang M, Lam T, Smith KL, and Swann JW. Novel hippocampal interneuronal subtypes identified using transgenic mice that express green fluorescent protein in GABAergic interneurons. *J Neurosci* 20: 3354-3368, 2000.

Park KS, Mohapatra DP, Misonou H, and Trimmer JS. Graded regulation of the Kv2.1 potassium channel by variable phosphorylation. *Science* 313: 976-979, 2006.

Perney TM, Marshall J, Martin KA, Hockfield S, and Kaczmarek LK. Expression of the mRNAs for the Kv3.1 potassium channel gene in the adult and developing rat brain. *Journal of neurophysiology* 68: 756-766, 1992.

Prinz AA, Bucher D, and Marder E. Similar network activity from disparate circuit parameters. *Nat Neurosci* 7: 1345-1352, 2004.

Quadroni R, and Knopfel T. Compartmental models of type A and type B guinea pig medial vestibular neurons. *Journal of neurophysiology* 72: 1911-1924, 1994.

Raman IM, and Bean BP. Ionic currents underlying spontaneous action potentials in isolated cerebellar Purkinje neurons. *J Neurosci* 19: 1663-1674, 1999.

Raman IM, and Bean BP. Resurgent sodium current and action potential formation in dissociated cerebellar Purkinje neurons. *J Neurosci* 17: 4517-4526, 1997.

Raman IM, Gustafson AE, and Padgett D. Ionic currents and spontaneous firing in neurons isolated from the cerebellar nuclei. *J Neurosci* 20: 9004-9016, 2000.

Rudy B, and McBain CJ. Kv3 channels: voltage-gated K+ channels designed for high-frequency repetitive firing. *Trends Neurosci* 24: 517-526, 2001.

Sacco T, and Tempia F. A-type potassium currents active at subthreshold potentials in mouse cerebellar Purkinje cells. *J Physiol* 543: 505-520, 2002.

Sah P, and Faber ES. Channels underlying neuronal calcium-activated potassium currents. *Prog Neurobiol* 66: 345-353, 2002.

Sansom SC, Ma R, Carmines PK, and Hall DA. Regulation of Ca(2+)-activated K(+) channels by multifunctional Ca(2+)/calmodulin-dependent protein kinase. *Am J Physiol Renal Physiol* 279: F283-288, 2000.

Schulz DJ, Goaillard JM, and Marder E. Variable channel expression in identified single and electrically coupled neurons in different animals. *Nat Neurosci* 9: 356-362, 2006.

Sekirnjak C, and du Lac S. Intrinsic firing dynamics of vestibular nucleus neurons. *J Neurosci* 22: 2083-2095, 2002.

Sekirnjak C, and du Lac S. Physiological and anatomical properties of mouse medial vestibular nucleus neurons projecting to the oculomotor nucleus. *Journal of neurophysiology* 2006.

Sekirnjak C, Vissel B, Bollinger J, Faulstich M, and du Lac S. Purkinje cell synapses target physiologically unique brainstem neurons. *J Neurosci* 23: 6392-6398, 2003.

Serafin M, de Waele C, Khateb A, Vidal PP, and Muhlethaler M. Medial vestibular nucleus in the guinea-pig. I. Intrinsic membrane properties in brainstem slices. *Exp Brain Res* 84: 417-425, 1991.

Sergeant GP, Ohya S, Reihill JA, Perrino BA, Amberg GC, Imaizumi Y, Horowitz B, Sanders KM, and Koh SD. Regulation of Kv4.3 currents by Ca2+/calmodulin-dependent protein kinase II. *Am J Physiol Cell Physiol* 288: C304-313, 2005.

Smith MR, Nelson AB, and Du Lac S. Regulation of firing response gain by calcium-dependent mechanisms in vestibular nucleus neurons. *Journal of neurophysiology* 87: 2031-2042, 2002.

Song P, Yang Y, Barnes-Davies M, Bhattacharjee A, Hamann M, Forsythe ID, Oliver DL, and Kaczmarek LK. Acoustic environment determines phosphorylation state of the Kv3.1 potassium channel in auditory neurons. *Nat Neurosci* 8: 1335-1342, 2005.

Song WJ, Tkatch T, Baranauskas G, Ichinohe N, Kitai ST, and Surmeier DJ. Somatodendritic depolarization-activated potassium currents in rat neostriatal cholinergic interneurons are predominantly of the A type and attributable to coexpression of Kv4.2 and Kv4.1 subunits. *J Neurosci* 18: 3124-3137, 1998.

Straka H, Vibert N, Vidal PP, Moore LE, and Dutia MB. Intrinsic membrane properties of vertebrate vestibular neurons: function, development and plasticity. *Prog Neurobiol* 76: 349-392, 2005.

Swensen AM, and Bean BP. Ionic mechanisms of burst firing in dissociated Purkinje neurons. *J Neurosci* 23: 9650-9663, 2003.

Swensen AM, and Bean BP. Robustness of burst firing in dissociated purkinje neurons with acute or long-term reductions in sodium conductance. *J Neurosci* 25: 3509-3520, 2005.

Takazawa T, Saito Y, Tsuzuki K, and Ozawa S. Membrane and firing properties of glutamatergic and GABAergic neurons in the rat medial vestibular nucleus. *Journal of neurophysiology* 92: 3106-3120, 2004.

Uusisaari M, Obata K, and Knopfel T. Morphological and electrophysiological properties of GABAergic and non-GABAergic cells in the deep cerebellar nuclei. *Journal of neurophysiology* 97: 901-911, 2007.

Vergara C, Latorre R, Marrion NV, and Adelman JP. Calcium-activated potassium channels. *Curr Opin Neurobiol* 8: 321-329, 1998.

Weiser M, Bueno E, Sekirnjak C, Martone ME, Baker H, Hillman D, Chen S, Thornhill W, Ellisman M, and Rudy B. The potassium channel subunit KV3.1b is localized to somatic and axonal membranes of specific populations of CNS neurons. *J Neurosci* 15: 4298-4314, 1995.

Weiser M, Vega-Saenz de Miera E, Kentros C, Moreno H, Franzen L, Hillman D, Baker H, and Rudy B. Differential expression of Shaw-related K+ channels in the rat central nervous system. *J Neurosci* 14: 949-972, 1994.

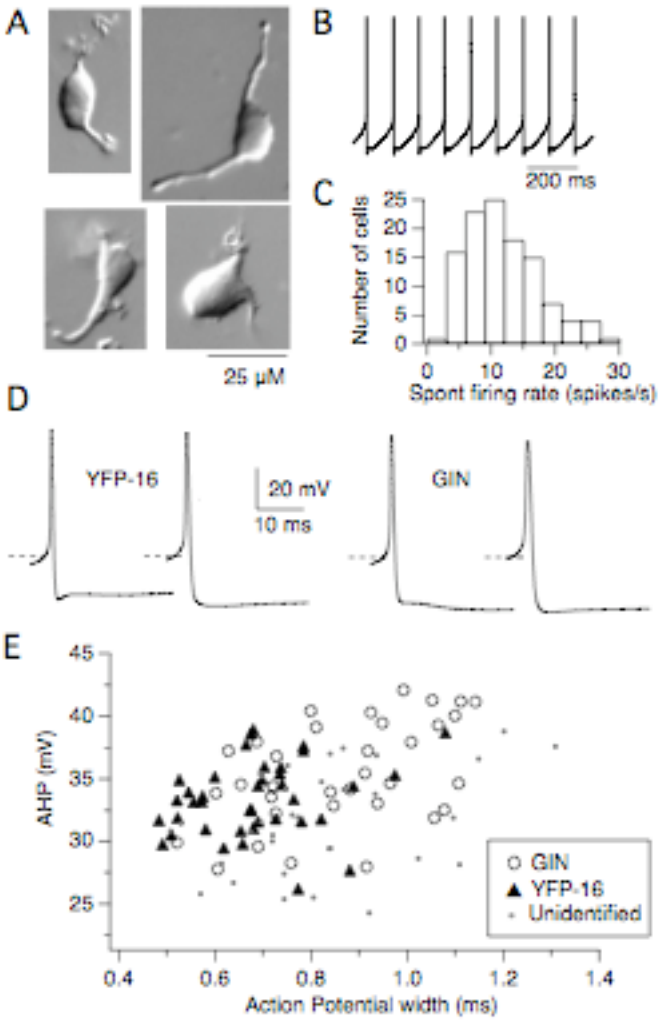

Fig 3.1: Acutely dissociated MVN neurons fire spontaneously and exhibit differences in action potential parameters between GIN and YFP-16 neurons. **A.** DIC images of dissociated MVN neurons. Typically, processes did not extend beyond 30 µm and soma sizes ranged from 15-30 µm in diameter. **B.** An example of the spontaneous, tonic firing pattern recorded from a dissociated MVN neuron. **C.** Histogram of the spontaneous firing rates across the population of dissociated MVN neurons (avg. = 12.7 ± 6.8 spikes/s, n = 126). **D.** Representative action potentials recorded from GIN (right) and YFP-16 neurons (left). Dashed lines are at -55 mV. **E.** Peak AHP amplitude is plotted vs. action potential width (defined at half-height, see Methods) for GIN neurons (open circles), YFP-16 neurons (filled triangles) and a population of unidentified MVN neurons (small, grey dots). GIN neurons tended to have wider action potentials and larger AHPs than YFP-16 neurons. Action potential parameters from GIN and YFP-16 neurons overlap with those from unidentified neurons, forming a continuum.

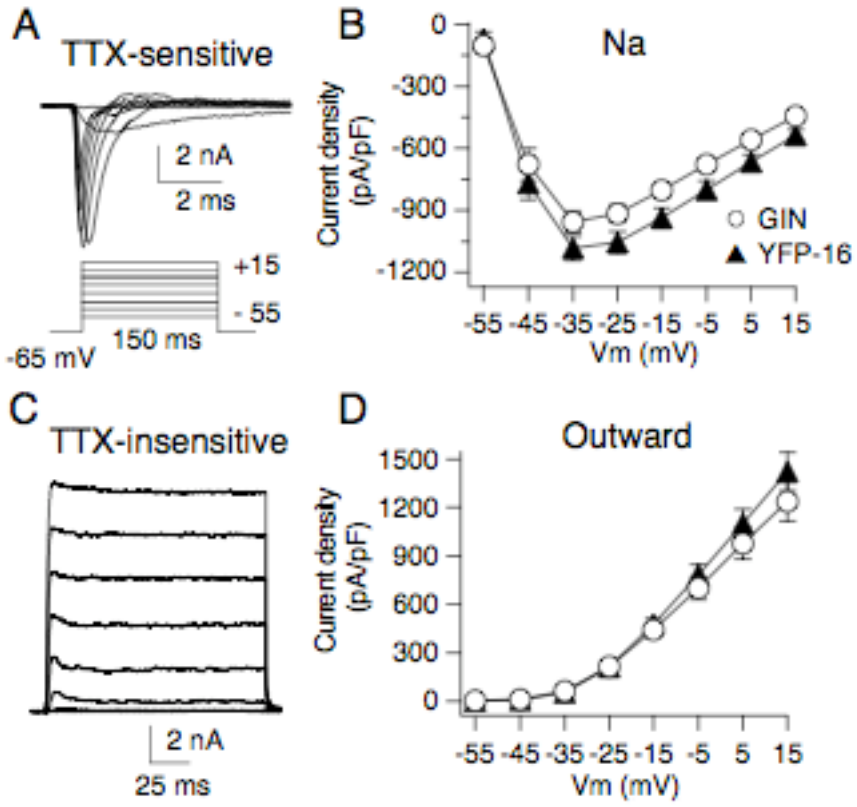

Fig 3.2: Whole cell inward and outward currents are similar in GIN and YFP-16 neurons. **A.** A family of TTX-sensitive transient Na^+ currents (I_{NaT}) recorded from a GIN neuron. The voltage protocol used to evoke the currents is illustrated: neurons were held at -65 mV and stepped for 150 ms to voltages between -55 and +15 mV in 10 mV increments. **B**. Plot of the peak current density of I_{NaT} in GIN and YFP-16 neurons at each voltage. There was no difference in I_{NaT} density between GIN (956 ± 313 pA/pF; n = 35) and YFP-16 neurons (1085 ± 353 pA/pF; n = 40) at -35 mV (p = 0.10). **C**. The TTX-insensitive current (I_{total}) recorded from the same neuron as in A. **D**. Plot of the current density of I_{total} in GIN and YFP-16 neurons at each voltage, measured as the average steady-state current density over the last 50 ms of the trace. The density of I_{total} did not differ significantly between GIN (1239 ± 524 pA/pF) and YFP-16 (1423 ± 532 pA/pF) neurons at + 15 mV, p = 0.29. Error bars represent sem.

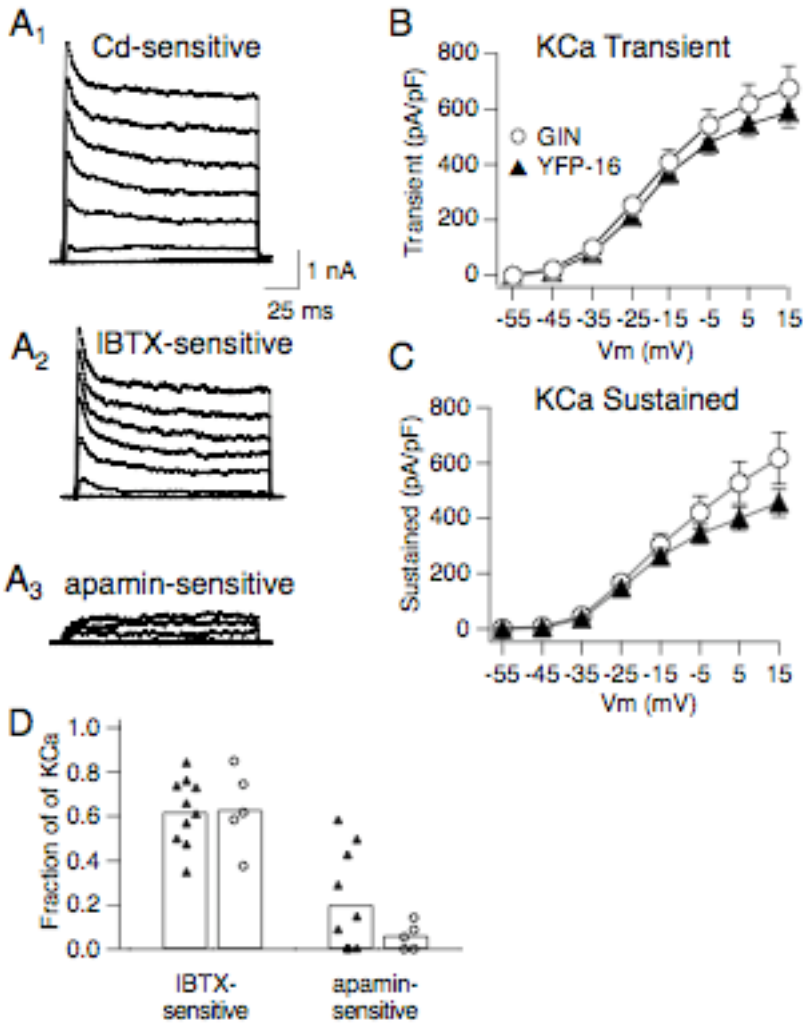

Fig 3.3: Ca^{2+}-dependent K^+ currents (I_{KCa}) in GIN and YFP-16 neurons. **A_{1-3}**. Family of Cd-sensitive I_{KCa}, divided into IBTX-sensitive I_{BK} (A_2) and apamin-sensitive I_{SK} (A_3) components from the same YFP-16 neuron. **B**. Plot of the current density of the transient component (peak amplitude within the first 10 ms) of I_{KCa} at each voltage in GIN and YFP-16 neurons. There was no difference in I_{KCa} density of the transient component between GIN (678 ± 351 pA/pF; n = 19) and YFP-16 neurons (585 ± 243 pA/pF; n = 20) at + 15 mV, p = 0.34. **C**. Plot of the peak current density of the sustained component (average over the last 50 ms) of I_{KCa} at each voltage in GIN and YFP-16 neurons. There was no difference in I_{KCa} density of the sustained component between GIN (616 ± 404 pA/pF) and YFP-16 neurons (455 ± 221 pA/pF,) at + 15 mV, p = 0.42. **D**. Bar graph showing fraction of I_{KCa} that was sensitive to IBTX and apamin in YFP-16 (0.62 ± 15; 0.20 ± 23) and GIN neurons (0.63 ± 18 ; 0.11 ± 14) at + 15 mV, calculated as the average current density over the entire 150 ms step. Error bars represent sem.

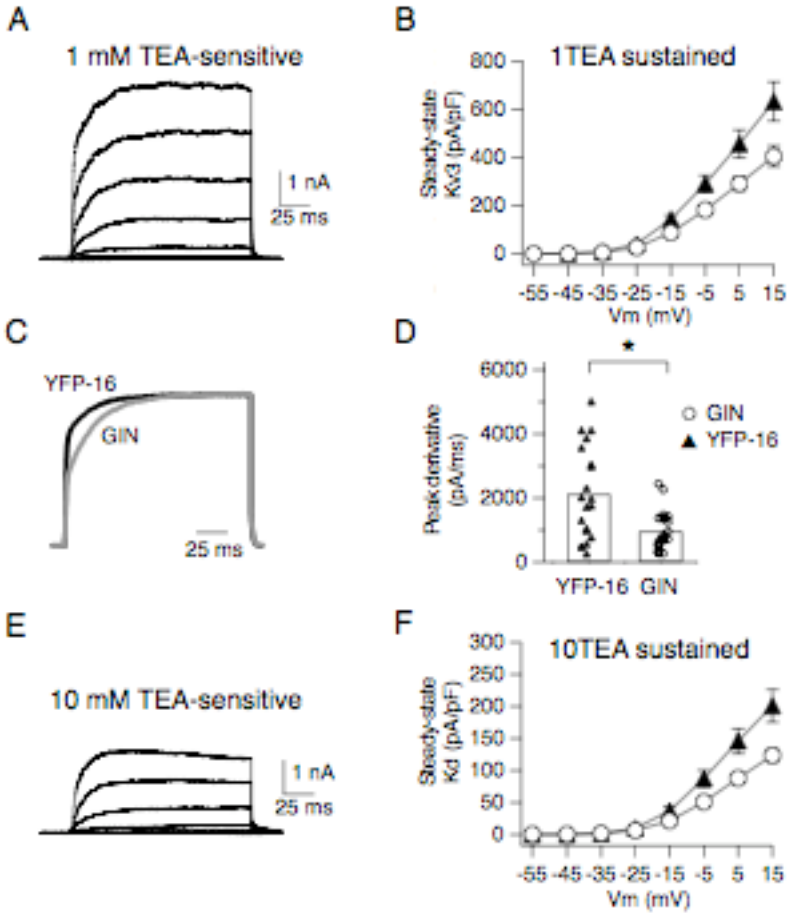

Fig 3.4: TEA-sensitive K^+ currents in GIN and YFP-16 neurons. **A**. Family of 1 mM TEA-sensitive I_{1TEA} with typical kinetics, recorded from a YFP-16 neuron. **B**. Plot of the current density of I_{1TEA} in GIN and YFP-16 neurons at each voltage, measured as the average steady-state current density over the last 50 ms of the trace. There was more I_{1TEA} in YFP-16 (634 ± 361 pA/pF; n = 20) than in GIN neurons (406 ± 186 pA/pF; n = 19) at + 15 mV, p = 0.05. **C**. Average current waveforms at +15 mV from GIN and YFP-16 neurons. I_{1TEA} from GIN neurons was scaled by a factor of 1.6 to match the steady-state value of I_{1TEA} from YFP-16 neurons. Note the faster kinetics of I_{1TEA} in YFP-16 neurons. **D.** Quantification of faster rise time of I_{1TEA} in YFP-16 neurons. The rate of rise was calculated as the maximum derivative over the rising phase of the current at + 15 mV. The rate of rise of I_{1TEA} was faster in YFP-16 (2121 ± 1444 pA/ms) than in GIN neurons (999 ± 328 pA/ms, p = 0.01). **E**. Family of the 10 mM TEA-sensitive I_{10TEA} from a YFP-16 neuron. I_{10TEA} displayed similar kinetics in GIN and YFP-16 neurons. **F**. Plot of the current density of I_{10TEA} in GIN and YFP-16 neurons at each voltage, measured as the average steady-state current density over the last 50 ms of the trace. There was more I_{10TEA} in YFP-16 (201 ± 115 pA/pF; n = 20) than in GIN neurons (123 ± 42 pA/pF; n = 19) at + 15 mV, p = 0.05. Error bars represent sem.

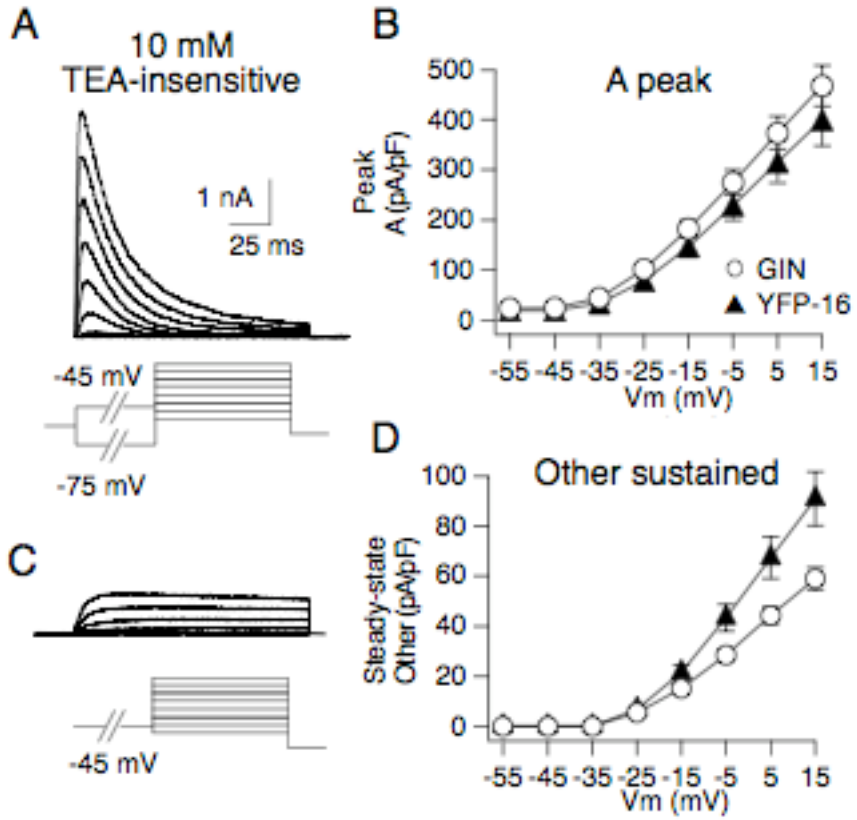

Fig. 3.5: TEA-insensitive K^+ currents in GIN and YFP-16 neurons. **A**. Family of I_A from a GIN neuron, isolated as the difference current inactivated by a 500 ms pre-depolarizing step to -45 mV, voltage protocol shown. **B**. Plot of the current density of I_A at each voltage in GIN and YFP-16 neurons, measured as the peak amplitude over the first 50 ms. There was no difference in I_A density between GIN (468 ± 179 pA/pF, n = 19) and YFP-16 neurons (400 ± 234 pA/pF; n = 20) at + 15 mV, p = 0.25. **C**. Representative trace of I_{other} from a YFP-16 neuron. **D**. Plot of the current density of I_{other} in GIN and YFP-16 neurons, measured as the average steady-state current density over the last 50 ms of the trace. The density of I_{other} was greater in YFP-16 (91 ± 48 pA/pF; n = 20) than in GIN neurons (59 ± 20 pA/pF; n = 19) at + 15 mV, p = 0.01. Error bars represent sem.

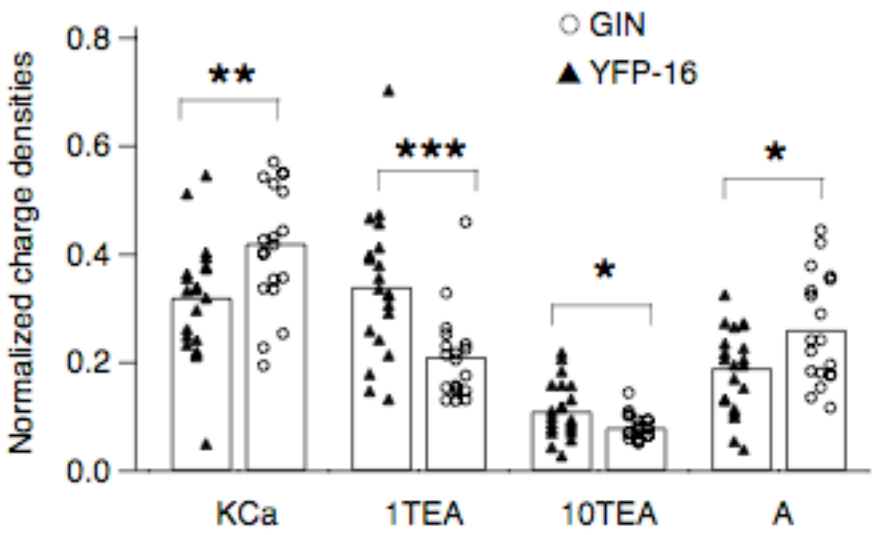

Fig. 3.6: The balance of outward current expression is different in GIN and YFP-16 neurons. The charge density of each current was calculated by integrating the current at +15 mV over the first 30 ms of the trace. The charge densities of the four major current components were normalized by the charge density of I_{total} to control for differences in I_{total} density across cells. All four currents were found in GIN and YFP-16 neurons, but GIN neurons had proportionately more I_{KCa} and I_A and YFP-16 had proportionately more I_{1TEA} and I_{10TEA}. * $p < 0.05$, ** $p < 0.01$, *** $p < 0.005$.

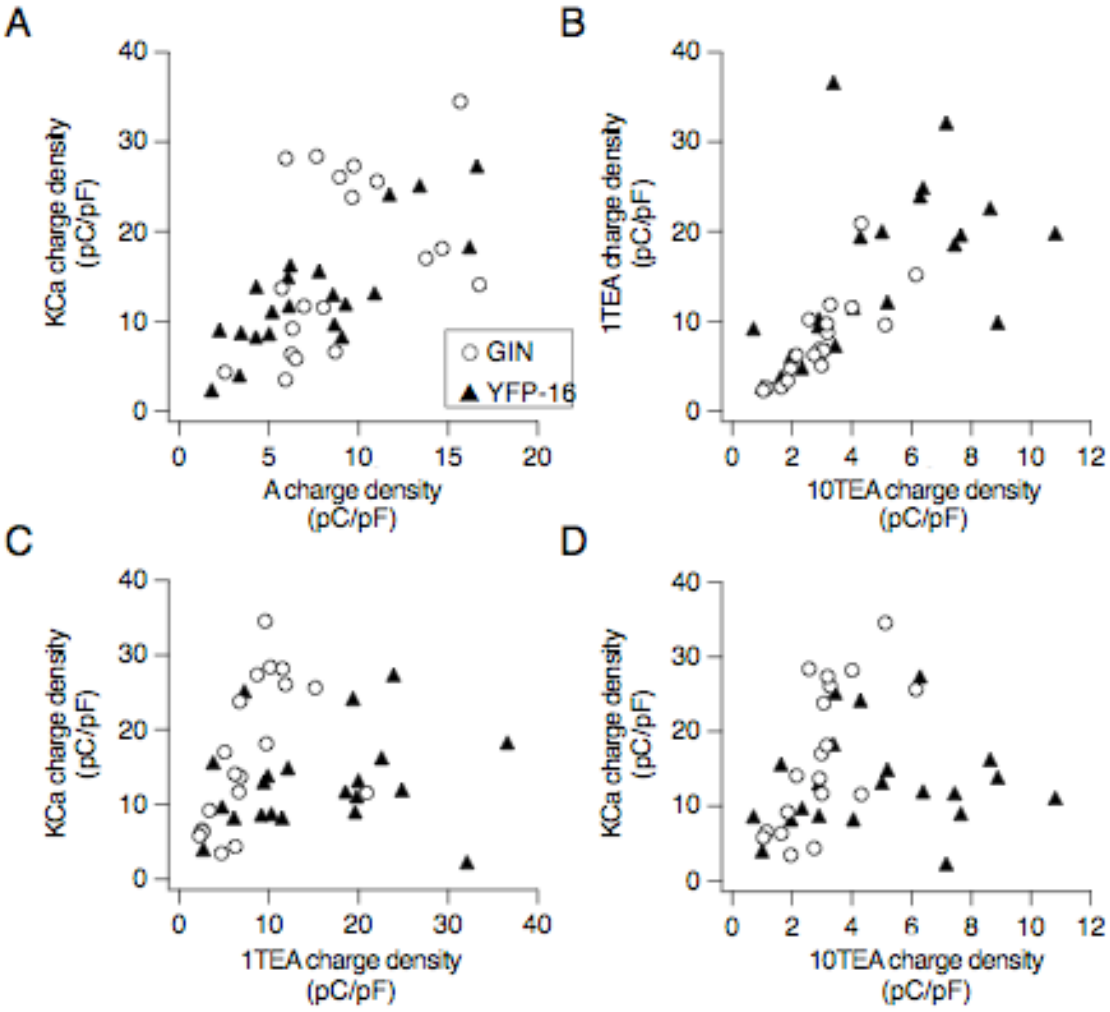

Fig. 3.7: The expression of currents is correlated in GIN and YFP-16 neurons. **A**. The charge density of I_{KCa} over the first 30 ms was correlated with the charge density of I_A, weakly in GIN neurons ($r^2 = 0.22$, n = 19, p = 0.04) and strongly in YFP-16 neurons ($r^2 = 0.64$, n = 20, $p < 0.0001$). **B**. The charge density of I_{1TEA} over the first 30 ms was correlated with the charge density of I_{10TEA}, strongly in GIN neurons ($r^2 = 0.62$, n = 19, $p < 0.0001$) and weakly in YFP-16 neurons ($r^2 = 0.29$, n = 20, p = 0.01). **C**. The charge density of I_{KCa} over the first 30 ms was correlated with the charge density of I_{1TEA} in GIN ($r^2 = 0.26$, n = 19, p = 0.03) but not YFP-16 neurons ($r^2 = 0.17$, n = 20, p = 0.46). **D**. The charge density of I_{KCa} over the first 30 ms was correlated with the charge density of I_{10TEA} in GIN ($r^2 = 0.42$, n = 19, p = 0.001) but not YFP-16 neurons ($r^2 = 0.01$, n = 20, p = 0.71). GIN = open circles. YFP-16 = filled triangles.

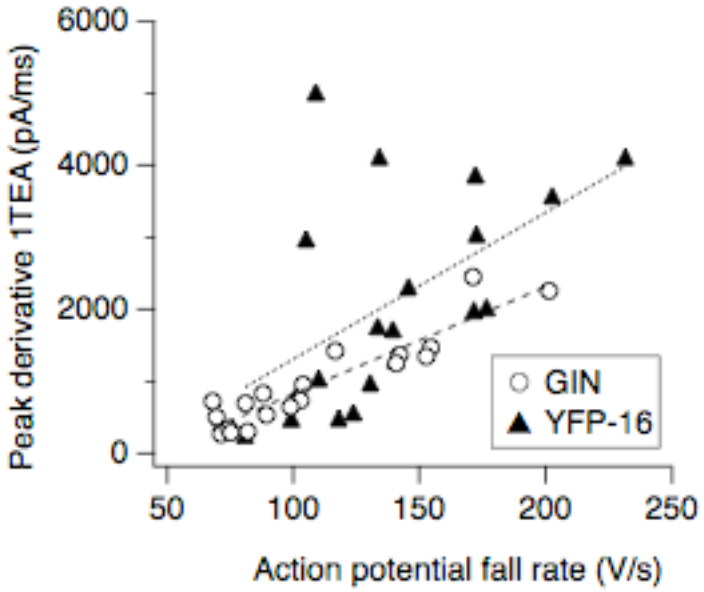

Fig. 3.8: The rate of action potential repolarization correlated with the rate of rise of I_{1TEA} in both GIN and YFP-16 neurons. Rate of rise was calculated as the maximum derivative over the rising phase of the current (see Fig. 4C). This correlation was stronger in GIN neurons ($r^2 = 0.85$, $n = 19$, $p < 0.001$) than in YFP-16 neurons ($r^2 = 0.28$, $n = 20$, $p = 0.02$).

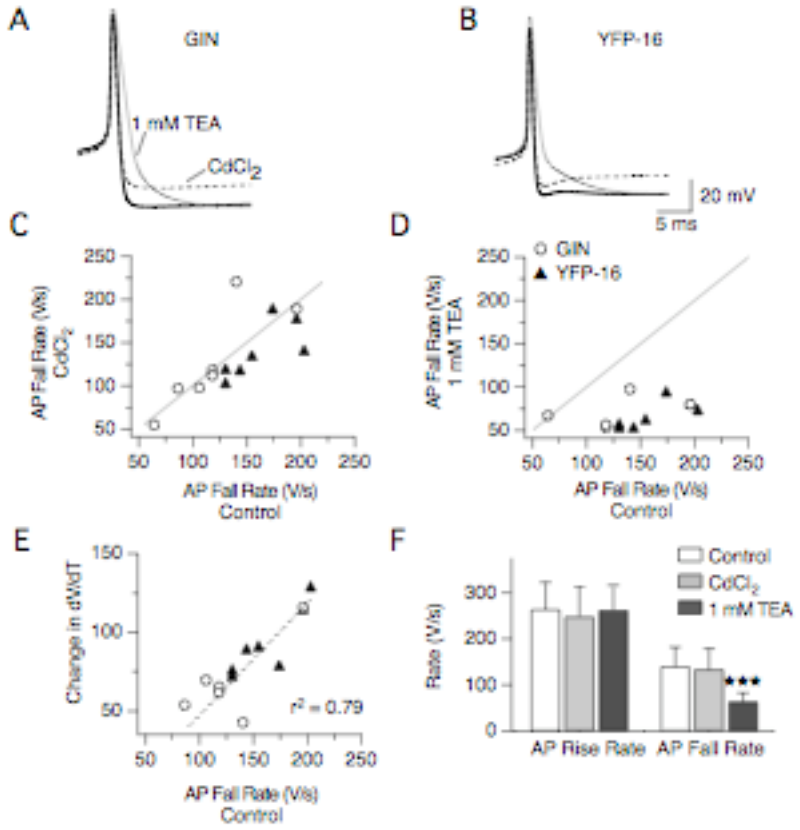

Fig. 3.9: Variability in I_{1TEA} underlies diversity in action potential repolarization in GIN and YFP-16 neurons. **A**. Action potential from an example GIN neuron in control solution (thick, black line); in 0 Ca^{2+} 0.3 mM $CdCl_2$ (dotted line); and in 1 mM TEA (grey line). **B**. Same as A but from a YFP-16 neuron. **C**. Rate of action potential repolarization was not slowed in the presence of $CdCl_2$. Solid line represents no change in repolarization rate between Tyrode's and $CdCl_2$. **D**. Rate of action potential repolarization was slowed in the presence of 1 mM TEA. Solid line represents no change in repolarization rate between control and 1 mM TEA solutions. Before application of 1 mM TEA, YFP-16 neurons repolarized more quickly than GIN neurons (162 ± 30, n = 7; 119 ± 42, n = 7; p = 0.05), but in 1 mM TEA, GIN and YFP-16 neurons repolarized at the same rate (68 ± 16, n = 7; 61 ± 23, n = 7; p = 0.46). **E**. The extent to which 1 mM TEA slowed action potential repolarization was correlated with the initial rate of repolarization. Neurons that repolarized faster in 1 mM TEA were more strongly affected by 1 mM TEA than those that initially repolarized slower ($r^2 = 0.79$, $p < 0.001$). **F**. Summary of the effects of 1 mM TEA and $CdCl_2$ on the rate of action potential (AP) rise and fall. Blocking neither I_{KCa} nor I_{1TEA} affected the rate of action potential rise. The action potential fall rate was significantly slowed in 1 mM TEA (p = 0.0002) but not $CdCl_2$ (p = 0.17), indicating the effect of 1 mM TEA on action potential fall rate is specific to I_{1TEA}.

Table 3.1 Differences in the firing properties of GIN and YFP-16 neurons are preserved in dissociated cells. The table lists averages and standard deviations of parameters used to quantify action potential (AP) shapes and firing propertiesin dissociated YFP-16 (n = 39) and GIN (n = 35) neurons. Spont FR = spontaneous firing rate; CV= coefficient of variation of the inter-spike interval. Cell health, size, and quality of the recording, assessed with input resistance (R_{input}), whole cell capacitance, and series resistance (R_{series}), respecitvely were not different between the two populations of neurons.

	YFP-16 (n = 39)	**GIN (n =35)**	**p**
AP half width, ms	0.69 ± 0.19	0.88 ± 0.13	< 0.0001
AP height, mV	73.2 ± 7.9	70.3 ± 7.8	0.11
AP peak, mV	37.8 ± 6.2	36.2 ± 5.4	0.24
AP Rise rate, V/s	263 ± 66	218 ± 63	0.005
AP Fall rate, V/s	142 ± 39	107 ± 33	0.0001
ADP, V/s	0.96 ± 0.8	0.47 ± 0.7	0.008
AHP, mV	33.3 ± 3.0	35.4 ± 4.7	0.04
Spont FR, Hz	13.9 ± 5.8	10.5 ± 5.1	0.02
CV	0.077 ± 0.099	0.063 ± 0.05	0.88
R_{input}, MΩ	1626 ± 760	1685 ± 582	0.48
Capacitance, pF	8.0 ± 2.3	7.2 ± 1.6	0.13
R_{series}, MΩ	8.1 ± 3.3	9.8 ± 3.9	0.07

Table 3.2 Voltage-dependent properties of somatic currents recorded from YFP-16 (n= 20) and GIN (n = 19) neurons, measured by fitting normalized conductance graphs with a Boltzmann fit: $g_{max} / (1 + \exp(v_{1/2}-v)/k)$, where g_{max} is the normalized maximum conductance, $v_{1/2}$ is the voltage at which half of the channels are open or closed, v is the voltage at which conductance was calculated, corrected for R_{series} errors, and k is the slope, a measure of the voltage-dependence of the channel. Averages and standard deviations of $v_{1/2}$ and k are shown for each current in YFP-16 and GIN neurons. Significant differences are indicated with astrices, ** $p < 0.01$, ***$p < 0.0005$.

	YFP-16 (n = 20)	**GIN (n = 19)**
I_{total} (TTX-insensitive)		
v ½ (mV)	-18.2 ± 3.8	-17.4 ± 6.0
k (mV)	7.1 ± 1.9	8.1 ± 2.8
I_{KCa} (Cd-sensitive)		
v ½ (mV)	-27.0 ± 4.9	-22.1 ± 5.3**
k (mV)	5.3 ± 2.8	8.2 ± 2.5***
I_{Kv3} (1mM TEA-sens)		
v ½ (mV)	-9.3 ± 2.4	-7.6 ± 3.2
k (mV)	7.4 ± 1.3	8.2 ± 1.8
I_{Kd} (10mM TEA-sens)		
v ½ (mV)	-4.3 ± 5.0	-2.8 ± 4.3
k (mV)	8.6 ± 1.5	9.1 ± 1.6
I_A (10mM TEA-insens)		
v ½ (mV)	-12.5 ± 3.8	-13.3 ± 4.2
k (mV)	10.0 ± 1.4	10.3 ± 2.4

IV. Similar Properties of Transient, Persistent, and Resurgent Na Currents in GABAergic and non-GABAergic MVN neurons

Abstract

Sodium currents in fast firing neurons are tuned to support sustained firing rates > 50-60 Hz. This is typically accomplished with fast channel kinetics and the ability to minimize the accumulation of Na channels into inactivated states. Neurons in the medial vestibular nuclei (MVN) can fire at exceptionally high rates, but their Na currents have never been characterized. In this study, Na current kinetics and voltage dependent properties were compared in two classes of MVN neurons with distinct firing properties. Non-GABAergic neurons (fluorescently labeled in YFP-16 transgenic mice) have action potentials with faster rise and fall kinetics and sustain higher firing rates than GABAergic neurons (fluorescently labeled in GIN transgenic mice). A previous study showed that these neurons express a differential balance of K currents. To determine whether the Na currents in these two populations were different, their kinetics and voltage dependent properties were measured in acutely dissociated neurons from 24 - 40 day-old mice. All neurons expressed persistent Na currents and large transient Na currents with resurgent kinetics tuned for fast firing. No differences were found between the Na currents expressed in GABAergic and non-GABAergic MVN neurons, suggesting that differences in properties of these neurons are tuned by their K currents.

Introduction

Different firing properties of neurons are established by the tuning of ionic currents, apparent at the molecular level in the diversity of potassium (K) channel and sodium (Na) channel expression across cell types (Catterall et al. 2005; Coetzee et al. 1999). Historically, the kinetic properties of voltage-gated Na channels were considered to be relatively homogeneous, but more recently, important differences in their kinetic and voltage dependent properties have been identified across cell types with different firing properties (reviewed in Bean 2007). For example, Na currents in regular spiking hippocampal neurons have different inactivation kinetics and voltage dependences than Na currents in fast firing interneurons in the hippocampus (Martina and Jonas 1997) and Purkinje cells in the cerebellum (Raman and Bean 1997).

During firing, Na current availability is limited by the accumulation of Na channels into fast (Armstrong 1981; Stuhmer et al. 1989; Vassilev et al. 1988) and slow inactivated states (Mitrovic et al. 2000; Ong et al. 2000; reviewed in Ulbricht 2005). Na currents in fast firing neurons are slower to enter and faster to recover from these inactivated states than Na currents in slower firing neurons (Martina and Jonas 1997). Additionally, Na currents in many fast firing neurons are protected from inactivation by an endogenous blocking particle that competes for position in a Na channel pore with the channel's inactivation gate (Grieco et al. 2005; Raman and Bean 1997). This mechanism is revealed in voltage clamp experiments by the presence of a resurgent Na current (Afshari et

al. 2004; Aman and Raman 2007; Baufreton et al. 2005; Do and Bean 2003; Raman and Bean 1997; Raman et al. 2000).

Neurons in the medial vestibular nuclei (MVN) rapidly encode changes in head and image motion with linear changes in firing rate and can sustain firing rates up to hundreds of Hz. In contrast to the cellular framework in the hippocampus and cortex, both GABAergic and non-GABAergic neurons in the MVN are fast firing, and non-GABAergic neurons have narrower action potentials and higher maximum firing rates than GABAergic neurons (Bagnall et al. 2007). Although GABAergic and non-GABAergic MVN neurons express a different balance of K currents that contributes to differences in their action potential repolarization (Gittis and du Lac 2007), the properties of their Na currents have never been characterized.

Neurons from the same structure with different firing properties often express Na currents with distinct properties (Afshari et al. 2004; Aman and Raman 2007; Martina and Jonas 1997), however all MVN neurons are expected to express Na currents with properties tuned to support fast firing. To determine whether Na currents are differentially tuned between GABAergic and non-GABAergic MVN neurons, the amplitude and kinetic properties of Na currents, including persistent and resurgent currents, were measured from acutely dissociated MVN neurons. The results of this study show that Na currents in MVN neurons are similarly tuned to support fast firing in both GABAergic and non-GABAergic MVN neurons.

Methods

Cell preparation: 350 μM coronal slices through the rostral 2/3 of the MVN were prepared with a DSK-1500E or Leica VT1000S Vibratome in carbogenated ACSF containing (in mM) 125 NaCl, 26 $NaCHO_3$, 5 KCl, 1.3 $MgCl_2$, 2.5 $CaCl_2$, 1 NaH_2PO_4, and 11 glucose. Slices were heated for 10-30 minutes at 34°C then maintained at room temperature. Neurons were enzymatically dissociated as described in Gittis and du Lac, 2007 from 24-40-day-old mice, either GIN (Oliva et al. 2000) for GABAergic neurons, or YFP-16 (Feng et al. 2000) for non-GABAergic neurons, both in c57bl6 backgrounds. Briefly, slices were treated with 40 U/mL papain (Worthington) in 9.4 mg/mL MEM powder (Gibco), 10 mM Hepes, 0.2 mM cysteine, for 10 min at 30ºC. The bilateral vestibular nuclei were removed from a slice, triturated with fire polished Pasteur pipets, and dissociated neurons were plated on the glass slide of the recording chamber.

Electrophysiological recording: For the duration of a recording session (2-3 hours), neurons were continuously perfused with oxygenated Tyrode's solution (in mM: 150 NaCl, 3.5 KCl, 2 $CaCl_2$, 1 $MgCl_2$, 10 Hepes, 10 glucose) and all recordings were done at room temperature. Whole cell recordings were made with Borosilicate pipettes (2-4 MΩ), filled with a K-gluconate based intracellular solution (in mM: 140 Kgluc, 8 NaCl, 10 Hepes, 0.02 EGTA, 2 Mg_2-ATP, 0.3 Na_2-GTP, and 14 Tris-creatine PO_4).

The measured liquid junction potential was +15 mV and was corrected off-line. Sodium currents were isolated by digital subtraction following application of 1

μM TTX (Tocris) in the presence of Tyrode's solution containing 20 mM TEA, 5 mM 4-AP, and 2 mM $MgCl_2$ substituted for 2 mM $CaCl_2$ (Sigma).

Data were collected and analyzed using IGOR software with a MultiClamp 700B amplifier (Axon Instruments) and an ITC-16 interface (Instrutech). Ionic currents were recorded in voltage clamp mode, filtered at 8 kHz and digitized at 40 kHz. Whole cell capacitance was compensated through the amplifier circuitry and series resistance (R_{series}) was compensated at 70-90%. The average uncompensated series resistance was 1.9 ± 1.0 MΩ (n = 25) in GABAergic and 1.6 ± 0.8 MΩ (n = 25) in non-GABAergic neurons (p = 0.27). The capacitance was measured off the amplifier or by integrating the area of the transient following a step from -65 mV to -75 mV with whole cell capacitance and series resistance compensation turned off. Average cell capacitance was 7.2 ± 2.8 pF (n = 25) for GABAergic and 8.5 ± 3.5 pF (n = 25) for non-GABAergic neurons (p = 0.15).

Data Analysis

Na conductance (g_{Na}) was calculated with the equation $g_{Na} = I/(V-E_{rev})$, where E_{rev} was calculated to be +46 mV in 50 mM NaCl at 22°C. Na conductance at each voltage was normalized to the maximum conductance (usually at -25 mV in 50 mM NaCl) in each cell to create a normalized conductance plot. The normalized conductance plot in each neuron was fit with a Boltzmann equation: $g_{max} / (1 + \exp(V_{1/2}-V)/k)$, where g_{max} is the normalized maximum conductance, $V_{1/2}$ is the voltage at which half of the channels are open or closed, V is the

voltage at which conductance was calculated, and k is the slope, a measure of the voltage-dependence of the channels.

To calculate the voltage-dependence of fast inactivation, Na current availability was measured at +15 mV after 100 ms voltage steps to potentials between -95 and 0 mV. Availability after the 100 ms voltage steps was assessed by normalizing the amplitude of the non-inactivated current by the amplitude of the non-inactivated current after the 100 ms voltage step to -95 mV.

Statistical differences were tested with the non-parametric Wilcoxon test for unpaired data and variances reported in the text are standard deviations.

Results

Transient Na current

To determine whether Na currents were differentially tuned in GABAergic vs. non-GABAergic MVN neurons, transient Na currents were recorded from fluorescently labeled neurons, acutely dissociated from lines of mice established to label GABAergic (GIN) or non-GABAergic (YFP-16) neurons in the MVN (Bagnall et al. 2007). Transient Na currents were elicited with 20 ms voltage steps to positive potentials from a holding potential of -80 mV. The amplitudes of transient Na currents in non-GABAergic neurons tended to be larger than those in GABAergic neurons (13.8 ± 4.5 nA, n = 24 vs. 10.8 ± 4.7 nA, n = 22, p = 0.04) but their current densities were similar (1.9 ± 0.7 nA/pF vs. 1.8 ± 0.9 nA/pF, p = 0.47), suggesting their different current amplitudes reflected larger surface areas

of non-GABAergic neurons (Bagnall et al. 2007) rather than differences in Na current expression.

Activation of the transient Na current at 0 mV was complete within 0.34 ± 0.04 ms in GABAergic (n = 13) and 0.31 ± 0.04 ms in non-GABAergic (n = 15) neurons (p = 0.24). To measure the voltage dependence of activation, a family of voltage steps was delivered in a low Na external solution [50 mM] to reduce the current amplitude and minimize R_{series} errors (Fig. 1A). Even in 50 mM NaCl, the maximum transient Na current was often > 6 nA, creating 8-12 mV deviations between the command potential of the amplifier and the voltage experienced by the cell. To decrease these errors, the peak Na current was further reduced to < 3.5 nA with subsaturating concentrations of TTX. This allowed for accurate measurement of the voltage-dependence of activation, but precluded measurements of true maximum conductance. As a result, normalized conductance plots were compared across neurons (see methods). In both cell types, Na currents began to activate around -55 mV and were fully activated by about -5 mV (Fig. 1C). Boltzmann fits from individual neurons to determine the voltage of half-maximal activation ($V_{1/2}$) and the slope (k) yielded no differences between the cell types ($V_{1/2}$, p = 1; k, p = 0.89, n = 11 GABAergic and 10 non-GABAergic).

To measure the kinetics of inactivation, the decay of transient Na currents at 0 mV (in 150 mM NaCl) were fit with a single exponential. The τ of fast inactivation was the same in GABAergic (0.34 ± 0.03 ms, n = 13) and non-GABAergic neurons (0.34 ± 0.05 ms, n = 15) (p = 0.96). To compare the voltage

dependence of inactivation, Na channel availability at + 15 mV was assessed following a 100 ms pre-step to different potentials (Fig. 1B). Na channels began to inactivate during 100 ms steps to -70 mV in both cell types and were fully inactivated by 100 ms steps to -35 mV (Fig. 1C). Boltzmann fits of the steady-state inactivation curves from individual cells yielded no differences in $V_{1/2}$ or k ($V_{1/2}$, p = 0.28; k, p = 1) between GABAergic (n = 12) and non-GABAergic neurons (n = 11).

Na current inactivation and recovery

The time courses of recovery of transient Na currents in GABAergic and non-GABAergic MVN neurons were compared following either a 2 ms step or a 500 ms step to 0 mV to drive Na channels into fast and slow inactivated states, respectively. Recovery from inactivation was assessed by measuring the Na current availability 1 ms – 1 s after the initial depolarizing step (Fig. 2A).

In both GABAergic and non-GABAergic neurons, transient Na currents were initially reduced to 41% following a 2 ms step to 0 mV (p = 0.86). Within 10 ms, more than 80% of the Na current had recovered. Recovery followed a double exponential time course with similar time constants for both GABAergic (1.7 ± 0.3 ms and 138 ± 38 ms, n = 12) and non-GABAergic neurons (1.7 ± 0.4 ms and 117 ± 58 ms, n =11) (τ_1 p = 0.64; τ_2 p = 0.11) (Fig. 2B).

Following a 500 ms voltage step to 0 mV, transient Na currents were reduced to 10-13% their initial value in both GABAergic and non-GABAergic neurons (p = 0.25) (Fig. 2B). Recovery was considerably slower, requiring

almost 500 ms for 80% recovery and followed a double exponential time course with similar time constants for GABAergic (3.6 ± 1.6 ms and 248 ± 103 ms, n = 12) and non-GABAergic neurons (3.9 ± 2.1 ms and 220 ± 134 ms, n =11) (τ_1 p = 0.97; τ_2 p = 0.25) (Fig. 2B).

To test for cell type differences in the rate of entry into the slow inactivated state, neurons were held at 0 mV for durations of 1 ms – 2.5 s and Na channel availability was assessed after 75 ms at -80 mV to relieve fast inactivation (Fig 2C). Slow inactivation in both GABAergic and non-GABAergic MVN neurons took almost 100 ms to accumulate at 0 mV and followed a similar time course in both cell types (Fig. 2D). Although τ_1 was significantly shorter in GABAergic neurons (60 ± 41 ms vs. 121 ± 53 ms, p = 0.01), there was no differences in the dominant time constant (τ_2) between the cell types (GABAergic: 1125 ± 415 ms, n =12; non-GABAergic: 1360 ± 489 ms, n =8) (Fig. 2D).

Persistent Na current

Persistent Na currents are present in a number of diverse cell types (reviewed in Crill 1996) and can contribute to autonomous pacemaking (Bevan and Wilson 1999; Do and Bean 2003; Raman and Bean 1999; Shao et al. 2006; Taddese and Bean 2002) or burst firing (Enomoto et al. 2006; Wu et al. 2005; Del Negro et al. 2002). To isolate persistent Na currents in MVN neurons, cells were slowly depolarized with a 1 s ramp stimulus from -95 mV to +20 mV (115 mV/s), before and after application of 1 μM TTX (Fig. 3A). Both cell types expressed a

persistent Na current between -70 and -20 mV and there was no difference in the maximum amplitude or voltage dependence of the current between GABAergic (233 ± 113 pA, n = 11) and non-GABAergic neurons (232 ± 148 pA, n = 11; p = 0.95) (Fig. 3B). Across the population of MVN neurons, the amplitude of the persistent Na current at voltages more hyperpolarized than -55 mV correlated with the rate of rise of the action potential ($r^2 = 0.36$, $p < 0.01$, n = 18), but not at voltages more depolarized than -55 mV, including -50 mV where persistent Na currents were largest ($r^2 = 0.18$, p = 0.1, n = 18).

Resurgent Na current

To measure resurgent Na currents in MVN neurons, cells were held at 0 mV for 10 ms, then repolarized to voltages between -60 and -10 mV (Fig. 4A). At these voltages, a 'resurgent' Na current flows through channels that were protected from inactivation during the 10 ms depolarization step by a peptide blocking particle (Grieco et al. 2005; Raman and Bean 1997). In both GABAergic and non-GABAergic MVN neurons, resurgent Na currents were largest at -35 mV and were 13 ± 3% and 15 ± 5% of the transient Na current (measured at 0 mV), respectively. At -35 mV, the resurgent current reached its peak amplitude within 2.8 ± 0.6 ms (n = 13) in GABAergic and 2.9 ± 0.4 ms (n = 14) in non-GABAergic neurons (p = 0.54) and decayed exponentially with a time constant of 9.6 ± 1.3 ms in GABAergic and 10.8 ± 1.9 ms in non-GABAergic neurons (p = 0.13). The resurgent Na current tended to be larger in non-GABAergic neurons (-797 ± 304 pA, n = 14) compared to GABAergic neurons (-

697 ± 282, n = 13), but this difference was not significant (p = 0.23) (Fig. 4B). Across the population, the peak amplitude of the resurgent Na current (at -35 mV) and the rate of action potential depolarization were weakly correlated $r^2 = 0.24$ (p = 0.03, n = 21).

Discussion

This study is the first to describe the biophysical properties of Na currents in MVN neurons which fire at exceptionally high rates. All MVN neurons had persistent Na currents as well as large transient Na currents with resurgent kinetics and voltage dependences similar to those of other fast firing neurons. A comparison of the Na currents expressed in two classes of MVN neurons with different firing properties, GABAergic and non-GABAergic neurons, revealed that their Na currents were very similar. This finding was surprising given that neurons with different firing properties from the same structure more commonly express Na currents with distinct properties (Afshari et al. 2004; Aman and Raman 2007; Martina and Jonas 1997) but see also (Huguenard et al. 1988).

Neurons that can sustain firing rates > 50-60 Hz express ionic currents that are tuned to generate brief action potentials with short refractory periods (reviewed in Bean 2007). This tuning is often associated with the expression of Kv3-type K currents, but it is evident that some properties of voltage gated Na currents are tuned to promote fast firing as well. These include rapid recovery from inactivated states as well as resistance to entry into slow inactivated states (Martina and Jonas 1997) and the expression of transient Na currents with

resurgent kinetics, reflecting a mechanism of protection from fast inactivation during repetitive firing (Afshari et al. 2004; Do and Bean 2003; Mercer et al. 2007; Raman and Bean 1997; Raman et al. 2000). In Nav1.6$^{-/-}$ mice, where resurgent Na currents were reduced, the maximum firing rates of some previously fast firing neurons were diminished to < 50 Hz (Khaliq et al. 2003; Mercer et al. 2007; Van Wart and Matthews 2006), demonstrating the importance of this mechanism in supporting fast firing.

With sustained maximum firing rates often exceeding 150 spikes/s, MVN neurons are among the fastest firing neurons in the brain (Bagnall et al., 2007). In support of the link between a neuron's firing capabilities and its expression of resurgent Na current, MVN neurons express large resurgent Na currents (13-15% the size of the transient Na current). Na currents from MVN neurons are exceptional in their ability to avoid accumulation into inactivated states. Na currents from MVN neurons are even faster to recover from inactivation than fast firing neurons in the hippocampus (Martina and Jonas 1997), and cerebellum (Aman and Raman 2007) and are more resistant to entry into the slow inactivated state. Both of these properties could enhance Na channel availability beyond levels observed in other fast firing neurons, likely contributing to the capacity of MVN neurons to sustain such high maximum firing rates.

The finding that GABAergic and non-GABAergic MVN neurons express similar persistent Na currents was unexpected given predictions from previous current clamp studies of the firing properties of MVN neurons (Johnston et al. 1994; Serafin et al. 1991). In these studies, TTX-sensitive plateau potentials were

observed during firing in MVN neurons classified as ‘Type B’ but not ‘Type A’. The Type A / Type B classification scheme in these studies was applied largely on the basis of action potential shape, but subsequent studies have shown that ‘Type A’ neurons are GABAergic and ‘Type B’ can be glutamatergic, glycinergic, or GABAergic (Bagnall et al. 2007; Takazawa et al. 2004). The fact that persistent Na currents were similarly expressed in both GABAergic and non-GABAergic neurons suggests that differences in K currents mask the contribution of persistent Na currents to plateau potentials in GABAergic but not non-GABAergic MVN neurons, demonstrating the importance of both inward and outward currents in shaping a neuron’s firing properties.

Although Na current expression in GABAergic and non-GABAergic MVN neurons was quite similar, these cell types have different action potential shapes and maximum firing rates (Bagnall et al. 2007). Therefore, the differences previously described in the outward current between these two cell types must play a critical role in sculpting the firing properties of these neurons (Gittis and du Lac 2007). An explanation of why non-GABAergic neurons are better able to utilize their Na currents to sustain higher maximum firing rates than GABAergic neurons will require understanding how Na and K currents cooperate during naturalistic firing activity in these neurons.

Acknowledgments

Chapter 4 is original work submitted as Gittis AH, du Lac S. J Neurophysiol Similar Properties of Transient, Persistent, and Resurgent Na Currents in GABAergic and non-GABAergic MVN neurons. in press. It is included with the permission of all the authors on the final publication.

References

Afshari FS, Ptak K, Khaliq ZM, Grieco TM, Slater NT, McCrimmon DR, and Raman IM. Resurgent Na currents in four classes of neurons of the cerebellum. *J Neurophysiol* 2004.

Aman TK, and Raman IM. Subunit dependence of Na channel slow inactivation and open channel block in cerebellar neurons. *Biophysical journal* 92: 1938-1951, 2007.

Armstrong CM. Sodium channels and gating currents. *Physiol Rev* 61: 644-683, 1981.

Bagnall MW, Stevens RJ, and du Lac S. Transgenic mouse lines subdivide medial vestibular nucleus neurons into discrete, neurochemically distinct populations. *J Neurosci* 27: 2318-2330, 2007.

Baufreton J, Atherton JF, Surmeier DJ, and Bevan MD. Enhancement of excitatory synaptic integration by GABAergic inhibition in the subthalamic nucleus. *J Neurosci* 25: 8505-8517, 2005.

Bean BP. The action potential in mammalian central neurons. *Nature reviews* 8: 451-465, 2007.

Bevan MD, and Wilson CJ. Mechanisms underlying spontaneous oscillation and rhythmic firing in rat subthalamic neurons. *J Neurosci* 19: 7617-7628, 1999.

Catterall WA, Goldin AL, and Waxman SG. International Union of Pharmacology. XLVII. Nomenclature and structure-function relationships of voltage-gated sodium channels. *Pharmacological reviews* 57: 397-409, 2005.

Coetzee WA, Amarillo Y, Chiu J, Chow A, Lau D, McCormack T, Moreno H, Nadal MS, Ozaita A, Pountney D, Saganich M, Vega-Saenz de Miera E, and Rudy B. Molecular diversity of K+ channels. *Ann N Y Acad Sci* 868: 233-285, 1999.

Crill WE. Persistent sodium current in mammalian central neurons. *Annu Rev Physiol* 58: 349-362, 1996.

Del Negro CA, Koshiya N, Butera RJ, Jr., and Smith JC. Persistent sodium current, membrane properties and bursting behavior of pre-botzinger complex inspiratory neurons in vitro. *J Neurophysiol* 88: 2242-2250, 2002.

Do MT, and Bean BP. Subthreshold sodium currents and pacemaking of subthalamic neurons: modulation by slow inactivation. *Neuron* 39: 109-120, 2003.

Enomoto A, Han JM, Hsiao CF, Wu N, and Chandler SH. Participation of sodium currents in burst generation and control of membrane excitability in mesencephalic trigeminal neurons. *J Neurosci* 26: 3412-3422, 2006.

Feng G, Mellor RH, Bernstein M, Keller-Peck C, Nguyen QT, Wallace M, Nerbonne JM,
Lichtman JW, and Sanes JR. Imaging neuronal subsets in transgenic mice expressing multiple spectral variants of GFP. *Neuron* 28: 41-51, 2000.

Gittis AH, and du Lac S. Firing properties of GABAergic versus non-GABAergic vestibular nucleus neurons conferred by a differential balance of potassium currents. *J Neurophysiol* 97: 3986-3996, 2007.

Grieco TM, Malhotra JD, Chen C, Isom LL, and Raman IM. Open-Channel Block by the Cytoplasmic Tail of Sodium Channel beta4 as a Mechanism for Resurgent Sodium Current. *Neuron* 45: 233-244, 2005.

Huguenard JR, Hamill OP, and Prince DA. Developmental changes in Na+ conductances in rat neocortical neurons: appearance of a slowly inactivating component. *J Neurophysiol* 59: 778-795, 1988.

Johnston AR, MacLeod NK, and Dutia MB. Ionic conductances contributing to spike repolarization and after-potentials in rat medial vestibular nucleus neurones. *J Physiol* 481 (Pt 1): 61-77, 1994.

Khaliq ZM, Gouwens NW, and Raman IM. The contribution of resurgent sodium current to high-frequency firing in Purkinje neurons: an experimental and modeling study. *J Neurosci* 23: 4899-4912, 2003.

Martina M, and Jonas P. Functional differences in Na+ channel gating between fast-spiking interneurones and principal neurones of rat hippocampus. *J Physiol* 505 (Pt 3): 593-603, 1997.

Mercer JN, Chan CS, Tkatch T, Held J, and Surmeier DJ. Nav1.6 sodium channels are critical to pacemaking and fast spiking in globus pallidus neurons. *J Neurosci* 27: 13552-13566, 2007.

Mitrovic N, George AL, Jr., and Horn R. Role of domain 4 in sodium channel slow inactivation. *The Journal of general physiology* 115: 707-718, 2000.

Oliva AA, Jr., Jiang M, Lam T, Smith KL, and Swann JW. Novel hippocampal interneuronal subtypes identified using transgenic mice that express green

fluorescent protein in GABAergic interneurons. *J Neurosci* 20: 3354-3368, 2000.

Ong BH, Tomaselli GF, and Balser JR. A structural rearrangement in the sodium channel pore linked to slow inactivation and use dependence. *The Journal of general physiology* 116: 653-662, 2000.

Raman IM, and Bean BP. Ionic currents underlying spontaneous action potentials in isolated cerebellar Purkinje neurons. *J Neurosci* 19: 1663-1674, 1999.

Raman IM, and Bean BP. Resurgent sodium current and action potential formation in dissociated cerebellar Purkinje neurons. *J Neurosci* 17: 4517-4526, 1997.

Raman IM, Gustafson AE, and Padgett D. Ionic currents and spontaneous firing in neurons isolated from the cerebellar nuclei. *J Neurosci* 20: 9004-9016, 2000.

Serafin M, de Waele C, Khateb A, Vidal PP, and Muhlethaler M. Medial vestibular nucleus in the guinea-pig. II. Ionic basis of the intrinsic membrane properties in brainstem slices. *Exp Brain Res* 84: 426-433, 1991.

Shao M, Hirsch JC, and Peusner KD. Maturation of firing pattern in chick vestibular nucleus neurons. *Neuroscience* 141: 711-726, 2006.

Stuhmer W, Conti F, Suzuki H, Wang XD, Noda M, Yahagi N, Kubo H, and Numa S. Structural parts involved in activation and inactivation of the sodium channel. *Nature* 339: 597-603, 1989.

Taddese A, and Bean BP. Subthreshold sodium current from rapidly inactivating sodium channels drives spontaneous firing of tuberomammillary neurons. *Neuron* 33: 587-600, 2002.

Takazawa T, Saito Y, Tsuzuki K, and Ozawa S. Membrane and firing properties of glutamatergic and GABAergic neurons in the rat medial vestibular nucleus. *J Neurophysiol* 92: 3106-3120, 2004.

Ulbricht W. Sodium channel inactivation: molecular determinants and modulation. *Physiol Rev* 85: 1271-1301, 2005.

Van Wart A, and Matthews G. Impaired firing and cell-specific compensation in neurons lacking nav1.6 sodium channels. *J Neurosci* 26: 7172-7180, 2006.

Vassilev PM, Scheuer T, and Catterall WA. Identification of an intracellular peptide segment involved in sodium channel inactivation. *Science (New York, NY* 241: 1658-1661, 1988.

Wu N, Enomoto A, Tanaka S, Hsiao CF, Nykamp DQ, Izhikevich E, and Chandler SH. Persistent sodium currents in mesencephalic v neurons participate in burst generation and control of membrane excitability. *J Neurophysiol* 93: 2710-2722, 2005.

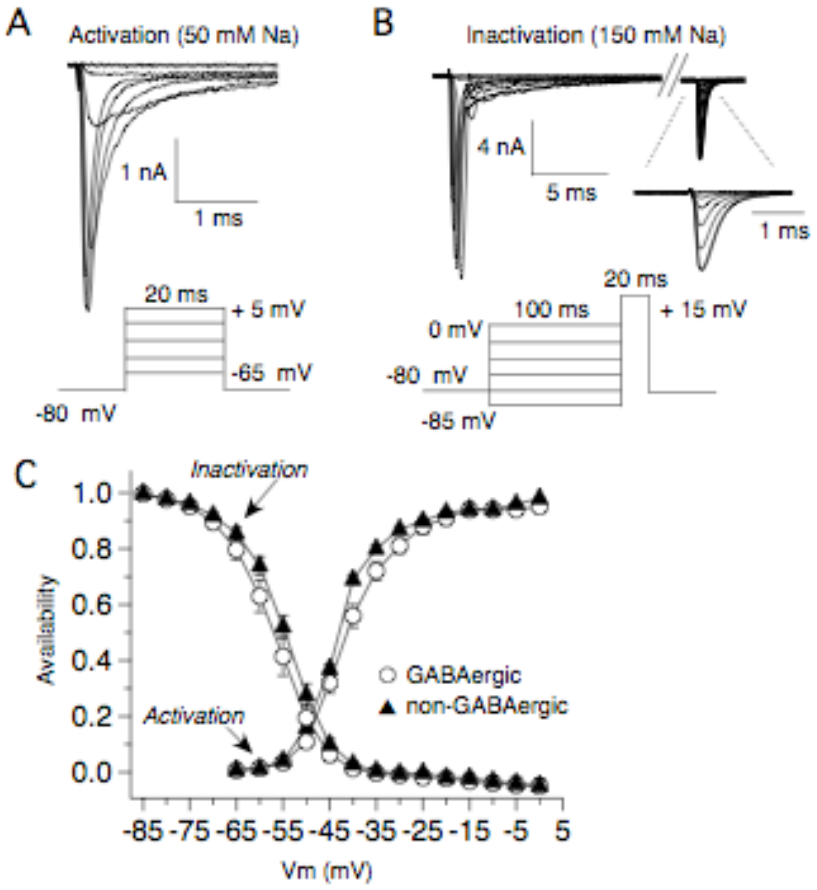

Fig. 4.1: Properties of transient Na currents are similar in GABAergic and non-GABAergic MVN neurons. **A.** Transient Na currents, measured in a non-GABAergic neuron during 20 ms depolarizing steps from a holding potential of -80 mV (voltage protocol shown below). Extracellular NaCl was reduced to 50 mM to reduce voltage errors. In some neurons, subsaturating TTX was also applied to reduce the transient Na current to < 3.5 nA. Currents were obtained by digital subtraction after application of 1 µM TTX. **B.** Voltage protocol and representative Na currents, recorded from a non-GABAergic neuron, measuring the voltage dependence of fast inactivation. Recordings were done in 150 mM NaCl and Na currents were isolated by digital subtraction, following application of 1 µM TTX. *Inset*, Non-inactivated Na currents after the depolarizing steps on an expanded time scale for clarity. **C.** Averages of the Na current activation and inactivation curves from the population of GABAergic vs. non-GABAergic neurons. Error bars are SEM. GABAergic neurons: $V_{1/2}$ activation = -41 ± 3 mV, n = 11; k activation = 5.3 ± 1.8 mV, n = 11; $V_{1/2}$ inactivation = -56 ± 4 mV, n = 12; k inactivation = 4.7 ± 1.5 mV, n = 12. Non-GABAergic neurons: $V_{1/2}$ activation = -40 ± 7 mV, n = 10; k activation = 5.0 ± 1.8 mV n = 10; $V_{1/2}$ inactivation = -55 ± 3, n = 11; k inactivation = 5.0 ± 0.9 mV, n = 11.

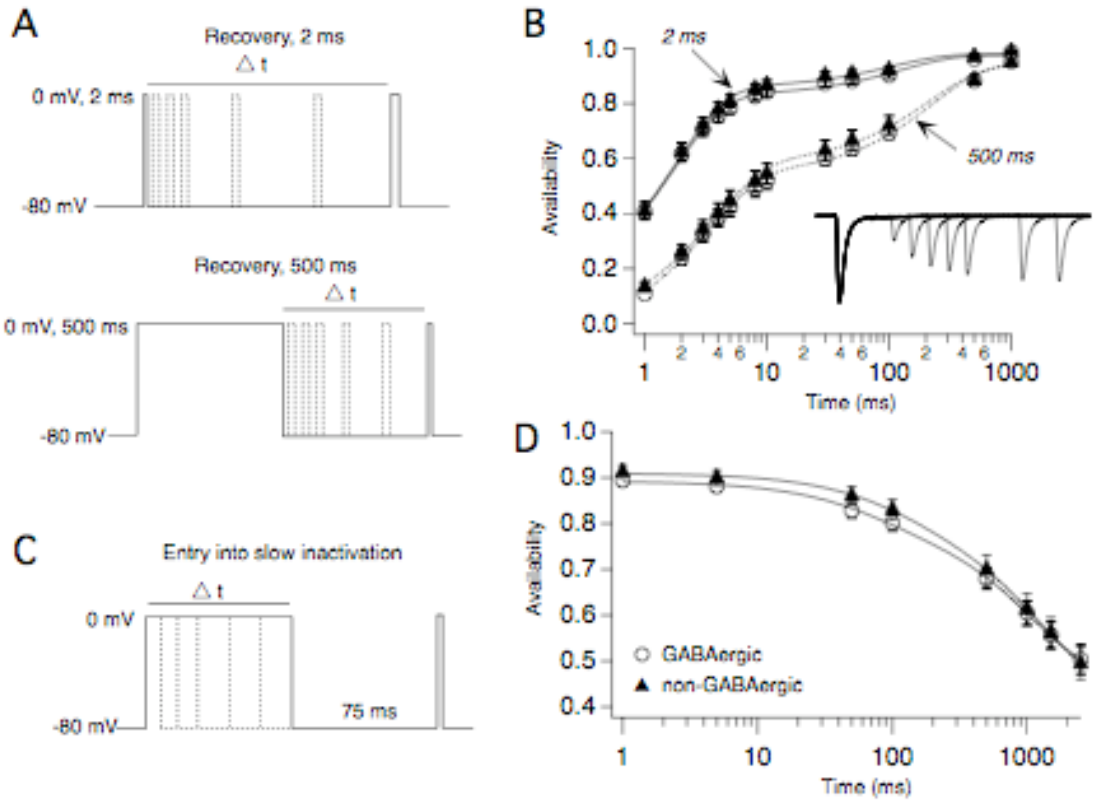

Fig. 4.2: Kinetics of recovery from inactivation are similar in GABAergic and non-GABAergic neurons **A.** Illustration of voltage protocols used to measure recovery from inactivation after a 2 ms step to 0 mV (fast inactivation) and 500 mV step to 0 mV (slow inactivation). **B.** Population averages of recovery from fast (solid line) and slow (dotted line) inactivation in GABAergic (n = 13) and non-GABAergic neurons (n = 11) , fit with double exponential functions for visual comparison. Error bars are SEM. *Inset*, Na currents, isolated by digital subtraction after 1 μM TTX application, in a non-GABAergic neuron recovering from fast inactivation. **C.** Illustration of voltage protocol used to measure the rate of entry into the slow inactivated state. **D.** Population averages of the time course of Na channel entry into the slow inactivated state in GABAergic (n = 12) and non-GABAergic neurons (n = 10), fit with a double exponential function for visual comparison. Error bars are SEM.

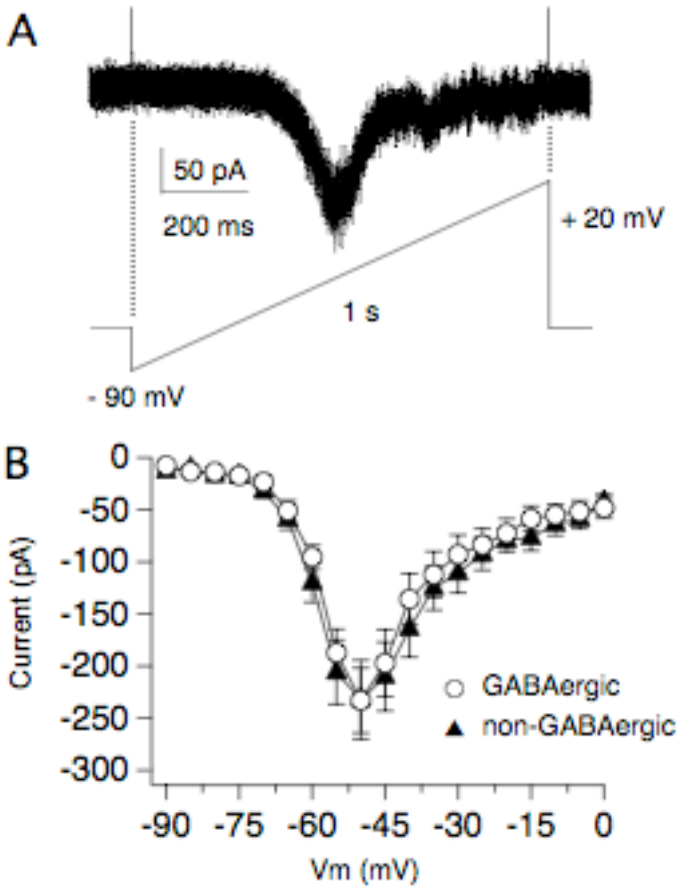

Fig. 4.3: Persistent Na currents are similar in both GABAergic and non-GABAergic neurons. **A.** A 1 µM TTX-sensitive persistent Na current (top) measured in a non-GABAergic neuron with a 115 mV/s ramp stimulus from -95 mV to + 20 mV (bottom). **B.** IV curves of the average persistent Na currents measured in GABAergic (n = 11) and non-GABAergic (n = 11) neurons. The current reached similar peak amplitudes at -50 mV in both cell types. Error bars are SEM.

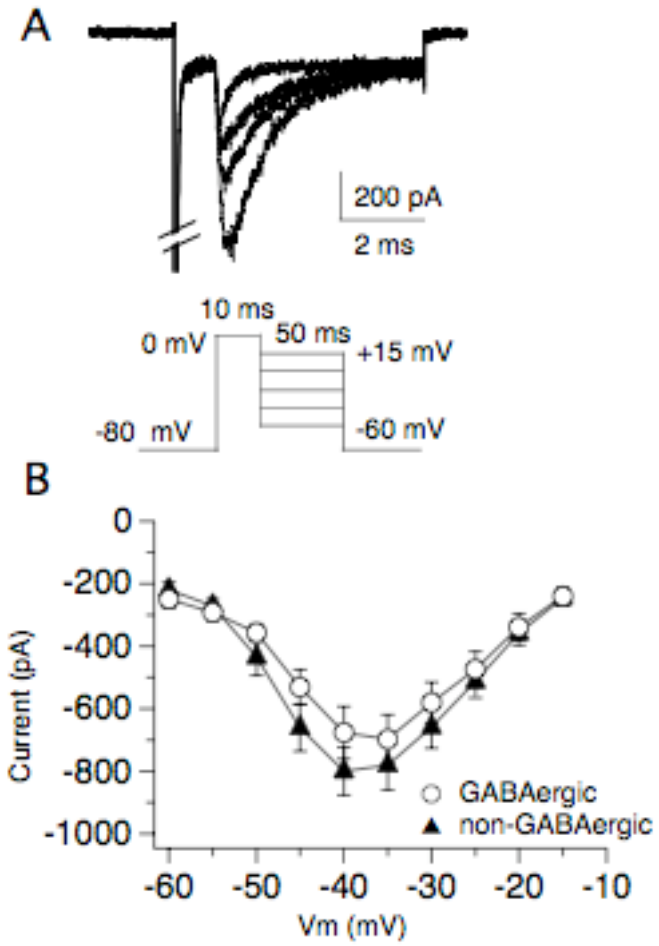

Fig. 4.4: Resurgent Na currents are similar in both GABAergic and non-GABAergic neurons. **A.** Resurgent Na currents from a non-GABAergic MVN neuron, observed at different potentials after a 10 ms voltage step to 0 mV (voltage protocol shown below). The transient current is truncated where indicated for clarity. **B.** IV curves of the average resurgent Na currents measured in GABAergic (n = 13) and non-GABAergic neurons (n = 14). Error bars are SEM. The resurgent Na currents were maximal at voltage steps to -35 mV in both cell types. Although non-GABAergic neurons tended to have more resurgent Na current, this differences was not significant ($p = 0.23$).

V: Functional regulation of ionic currents during firing establishes distinct firing properties of GABAergic and non-GABAergic neurons in the medial vestibular nuclei

Abstract

Intrinsic excitability is established through a dynamic regulation of ionic currents which shape the firing properties of neurons in a network. In the medial vestibular nuclei (MVN), ionic currents are continuously distributed across neurons but generate distinct firing properties between cell types in the circuit. The functional regulation of ionic currents that generates this cell type diversity was studied in 2 classes of MVN neurons using action potential clamp. Trains of action potentials spanning a neuron's firing range were used as voltage stimuli to measure the ionic currents activated during firing. Specific contributions from Na, Kv3, and BK currents were isolated during firing with systematic pharmacology. In GABAergic neurons, identified in the GIN line of transgenic mice, action potential repolarization was dominated by Kv3 currents at low firing rates but by BK currents at firing rates greater than 30 – 40 Hz. In non-GABAergic neurons, identified in the YFP-16 line of transgenic mice, action potential repolarization was dominated by Kv3 currents at all firing rates. This led to functional differences in Na current availability at high firing rates between these cell types because Na currents in non-GABAergic neurons were protected from inactivation by a novel Kv3-mediated mechanism. In these neurons, Kv3 currents repolarized action potentials before Na channels had fully entered inactivated or blocked states, transitioning them directly to closed states where

they would be immediately available for the next action potential. This mechanism allows non-GABAergic neurons to fire with greater temporal precision than GABAergic neurons which has important functional implications for information processing in the circuit

Introduction

Intrinsic excitability determines how synaptic inputs are converted to meaningful patterns of spike output in a neuron. The appropriate balance between these parameters sets the baseline for stable network function and provides a modulatory framework for adaptive plasticity (Marder et al., 1996; Zhang and Linden, 2003). Maintaining the appropriate level of intrinsic excitability is a dynamic process that involves the coordination of multiple ionic currents (Turrigiano et al., 1995; Desai et al., 1999; Goldman et al., 2001; Schulz et al., 2006; Pratt and Aizenman, 2007). This dynamic balance creates a parameter space in which neurons with apparently similar output properties can have different responses to plasticity-inducing stimuli (Goldman et al., 2001).

Descriptions of the behavioral correlates of adaptive changes in intrinsic excitability have come largely from invertebrate preparations, where the elegant simplicity of neural networks allows for the direct correlation between neural activity and behavior (Alkon, 1984a, b). In vertebrates, the vestibular system shares many of these attributes, where changes in intrinsic excitability underlie adaptive plasticity of the vestibular-ocular reflex (VOR) (Ris et al., 1995; Darlington and Smith, 1996; Darlington et al., 2002). Although many neurons in

the bilateral vestibular nuclei exhibit changes in intrinsic excitability during recovery from labyrinthectomy, these changes are not uniformly distributed across the heterogeneous population of neurons (Beraneck et al., 2003; Beraneck et al., 2004). Understanding how changes across neurons are coordinated to appropriately modify the output of the network requires a better understanding of the ionic mechanisms regulating excitability of distinct cell types in the vestibular nuclei.

Although all neurons in the medial vestibular nuclei (MVN) exhibit tonic, spontaneous firing and respond to depolarizing inputs with linear increases in firing rate (du Lac and Lisberger, 1995; Ris et al., 2001; Smith et al., 2002), there is considerable variability in the more specific details of their intrinsic firing properties, including differences in action potential waveforms, rebound burst firing, spike adaptation, and maximum firing rates that set the dynamic range of a neuron (Serafin et al., 1991; Sekirnjak and du Lac, 2002; Bagnall et al., 2007). Recently, the use of transgenic mouse lines has enabled the unambiguous identification of distinct cell types in the vestibular nuclei whose intrinsic firing properties cluster in distinct regions of the distribution (Sekirnjak et al., 2003; Bagnall et al., 2007).

In MVN neurons, the expression levels of potassium (K) currents vary considerably from neuron to neuron, but correlations between several currents create a unique balance of current expression between populations of GABAergic and non-GABAergic neurons with distinct firing properties (Gittis and du Lac, 2007). This differential balance of K currents likely underlies the differences in

their intrinsic firing properties because the total amplitude of outward currents is no different between the cell types and their sodium (Na) currents are similar (Gittis and du Lac, 2007; Gittis and du Lac, in press). During firing, the contribution of any one current can be hard to predict by its biophysical properties alone because its activity is often influenced by the other currents in the neuron (Ma and Koester, 1995; Ma and Koester, 1996 ; Marder, 1998). For example, two recent papers show that Kv3.3 currents mediating rapid action potential repolarization can change the gating kinetics of Na channels to better protect them from inactivation during firing (Akemann and Knopfel, 2006; Zagha et al., 2008). The fact that GABAergic and non-GABAergic MVN neurons express different balances of outward currents but similar inward : outward current ratios (Gittis and du Lac, 2007) suggests that differences in their firing properties arise through the complex regulation of their ionic currents during firing.

To measure directly how different ionic currents contribute to firing in MVN neurons, a neuron's own action potentials at multiple firing rates were used as voltage stimuli (Llinas et al., 1982; Bean, 2007) and different classes of ionic currents were isolated with systematic pharmacology. Different voltage-dependencies of ionic currents can lead to firing rate-dependent shifts in their relative contributions(Ma and Koester, 1996; Gu et al., 2007). Because the functional range of MVN neurons is hundreds of Hz *in vivo* (Cullen and Roy, 2004), these firing rate-dependent shifts are an integral part of their normal function. Our results show that in GABAergic neurons, the current driving action potential repolarization shifts from Kv3 to BK at high firing rates (> 20 – 30 Hz)

but that in non-GABAergic neurons, Kv3 currents repolarize the action potential over the entire firing range. This has important consequences for Na current availability because Kv3 currents repolarize action potentials more rapidly than BK currents, engaging a novel mechanism of Na current protection during firing in non-GABAergic neurons that is not present in most GABAergic neurons. This mechanism creates broader firing ranges in non-GABAergic compared to GABAergic neurons which may have important functional implications for information processing in the vestibular system.

Methods

Cell preparation: 350 μM coronal slices through the rostral 2/3 of the MVN were prepared with a DSK-1500E or Leica VT1000S Vibratome in carbogenated ACSF containing (in mM) 125 NaCl, 26 $NaCHO_3$, 5 KCl, 1.3 $MgCl_2$, 2.5 $CaCl_2$, 1 NaH_2PO_4, and 11 glucose. Slices were heated for 10-30 minutes at 34°C then maintained at room temperature. Neurons were enzymatically dissociated as described in Gittis and du Lac, 2007 from 24-40-day-old mice, either GIN (Oliva et al., 2000) for GABAergic neurons, or YFP-16 (Feng et al., 2000) for non-GABAergic neurons, both in c57bl6 backgrounds. Briefly, slices were treated with 40 U/mL papain (Worthington) in 9.4 mg/mL MEM powder (Gibco), 10 mM Hepes, 0.2 mM cysteine, for 10 min at 30ºC. The bilateral vestibular nuclei were removed from a slice, triturated with fire polished Pasteur pipets, and dissociated neurons were plated on the glass slide of the recording chamber.

Electrophysiological recording: For the duration of a recording session (2-3 hours), neurons were continuously perfused with oxygenated Tyrode's solution (in mM: 150 NaCl, 3.5 KCl, 2 $CaCl_2$, 1 $MgCl_2$, 10 Hepes, 10 glucose) and all recordings were done at room temperature. Whole cell recordings were made with Borosilicate pipettes (2-4 MΩ), filled with a K-gluconate based intracellular solution (in mM: 140 Kgluc, 8 NaCl, 10 Hepes, 0.02 EGTA, 2 Mg-ATP, 0.3 Na_2-GTP, and 14 Tris-creatine PO_4).

The measured liquid junction potential was +15 mV and was corrected off-line. All experiments were done at room temperature (22°C) because dissociated neurons were not stable at higher physiological temperatures.

Data were collected and analyzed using IGOR software with a MultiClamp 700B amplifier (Axon Instruments) and an ITC-16 interface (Instrutech). Upon establishment of the whole cell configuration, neurons exhibited regular, spontaneous action potentials at rates of 8.3 ± 4.8 Hz, n = 16 in GABAergic and 15.7 ± 7.7 Hz, n = 11 in non-GABAergic neurons (p = 0.007) and average membrane potentials of -65.8 ± 3.4 mV in GABAergic and -66.6 ± 2.2 mV in non-GABAergic neurons (p = 0.23) . Action potentials were recorded in current clamp mode, filtered at 10 kHz and digitized at 40 kHz. To measure action potentials at increased firing rates, neurons were injected with DC current for 1 s in 5 s intervals. Data were collected in discrete epochs, 3 s long consisting of 1 s of spontaneous firing, 1 s of firing in response to DC current injection, and 1 s of the subsequent spontaneous firing. The amplitude of current injection was

increased, usually in 40 pA intervals, until neurons could not sustain firing over the 1 s step, typically once current injections reached 200-300 pA.

Once action potentials had been collected at rates spanning a neuron's firing range, the amplifier was switched to voltage clamp mode and the 3 s epochs of action potentials were used as a command voltage. Hybrid spikes were created from a neuron's own action potentials during an experiment by detecting action potential peaks in a train, then changing the membrane voltage over a 3 ms window prior to each peak.

In voltage clamp mode, ionic currents were filtered at 8 kHz and digitized at 40 kHz. Whole cell capacitance was compensated through the amplifier circuitry and series resistance (R_{series}) was compensated at 70-90%. The average uncompensated series resistance was 2.4 ± 1.3 MΩ in GABAergic and 2.3 ± 1.2 MΩ in non-GABAergic neurons ($p = 0.66$). The capacitance was measured off the amplifier or by integrating the area of the transient following a step from -65 mV to -75 mV with whole cell capacitance and series resistance compensation turned off. Average cell capacitance was 5.9 ± 1.5 pF for GABAergic and 8.6 ± 3.3 pF for non-GABAergic neurons ($p = 0.001$).

Pharmacology: To isolate individual ionic currents during action potentials, neurons were perfused with a series of pharmacological solutions, rapidly delivered using a gravity-driven, VC-6 perfusion valve control system (Warner). Transient Na currents were measured by digital subtraction following the application of 1 μM TTX (Tocris). The next solution consisted of either 1 uM Paxilline (Tocris) to block BK currents or 2mM $MgCl_2$ in place of 2 mM $CaCl_2$ to

block Ca and KCa currents. Once BK currents had been blocked with either of the previous 2 solutions, Kv3 currents were isolated by subtraction following application of 1 mM TEA, which under these conditions is specific for Kv3-containing channels (Gittis and du Lac, 2007). In about ¼ of the neurons, 2 additional voltage-gated K currents were also measured: non-Kv3-containing delayed rectifier K currents (by subtraction after 10 mM TEA), and A-type K currents (by subtraction after 5 mM 4-AP).

Ca currents were measured by replacing 2 mM $CaCl_2$ with 2 mM $MgCl_2$ in the presence of 1 μM TTX, 1 μM Paxilline, 20 mM TEA, and 5 mM 4-AP.

In experiments where Na currents were measured to test availability during modified action potential waveforms (Fig. 7-10), K and Ca currents were first blocked with 20 mM TEA, 5 mM 4-AP and 2 mM $MgCl_2$ substituted for 2 mM $CaCl_2$. Na currents were then isolated from the currents remaining by application of 1 μM TTX.

All stock solutions were prepared in water with the exception of Paxilline which was prepared as a 20,000 x stock in DMSO. TTX, TEA, and Paxilline were stored at 4ºC, 4-AP was stored at -20ºC. Unless otherwise noted, drugs were purchased from Sigma.

Data Analysis

Action potential width and rate of repolarization were calculated from the average action potential waveform during 3 s of spontaneous firing or during steady state firing at higher frequencies (0.3 s after the onset of DC depolarization until the offset of DC current). Action potential threshold was defined s the

voltage at which the rate of membrane depolarization exceeded 10 V/s. Action potential width was measured half way between action potential threshold and peak. The rate of action potential repolarization was measured as the greatest rate of change (minimum derivative V/s) during the falling phase of the action potential. The ionic currents flowing during action potentials were aligned using the peak of the action potential as time zero. The currents were averaged once the neuron was firing in steady state (0.3 s after the onset of DC depolarization).

Statistical differences between GABAergic and non-GABAergic neurons were tested with the non-parametric Wilcoxon test for unpaired data. Changes in Na current amplitudes in response to modified action potential waveforms were tested with the Wilcoxin test for paired data. Errors reported in the text are standard deviations.

Histology

Immunohistochemistry was performed on slices from GIN or YFP-16 transgenic mice. The tissue was fixed overnight at 4°C in 4% paraformaldehyde then treated in 30% sucrose at room temperature for 1 hour before re-sectioning. The tissue was re-sectioned into 30μm sections, blocked in phosphate-buffered saline containing: 2% normal goat serum, 1% BSA, 0.3% Triton-X-100 and incubated in primary antibody overnight at 4°C. Anti-Kv3.3 was used at a concentration of 1:2500. Goat anti-rabbit secondary, conjugated to Cy3 (1:200, Chemicon) and goat anti-mouse secondary, conjugated to Alexa-fluor 488 (1:500, Molecular Probes), were used to visualize the primary antibody.

Computer model

Simulations were performed using the NEURON 6.1 simulator (Hines & Carneval 1997). All simulations used 0.005 ms time steps. The MVN cell model was based on the Type A model of Akemann and Knopfel (2006) (http://senselab.med.yale.edu/ModelDB/ShowModel.asp?model=53876). To capture the properties of fast and slow inactivation as well as resurgent kinetics in the Na current, the transient and persistent Na currents in the Akemann model were replaced with the resurgent Na current model from Khaliq et al., (2003). The sodium current was based on the 13 state, allosteric sodium channel model of Raman and Bean (2001) in the modified form described by Khaliq et al., (2003) (obtained from http://senselab.med.yale.edu/ModelDB/ShowModel.asp?model=80769).

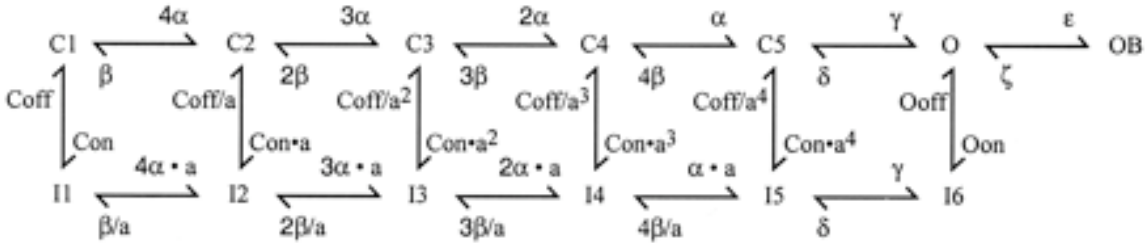

As in Goldfarb et al., (2007), the Coff parameter of the resurgent Na current was tuned to a value of 0.01 ms^{-1} to match the time course of recovery from fast and slow inactivation recorded in acutely dissociated MVN neurons (Gittis and du Lac, 2008, in press). Following a 2 ms voltage step to 0 mV, the Na current in the model was reduced to 37% its initial value compared with 41% in real neurons. Na currents in both the model and real neurons recovered exponentially with a time constant of 1.7 ms over the first 10 ms, recovering to 71% its initial value in the model and 84% its initial value in real neurons.

Following a 500 ms voltage step to 0 mV, the Na current in the model was reduced to 19% its initial value compared to 11% in real neurons. The Na current recovered exponentially over 10 ms with a time constant of 2.6 ms in the model and 2.8 ms in real neurons, recovering to 43% its initial value in the model and 52% its initial value in real neurons .

The surface area of the model MVN neurons was set to 1068.14 um^2 approximating the surface area for cells with a measured capacitance of 10 pF and the standard capacitance density of a membrane at 0.91 uF/cm^2.

The following adjustments were made to the maximal conductances set by the Akemann and Knopfel model to give good matches to experimentally recorded values of

cell excitability (aKfast (Kv3) = 0.0010667 S/cm^2; AHP (BK) = 0.0036117; A (A) =

0.003658 S/cm^2; Na leak = 3.75e-05 S/cm^2; Na = 0.022 S/cm^2). A low Kv3 condition was created by setting aKfast to 0.0003 and a high Kv3.3 condition was created by setting aKfast to 0.01. All other conductances remained the same. For comparing values across these conditions, simulations were injected with enough current to produce 60 Hz firing rates. Reversal potentials were modified to match calculated values, Na rev = +73; K rev = -92.9. The model is based on kinetics data obtained at 22°C.

Firing rates in the model were calculated by allowing the model to reach steady state and then counting the number of spikes in a 1 s period. Steady state was defined by a 1 a period with coefficient of variation less than 0.003.

Results

Intrinsic firing properties are preserved in acutely dissociated neurons

To achieve good space clamp, recordings were made from acutely dissociated neurons (Gittis and du Lac, 2007). Differences in action potential waveforms are preserved in this preparation (Gittis and du Lac, 2007), but previous studies did not address whether other aspects of intrinsic firing properties are preserved as well. To determine whether MVN neurons retain their linear input-output firing responses and high maximum firing rates in the acutely dissociated cell preparation, their firing rates were measured in response to 1 s depolarizing current injections of increasing intensity until neurons were unable to sustain firing across the step (Fig. 1A).

Similar to neurons in slice, dissociated MVN neurons linearly increased their firing rates in response to depolarizing current injections, but had lower maximum firing rates on average (101 ± 53 Hz vs. 213 ± 114 Hz, $p < 0.0001$) (Fig. 1B). Dissociated neurons that could fire > 100 Hz were less linear in this upper range than neurons in slice, suggesting that dendritic conductances are particularly important in this range. However, some dissociated neurons could still fire up to 250 Hz. Importantly for this study, cell type differences in maximum firing rate between GABAergic and non-GABAergic neurons were preserved (72 ± 35 Hz, GABAergic vs. 148 ± 58 Hz, non-GABAergic, $p = 0.0002$). Figure 1B shows that these differences in maximum firing rate were well correlated with differences in action potential widths described previously

(Gittis and du Lac, 2007), particularly in the non-GABAergic population with action potential widths < 0.8 ms (Fig. 1B).

Activation of ionic currents during firing

To measure how ionic currents in MVN neurons are engaged during firing, trains of a neuron's own action potentials were recorded and used as a voltage stimulus in the same cell. At spontaneous firing rates (~ 5 – 25 Hz), large inward and outward currents were active during action potentials but the net current flow in between spikes was virtually zero (Fig. 2A). Specific currents contributing to the generation and repolarization of action potentials were isolated with systematic pharmacology and averaged across spikes (Fig. 2B).

The rising phase of the action potential was driven by TTX-sensitive Na currents, which were larger in non-GABAergic (4.8 ± 1.4 nA, n = 11) vs. GABAergic neurons (3.0 ± 0.9 nA, n = 17, p = 0.002) (Fig. 2B-C). Towards the peak of the action potential, small inward Ca currents began to activate and reached peak amplitudes during the falling phase of the action potential of 365 ± 121 pA, n = 7 in GABAergic and 383 ± 64 pA, n = 4 in non-GABAergic neurons (p = 0.52).

At spontaneous firing rates, 1 mM TEA-sensitive Kv3-type K currents were nearly 3-fold larger in non-GABAergic (2.9 ± 1.1 nA. n = 11) vs. GABAergic neurons (1.2 ± 0.6 nA, n = 17, p = 0.0001) and dominated action potential repolarization, reflected by the tight correlation between Kv3 current amplitude and rate of action potential repolarization (r^2 = 0.74) (Fig. B-D). Small,

paxilline-sensitive BK-type K currents were also present during repolarization in both cell types, but their contribution to repolarization was only apparent in a subset of GABAergic neurons with small Kv3 currents (Fig. 2B). BK current amplitudes were small in both non-GABAergic (335 ± 180 pA, n = 5) and GABAergic neurons (410 ± 264 pA, n = 10, p = 0.54) (Fig. 2C).

At least 2 other voltage-gated K currents are expressed in MVN neurons: 10 mM TEA-sensitive delayed rectifier currents and 4 AP-sensitive A-type currents (Gittis and du Lac, 2007). Although these currents contributed about 30% of the total outward current during step depolarizations of 150-300 ms, these currents were not substantially activated during firing.

Na current availability determines firing range of neurons

The ability of a neuron to generate action potentials depends critically on the availability of its Na currents. To measure changes in the functional availability of Na currents during action potentials across a neuron's firing range, neurons were driven to fire at increasing frequencies with DC current injection until action potentials could not be sustained across the 1 s step. These trains of action potentials were then used as the voltage stimuli to measure the amplitude of TTX-sensitive Na currents during firing at different frequencies (Fig. 3A). As neurons approached their maximum firing rates, action potentials became shorter and broader. Na current amplitudes steeply declined over the first few action potentials in a train to reach a steady-state value within ~15 ms. Neurons could

not sustain firing across the step once Na current amplitudes dropped bellow 0.5 – 1.5 nA (data not shown).

The steady-state amplitude of Na currents during action potentials decreased exponentially with firing rate, shown for 3 neurons in Fig. 3B. The neurons selected had similar Na current amplitudes during spontaneous firing but different rates of Na current decline, resulting in a 2.4-fold difference in maximum firing rate. The range over which Na currents declined by 2/3 was significantly smaller ($p < 0.0001$) in GABAergic (54.5 ± 88 Hz, n = 15) vs. non-GABAergic neurons (502 ± 558 Hz, n = 10) (Fig. 3C). These results demonstrate that Na currents are better protected from inactivation during firing in non-GABAergic vs. GABAergic neurons, even when Na current availability was similar at spontaneous firing rates.

Changes in current ratios over a neuron's firing range

Neurons required at least 500 pA of outward current during action potential repolarization to maintain firing across a 1 s step (data not shown). In non-GABAergic neurons, Kv3 currents decayed exponentially as a function of firing rate, reaching 2/3 amplitude by 131 ± 103 Hz (n = 8). Given their large amplitudes to start with, they still provided the majority of the current driving action potential repolarization across a neuron's firing range (Fig. 4A-B). In GABAergic neurons, Kv3 currents were smaller and decayed more rapidly with firing rate ($p = 0.003$), reaching 2/3 amplitude by 30 ± 29 Hz (n = 12). As a result, Kv3 current amplitudes in GABAergic neurons were typically < 500 pA by

the time neurons were firing 30-40 Hz, too small to sufficiently repolarize action potentials alone (Fig. 4C-D). BK currents did not decline exponentially as a function of firing rate, resulting in a shift from Kv3-dominated action potential repolarization to BK-dominated action potential repolarization at frequencies beyond 30 – 40 Hz in most GABAergic neurons.

Kv3 currents protect Na currents from inactivation

Although both Kv3 and BK currents can drive action potential repolarization, the more Kv3 current a neuron expresses, the narrower its action potentials and the faster it can fire (Fig. 2D), suggesting that Kv3 currents preferentially enhance Na current availability. To test this hypothesis, trains of action potentials were recorded from neurons before and after application of 1 mM TEA to block Kv3 currents (Fig. 5A). Neurons with narrow action potentials (0.53 ± 0.13 ms, n = 7) were used to select for cells with large Kv3 currents.

Application of 1 mM TEA slowed action potential repolarization by 72 ± 7% and increased action potential width from 0.53 ± 0.13 ms to 1.19 ± 0.29 ms (n = 7) (Fig. 5B). These changes were specific for the effect of 1 mM TEA on Kv3 currents because application of paxilline to block BK currents (which are also sensitive to 1 mM TEA) only slowed action potential repolarization by 4.4 ± 6% (n = 3).

Blocking fast Kv3-mediated action potential repolarization had only modest effects on the amplitude of Na currents driving action potentials at spontaneous firing rates, reducing them by only 10 ± 12%, n = 7 (Fig. 5A). In

contrast, 1 mM TEA strongly affected Na currents flowing during action potential repolarization, representing the presence of Na channels that have escaped inactivation during the action potential (Fig. 5A, inset). Blocking fast Kv3-mediated repolarization decreased the amplitude of this protected current by 58 ± 16%, from 1250 ± 680 pA to 460 ± 240 pA and delayed its peak (relative to the peak of the action potential) by 1.0 ± 0.6 ms, from 1.3 ± 1.6 ms to 2.3 ± 1.2 ms.

One way Na channels can avoid inactivation during an action potential is through a resurgent Na current mechanism, first described in Purkinje cells and now recognized in a number of other fast firing cell types, including MVN neurons. To test for the presence of this mechanism during firing, neurons were depolarized for 3 ms to drive all of their Na channels into either inactivated or blocked states, then allowed to repolarize following their natural trajectory, releasing the blocking particle from channels that had escaped inactivation and generating a resurgent Na current (Do and Bean, 2003; Enomoto et al., 2006). The amplitude of the resurgent Na current measured with this hybrid spike protocol was 286 ± 167 pA (n = 7), only 26 ± 13% the size of the protected Na current during repolarization measured with the natural waveform (Fig. 5B). When action potential repolarization was slowed with 1 mM TEA, the amplitude of the resurgent Na current did not change significantly (286 ± 167 pA vs. 335 ± 184 pA, n = 7, p = 0.35), but its amplitude was almost as large (77 ± 20%) as the total protected Na current observed during the natural waveform when Kv3-mediated repolarization was blocked (Fig. 5C).

These data suggest that during firing, Na channels in MVN neurons can be protected from inactivation by at least 2 mechanisms. One mechanism is the resurgent Na current mechanism, due to the biophysical properties of Na channels expressed in MVN neurons. The other is a novel mechanism of Na current protection that precedes the resurgent mechanism, mediated by rapid action potential repolarization driven by Kv3 currents. The most likely mechanistic explanation for this novel form of protection is that Kv3 currents repolarize the membrane so quickly that some Na channels have not yet entered either the inactivated or blocked states. This produces a Na tail current through open channels during membrane repolarization.

Computer model of Na current protection by Kv3 currents

To test the hypothesis that Na channels could be protected from inactivation via a resurgent-independent mechanism under conditions of rapid membrane repolarization, trajectories for the state variables of the Na channel under different conditions of Kv3 conductance were tested in a computer model of an MVN neuron (see Methods). Figure 6 shows the state variable transitions of the Na channel and the current it produces under conditions of high, medium, and low Kv3 conductances. These changes in Kv3 conductance alone changed the maximum firing rate of the model neuron from 96 Hz (low) to 131 Hz (medium) to 176 Hz (high).

For comparison across conditions, simulations were run at matched firing rates of 60 Hz. Under conditions of high Kv3, the action potential width was 0.6

ms and Na current kinetics were similar to those measured under conditions of high Kv3 in real neurons (Fig. 5A). Under conditions of medium and low Kv3, action potential widths were broader (1.3 ms and 2.3 ms) and the amplitude of the Na current during the action potential and its kinetics during repolarization were distinct from those observed during the high Kv3 condition (Fig. 6B).

An analysis of the state transitions during firing revealed that with increasing levels of Kv3 conductance, the inactivation variable showed markedly less inactivation, but the peak amount of blocking increased only slightly. Instead, decreases in the inactivation variable could be attributed to increases in the closed variable. These behaviors are consistent with the idea of a mechanism of protection from inactivation that drives more Na current to a closed state with larger Kv3 conductances. By protecting Na current from inactivating, increased Kv3 conductance was capable of allowing neurons to reach higher maximal firing rates.

Na current are protected by Kv3 in non-GABAerigic but not GABAerigic neurons

The ability of Kv3 currents to protect Na currents from inactivation by driving them directly from open to closed states has been demonstrated with both recordings from fast repolarizing non-GABAergic neurons and computer simulations with high levels of Kv3 conductance. To determine how this mechanism of protection is utilized across the population of MVN neurons and whether it can account for cell-type differences in maximum firing rates, 2 trains of action potentials with different repolarization rates were used. The action

potential trains were pre-recorded from (1) a GABAergic neuron with a slow rate of action potential repolarization (76 V/s, action potential width = 1.1 ms) ("slow stimulus") and (2) a non-GABAergic neuron with an intermediate rate of action potential repolarization (125 V/s, action potential width =0.74 ms) ("fast stimulus") (Fig. 7A). The repolarization rate of the "fast stimulus" is consistent with repolarization driven largely by Kv3 currents, where as the repolarization rate of the "slow stimulus" is consistent with neurons in which repolarization is driven by a more equal contribution of Kv3 and BK currents.

The amplitude of the Na current protected by the "fast stimulus" was significantly larger than the amplitude of the current protected by the "slow stimulus" (323 ± 139 vs. 155 ± 87 pA, n = 10, p =0.002) (Fig. 7A). To determine whether this reflected different mechanisms of Na current protection (fast-close vs. resurgent), the amount of current predicted by a purely resurgent mechanism was estimated using the hybrid spike stimulus. The amount of Na current protected following the "fast stimulus" had faster kinetics and was 61 ± 9 % larger than that expected by the resurgent mechanism alone (322 ± 139 pA vs. 126 ± 61 pA, n = 10) (Fig. 7B). In contrast, the amount of protected current in response to the "slow stimulus" had similar kinetics as that generated by the resurgent mechanism alone and was only 18 ± 16 % larger (155 ± 88 pA vs. 122 ±58 pA, n = 10, p = 0.01) (Fig. 7C).

Across neurons, variability in Na current protection was correlated with action potential width, particularly for action potentials narrower than 0.8 ms (Fig. 7D). From Fig. 1B, most non-GABAergic neurons have action potential widths

narrower than 0.8 ms and most GABAergic neurons have action potential widths wider than 0.8 ms. These results suggest that Kv3 currents particularly in non-GABAergic neurons are tuned to mediate rapid action potential repolarization capable of protecting Na currents from inactivation, even before the resurgent mechanism fully engages.

To determine whether differences in Kv3 currents between GABAergic and non-GABAergic neurons had a molecular basis, brain sections from YFP-16 (non-GABAergic) and GIN (GABAergic) transgenic mouse lines were stained with antibodies against Kv3 subunits Kv3.1-Kv3.4. A particularly strong cell-type distinction eas observed for the expression pattern of Kv3.3. In non-GABAergic neurons 55 / 60 YFP+ neurons were positive for Kv3.3 (92 %) (Fig. 7E). In contrast, 0 / 65 GIN+ neurons were positive for Kv3.3 (Fig. 7F).

Fast Kv3-mediated repolarization enhances Na current availability at firing rates > 70

The model predicts that Na current protection by Kv3 currents influences a neuron's maximum firing rate. But at spontaneous firing rates, only subtle differences were observed in Na current availability when Kv3 currents were present vs. when they were absent (Fig. 5A). To determine at what firing rates Kv3-mediated protection of Na currents becomes functionally relevant to a neuron's firing capability, Na current availability with and without Kv3-mediated protection was measured in real neurons at different firing frequencies (Fig. 8). The stimuli for this experiment were generated from action potentials recorded

before and after application of 1 mM TEA in a neuron with an action potential width of 0.48 ms and a maximum firing rate of 162 Hz. Application of 1 mM TEA slowed action potential repolarization from 196 V/s to 65 V/s (corresponding to a broadening of the action potential from 0.48 ms to 1.0 ms) and reduced the maximum firing rate from 162 Hz to 69 Hz. The stimuli consisted of 2 action potentials, both recorded in ACSF at 20, 55, 88, 100, or 127 Hz (Fig. 8A). On some trials, the repolarization phase of the first action potential was substituted with the repolarization phase from an action potential whose fast repolarization mediated by Kv3 currents had been blocked with 1 mM TEA (Fig. 8B-C). After action potential repolarization, the membrane voltage was dropped to match that of the first condition and followed the same trajectory leading up to the second action potential to minimize. This was done to minimze differences in the membrane potential during the inter-spike interval, caused by reductions in the depth of the AHP when Kv3 currents are blocked.

Action potential repolarization in ACSF was sufficiently fast at all frequencies to protect Na currents from inactivation (Fig. 8A). When the rate of action potential repolarization was slowed by 1 mM TEA, the amplitude of the protected Na current was reduced and the kinetics were slowed to a rate consistent with a shift towards protection by the resurgent mechanism alone (Fig. 8B). The extent to which Kv3-mediate protection influenced Na current availability was measured by comparing the ratio of the Na current flowing during the 2^{nd} action potential compared to the first (Fig. 8C-D).

Across neurons, the rate of action potential repolarization had little affect on the availability of Na currents at firing rates < 55 Hz. At 20 Hz, blocking fast action potential repolarization only reduced Na current availability for the next action potential by 3 ± 3 % (n = 9) and at 55 Hz, availability was reduced by 14 ± 6 %. As firing rate became faster, the lack of Kv3-mediated action potential repolarization had a larger effect on Na current availability. At 88 Hz, Na current availability for the second action potential was reduced by 33 ± 5 % and remained reduced by 33 ± 7 % and by 35 ± 6 % at firing rates of 100 Hz and 127 Hz, respectively. These data suggest that the amount of Na current protection by Kv3 currents plays an important role in providing sufficient Na current availability to sustain firing at rates > 70 Hz, the approximate firing rate which divides the majority of GABAergic from non-GABAergic neurons in the population (Fig. 1A).

Discussion

Balance of currents is dynamically regulated over a neuron's firing range

In the MVN, GABAergic and non-GABAergic MVN neurons express a combination of BK and Kv3 currents whose relative ratios vary continuously across the population (Gittis and du Lac, 2007). At low firing rates, both BK and Kv3 currents are active during action potential repolarization, but Kv3 currents dominate in most neurons. The relative contributions from BK and Kv3 currents change as firing rates increase and in GABAergic neurons, action potential repolarization shifts from a Kv3-mediated process to a BK-mediated one at firing

rates > 30-40 Hz. Given that MVN neurons operate over firing ranges of hundereds of Hz *in vivo* (Cullen and Roy, 2004), this firing rate-dependent shift is likely to occur during normal signal processing in the circuit. Changes in the relative proportions of currents have been reported at different firing rates in other neurons (Ma and Koester, 1995, 1996; McKay and Turner, 2004; Gu et al., 2007), but this is the first example of a change in the dominant current driving action potential repolarization over a neuron's natural range of frequencies.

The shift from Kv3-mediated to BK-mediated action potential repolarization in GABAergic neurons was facilitated by the different voltage-dependent properties of Kv3 and BK currents. Kv3 currents are purely voltage-gated channels but the voltage-dependence of BK currents is influenced by intracellular calcium concentrations (Vergara et al., 1998). In MVN neurons, Kv3 current amplitudes decline exponentially with Na current amplitudes at elevate firing rates but BK current amplitudes remain more constant across the firing range. This creates a cellular system in GABAergic neurons where Kv3 currents repolarize action potentials at low firing rates, but when their amplitudes become too small at high firing rates, the presence of BK currents provides a failsafe mechanism to sustain firing. MVN neurons continue to act as linear filters over the course of this transition, demonstrating their precise functional coordination of ionic currents during firing.

Across many areas of the brain, Kv3 and BK currents can mediate action potential repolarization, however it has generally been observed that cells that sustain higher firing rates utilize Kv3 currents (Wang et al., 1998; Raman and

Bean, 1999; Rudy and McBain, 2001; Matsukawa et al., 2003; Kasten et al., 2007) and cells with lower firing rates utilize BK currents (Storm, 1987; Chen et al., 1996). Typically cells that rely on Kv3 have comparatively narrower action potentials than neurons that rely on BK. In fast firing neurons, the voltage dependence and kinetics of Kv3 currents are specifically tuned to facilitate the rapid generation and repolarization of action potentials which facilitates a high level of temporal precision (Erisir et al., 1999; Lien and Jonas, 2003; Macica et al., 2003; Kaczmarek et al., 2005). In slower firing neurons, BK control of action potential repolarization facilitates spike broadening (Shao et al., 1999; Gu et al., 2007) which may carry a history-dependent signal of neuronal activity important for short-term plasticity (Byrne and Kandel, 1996). This dichotomy has potentially important functional consequences for the 2 classes of cells studied in the MVN.

Tuning of firing properties by Kv3 currents during action potential repolarization

Voltage-gated Na channels are central to neuronal excitability for their fundamental role in action potential generation. During firing, Na current availability is limited by the entry of channels into inactivated states that develop during membrane depolarization (Armstrong, 1981; Stuhmer et al., 1989; Mitrovic et al., 2000). Na channels in MVN neurons, as in most other fast firing neurons, have biophysical properties tuned to minimize the accumulation of inactivation (Martina and Jonas, 1997; Raman and Bean, 1997; Leao et al., 2005)(Gittis and du Lac, in press), but inactivation still accumulates during firing,

causing an exponential decline in Na current amplitude. Although the biophysical properties of Na currents are similar between GABAergic and non-GABAergic MVN neurons (Gittis and du Lac, 2008, in press), Na currents in GABAergic neurons accumulate inactivation more quickly during firing than Na currents in non-GABAergic neurons, creating cell-type differences in maximum firing rates. This suggests the presence of distinct ionic mechanisms regulating Na current availability during firing that likely arise from interactions with other ionic currents.

Likely candidates are Kv3 currents, which are exceptional in their ability to protect Na currents from inactivation during firing (Erisir et al., 1999). Two recent papers use computer models to suggest that Kv3 currents influence Na current availability by changing the rate at which the channels enter and leave the blocked state (Akemann and Knopfel, 2006; Zagha et al., 2008), a gating mechanism that protects Na channels from inactivation in fast firing neurons (Raman and Bean, 1997, 2001; Khaliq et al., 2003; Mercer et al., 2007).

In this study, a combined approach of modeling and electrophysiology shows that rapid membrane repolarization mediated by Kv3 in most non-GABAergic MVN neurons is sufficiently fast to protect Na channels from inactivation by direct transitions from the open to closed state, precluding their entry into the inactivated or blocked states. This is a different mechanism of protection than that previously described in Purkinje cells (Akemann and Knopfel, 2006; Zagha et al., 2008). Electrophysiological recordings support the predictions of the model and suggest that Na currents are well protected by this

mechanism in non-GABAergic neurons but not in most GABAergic neurons, where action potential repolarization mediated by BK currents is slower. In GABAergic neurons, most Na currents that escape inactivation during firing are protected by the resurgent mechanism. At low firing rates, the functional consequences of these different protection mechanisms are indistinguishable, but at higher firing rates, particularly > 60 Hz, differences in Na current availability are more apparent. It is approximately this frequency range that distinguishes the maximum firing rates of GABAergic from non-GABAergic neurons, suggesting this mechanism establishes cell-type diversity in the MVN.

Expression of Kv3.3 differentiates GABAergic and non-GABAergic neurons in the MVN

The expression of Kv3.3 channels is particularly abundant in brainstem and cerebellar structures (Chang et al., 2007) and mutations or deletions of this subunit result in movement disorders and altered olivocerebellar functioning (Joho et al., 2006; Waters et al., 2006) (McMahon et al., 2004). Kv3.3 channels are particularly important for Purkinje cell physiology where they regulate both tonic firing (Akemann and Knopfel, 2006) and complex spike activity (Zagha et al., 2008).

Although all 4 major isoforms of Kv3 channels are present in the MVN (Weiser et al., 1994; Weiser et al., 1995), Kv3.3 subunits show the highest level of cell type-specific expression. Approximately 90% of non-GABAergic neurons labeled in the YFP-16 line of transgenic mice express Kv3.3 but this isoform is not present in GABAergic neurons labeled in the GIN line of transgenic mice.

These mouse lines also distinguish neurons with distinct roles in the vestibular circuit (Bagnall et al., 2007)(B. Zingg, unpublished). GABAergic neurons labeled in the GIN line of transgenic mice are probably local inhibitory neurons where as non-GABAergic neurons labeled in the YFP-16 line of transgenic mice are projection neurons. This suggests that the expression of Kv3.3 subunits distinguishes projection from intrinsic neurons in the vestibular circuit.

Ionic diversity provides stability and flexibility to the vestibular system

The vestibular system consists of networks of fast firing neurons where the temporal precision of its projection neurons exceeds that of its local inhibitory neurons (Bagnall et al., 2007). Ionic currents must be tuned to support this framework while at the same time providing variability of firing properties within a cell type, required for the distributive nature of vestibular processing. These data suggest one mechanism through which this is accomplished. Na current availability is dynamically regulated by the relative expression levels of Kv3 and BK currents across neurons. In non-GABAergic neurons, Kv3 currents regulate Na current availability by rapid action potential repolarization, whose variability is established by Kv3 current expression levels and kinetics across neurons. In GABAergic neurons, Na current availability is determined by BK currents and the resurgent kinetics of the Na channels themselves, both properties which have also been demonstrated to vary across neurons.

This framework provides an opportunity for cell type-specific expression of plasticity. For example, the downregulation of BK currents during firing rate

potentiation (FRP) (Nelson et al., 2003) might change the firing properties of GABAergic neurons, but have less of an effect on non-GABAergic neurons that do not rely on BK currents for action potential repolarization. Other potential mechanisms for cell type-sepcific plasticity would be the selective modulation of resurgent Na channel kinetics by phosphorylation (Grieco et al., 2002) or regulation of Kv3 currents by phosphorylation (Song et al., 2005; Song and Kaczmarek, 2006) or changes in accessory subunits (McCrossan et al., 2003; Lewis et al., 2004).

Acknowledgements

Chapter 5 is original work in preparation as Gittis AH, Larson SD, Mogadam S, du Lac S. Functional regulation of ionic currents during firing establishes distinct firing properties of GABAergic and non-GABAergic neurons in the medial vestibular nuclei and is included with permission from all the manuscript's authors. The dissertation author was the primary author of this paper.

References

Akemann W, Knopfel T (2006) Interaction of Kv3 potassium channels and resurgent sodium current influences the rate of spontaneous firing of Purkinje neurons. J Neurosci 26:4602-4612.

Alkon DL (1984a) Calcium-mediated reduction of ionic currents: a biophysical memory trace. Science 226:1037-1045.

Alkon DL (1984b) Changes of membrane currents during learning. J Exp Biol 112:95-112.

Armstrong CM (1981) Sodium channels and gating currents. Physiol Rev 61:644-683.

Bagnall MW, Stevens RJ, du Lac S (2007) Transgenic mouse lines subdivide medial vestibular nucleus neurons into discrete, neurochemically distinct populations. J Neurosci 27:2318-2330.

Bean BP (2007) The action potential in mammalian central neurons. Nat Rev Neurosci 8:451-465.

Beraneck M, Idoux E, Uno A, Vidal PP, Moore LE, Vibert N (2004) Unilateral labyrinthectomy modifies the membrane properties of contralesional vestibular neurons. J Neurophysiol 92:1668-1684.

Beraneck M, Hachemaoui M, Idoux E, Ris L, Uno A, Godaux E, Vidal PP, Moore LE, Vibert N (2003) Long-term plasticity of ipsilesional medial vestibular nucleus neurons after unilateral labyrinthectomy. J Neurophysiol 90:184-203.

Byrne JH, Kandel ER (1996) Presynaptic facilitation revisited: state and time dependence. J Neurosci 16:425-435.

Chang SY, Zagha E, Kwon ES, Ozaita A, Bobik M, Martone ME, Ellisman MH, Heintz N, Rudy B (2007) Distribution of Kv3.3 potassium channel subunits in distinct neuronal populations of mouse brain. J Comp Neurol 502:953-972.

Chen W, Zhang JJ, Hu GY, Wu CP (1996) Different mechanisms underlying the repolarization of narrow and wide action potentials in pyramidal cells and interneurons of cat motor cortex. Neuroscience 73:57-68.

Cullen KE, Roy JE (2004) Signal processing in the vestibular system during active versus passive head movements. J Neurophysiol 91:1919-1933.

Darlington CL, Smith PF (1996) The recovery of static vestibular function following peripheral vestibular lesions in mammals: the intrinsic mechanism hypothesis. J Vestib Res 6:185-201.

Darlington CL, Dutia MB, Smith PF (2002) The contribution of the intrinsic excitability of vestibular nucleus neurons to recovery from vestibular damage. Eur J Neurosci 15:1719-1727.

Desai NS, Rutherford LC, Turrigiano GG (1999) Plasticity in the intrinsic excitability of cortical pyramidal neurons. Nat Neurosci 2:515-520.

Do MT, Bean BP (2003) Subthreshold sodium currents and pacemaking of subthalamic neurons: modulation by slow inactivation. Neuron 39:109-120.

du Lac S, Lisberger SG (1995) Cellular processing of temporal information in medial vestibular nucleus neurons. J Neurosci 15:8000-8010.

Enomoto A, Han JM, Hsiao CF, Wu N, Chandler SH (2006) Participation of sodium currents in burst generation and control of membrane excitability in mesencephalic trigeminal neurons. J Neurosci 26:3412-3422.

Erisir A, Lau D, Rudy B, Leonard CS (1999) Function of specific K(+) channels in sustained high-frequency firing of fast-spiking neocortical interneurons. J Neurophysiol 82:2476-2489.

Feng G, Mellor RH, Bernstein M, Keller-Peck C, Nguyen QT, Wallace M, Nerbonne JM, Lichtman JW, Sanes JR (2000) Imaging neuronal subsets in transgenic mice expressing multiple spectral variants of GFP. Neuron 28:41-51.

Gittis AH, du Lac S (2007) Firing properties of GABAergic versus non-GABAergic vestibular nucleus neurons conferred by a differential balance of potassium currents. J Neurophysiol 97:3986-3996.

Goldfarb M, Schoorlemmer J, Williams A, Diwakar S, Wang Q, Huang X, Giza J, Tchetchik D, Kelley K, Vega A, Matthews G, Rossi P, Ornitz DM, D'Angelo E (2007) Fibroblast growth factor homologous factors control neuronal excitability through modulation of voltage-gated sodium channels. Neuron 55:449-463.

Goldman MS, Golowasch J, Marder E, Abbott LF (2001) Global structure, robustness, and modulation of neuronal models. J Neurosci 21:5229-5238.

Grieco TM, Afshari FS, Raman IM (2002) A role for phosphorylation in the maintenance of resurgent sodium current in cerebellar purkinje neurons. J Neurosci 22:3100-3107.

Gu N, Vervaeke K, Storm JF (2007) BK potassium channels facilitate high-frequency firing and cause early spike frequency adaptation in rat CA1 hippocampal pyramidal cells. J Physiol 580:859-882.

Hines ML and Carnevale NT (1997) The NEURON simulation environment. Neural Comput 9:1179-209.

Joho RH, Street C, Matsushita S, Knopfel T (2006) Behavioral motor dysfunction in Kv3-type potassium channel-deficient mice. Genes Brain Behav 5:472-482.

Kaczmarek LK, Bhattacharjee A, Desai R, Gan L, Song P, von Hehn CA, Whim MD, Yang B (2005) Regulation of the timing of MNTB neurons by short-term and long-term modulation of potassium channels. Hear Res 206:133-145.

Kasten MR, Rudy B, Anderson MP (2007) Differential regulation of action potential firing in adult murine thalamocortical neurons by Kv3.2, Kv1, and SK potassium and N-type calcium channels. J Physiol 584:565-582.

Khaliq ZM, Gouwens NW, Raman IM (2003) The contribution of resurgent sodium current to high-frequency firing in Purkinje neurons: an experimental and modeling study. J Neurosci 23:4899-4912.

Leao RM, Kushmerick C, Pinaud R, Renden R, Li GL, Taschenberger H, Spirou G, Levinson SR, von Gersdorff H (2005) Presynaptic Na+ channels: locus, development, and recovery from inactivation at a high-fidelity synapse. J Neurosci 25:3724-3738.

Lewis A, McCrossan ZA, Abbott GW (2004) MinK, MiRP1, and MiRP2 diversify Kv3.1 and Kv3.2 potassium channel gating. J Biol Chem 279:7884-7892.

Lien CC, Jonas P (2003) Kv3 potassium conductance is necessary and kinetically optimized for high-frequency action potential generation in hippocampal interneurons. J Neurosci 23:2058-2068.

Llinas R, Sugimori M, Simon SM (1982) Transmission by presynaptic spike-like depolarization in the squid giant synapse. Proc Natl Acad Sci U S A 79:2415-2419.

Ma M, Koester J (1995) Consequences and mechanisms of spike broadening of R20 cells in Aplysia californica. J Neurosci 15:6720-6734.

Ma M, Koester J (1996) The role of K+ currents in frequency-dependent spike broadening in Aplysia R20 neurons: a dynamic-clamp analysis. J Neurosci 16:4089-4101.

Macica CM, von Hehn CA, Wang LY, Ho CS, Yokoyama S, Joho RH, Kaczmarek LK (2003) Modulation of the kv3.1b potassium channel isoform adjusts the fidelity of the firing pattern of auditory neurons. J Neurosci 23:1133-1141.

Marder E (1998) From biophysics to models of network function. Annu Rev Neurosci 21:25-45.

Marder E, Abbott LF, Turrigiano GG, Liu Z, Golowasch J (1996) Memory from the dynamics of intrinsic membrane currents. Proc Natl Acad Sci U S A 93:13481-13486.

Martina M, Jonas P (1997) Functional differences in Na+ channel gating between fast-spiking interneurones and principal neurones of rat hippocampus. J Physiol 505 (Pt 3):593-603.

Matsukawa H, Wolf AM, Matsushita S, Joho RH, Knopfel T (2003) Motor dysfunction and altered synaptic transmission at the parallel fiber-Purkinje cell synapse in mice lacking potassium channels Kv3.1 and Kv3.3. J Neurosci 23:7677-7684.

McCrossan ZA, Lewis A, Panaghie G, Jordan PN, Christini DJ, Lerner DJ, Abbott GW (2003) MinK-related peptide 2 modulates Kv2.1 and Kv3.1 potassium channels in mammalian brain. J Neurosci 23:8077-8091.

McKay BE, Turner RW (2004) Kv3 K+ channels enable burst output in rat cerebellar Purkinje cells. Eur J Neurosci 20:729-739.

McMahon A, Fowler SC, Perney TM, Akemann W, Knopfel T, Joho RH (2004) Allele-dependent changes of olivocerebellar circuit properties in the absence of the voltage-gated potassium channels Kv3.1 and Kv3.3. Eur J Neurosci 19:3317-3327.

Mercer JN, Chan CS, Tkatch T, Held J, Surmeier DJ (2007) Nav1.6 sodium channels are critical to pacemaking and fast spiking in globus pallidus neurons. J Neurosci 27:13552-13566.

Mitrovic N, George AL, Jr., Horn R (2000) Role of domain 4 in sodium channel slow inactivation. J Gen Physiol 115:707-718.

Nelson AB, Krispel CM, Sekirnjak C, du Lac S (2003) Long-lasting increases in intrinsic excitability triggered by inhibition. Neuron 40:609-620.

Oliva AA, Jr., Jiang M, Lam T, Smith KL, Swann JW (2000) Novel hippocampal interneuronal subtypes identified using transgenic mice that express green fluorescent protein in GABAergic interneurons. J Neurosci 20:3354-3368.

Pratt KG, Aizenman CD (2007) Homeostatic regulation of intrinsic excitability and synaptic transmission in a developing visual circuit. J Neurosci 27:8268-8277.

Raman IM, Bean BP (1997) Resurgent sodium current and action potential formation in dissociated cerebellar Purkinje neurons. J Neurosci 17:4517-4526.

Raman IM, Bean BP (1999) Ionic currents underlying spontaneous action potentials in isolated cerebellar Purkinje neurons. J Neurosci 19:1663-1674.

Raman IM, Bean BP (2001) Inactivation and recovery of sodium currents in cerebellar Purkinje neurons: evidence for two mechanisms. Biophys J 80:729-737.

Ris L, de Waele C, Serafin M, Vidal PP, Godaux E (1995) Neuronal activity in the ipsilateral vestibular nucleus following unilateral labyrinthectomy in the alert guinea pig. J Neurophysiol 74:2087-2099.

Ris L, Hachemaoui M, Vibert N, Godaux E, Vidal PP, Moore LE (2001) Resonance of spike discharge modulation in neurons of the guinea pig medial vestibular nucleus. J Neurophysiol 86:703-716.

Rudy B, McBain CJ (2001) Kv3 channels: voltage-gated K+ channels designed for high-frequency repetitive firing. Trends Neurosci 24:517-526.

Schulz DJ, Goaillard JM, Marder E (2006) Variable channel expression in identified single and electrically coupled neurons in different animals. Nat Neurosci 9:356-362.

Sekirnjak C, du Lac S (2002) Intrinsic firing dynamics of vestibular nucleus neurons. J Neurosci 22:2083-2095.

Sekirnjak C, Vissel B, Bollinger J, Faulstich M, du Lac S (2003) Purkinje cell synapses target physiologically unique brainstem neurons. J Neurosci 23:6392-6398.

Serafin M, de Waele C, Khateb A, Vidal PP, Muhlethaler M (1991) Medial vestibular nucleus in the guinea-pig. I. Intrinsic membrane properties in brainstem slices. Exp Brain Res 84:417-425.

Shao LR, Halvorsrud R, Borg-Graham L, Storm JF (1999) The role of BK-type Ca2+-dependent K+ channels in spike broadening during repetitive firing in rat hippocampal pyramidal cells. J Physiol 521 Pt 1:135-146.

Smith MR, Nelson AB, Du Lac S (2002) Regulation of firing response gain by calcium-dependent mechanisms in vestibular nucleus neurons. J Neurophysiol 87:2031-2042.

Song P, Kaczmarek LK (2006) Modulation of Kv3.1b potassium channel phosphorylation in auditory neurons by conventional and novel protein kinase C isozymes. J Biol Chem 281:15582-15591.

Song P, Yang Y, Barnes-Davies M, Bhattacharjee A, Hamann M, Forsythe ID, Oliver DL, Kaczmarek LK (2005) Acoustic environment determines phosphorylation state of the Kv3.1 potassium channel in auditory neurons. Nat Neurosci 8:1335-1342.

Storm JF (1987) Action potential repolarization and a fast after-hyperpolarization in rat hippocampal pyramidal cells. J Physiol 385:733-759.

Stuhmer W, Conti F, Suzuki H, Wang XD, Noda M, Yahagi N, Kubo H, Numa S (1989) Structural parts involved in activation and inactivation of the sodium channel. Nature 339:597-603.

Turrigiano G, LeMasson G, Marder E (1995) Selective regulation of current densities underlies spontaneous changes in the activity of cultured neurons. J Neurosci 15:3640-3652.

Vergara C, Latorre R, Marrion NV, Adelman JP (1998) Calcium-activated potassium channels. Curr Opin Neurobiol 8:321-329.

Wang LY, Gan L, Forsythe ID, Kaczmarek LK (1998) Contribution of the Kv3.1 potassium channel to high-frequency firing in mouse auditory neurones. J Physiol 509 (Pt 1):183-194.

Waters MF, Minassian NA, Stevanin G, Figueroa KP, Bannister JP, Nolte D, Mock AF, Evidente VG, Fee DB, Muller U, Durr A, Brice A, Papazian DM, Pulst SM (2006) Mutations in voltage-gated potassium channel KCNC3 cause degenerative and developmental central nervous system phenotypes. Nat Genet 38:447-451.

Weiser M, Vega-Saenz de Miera E, Kentros C, Moreno H, Franzen L, Hillman D, Baker H, Rudy B (1994) Differential expression of Shaw-related K+ channels in the rat central nervous system. J Neurosci 14:949-972.

Weiser M, Bueno E, Sekirnjak C, Martone ME, Baker H, Hillman D, Chen S, Thornhill W, Ellisman M, Rudy B (1995) The potassium channel subunit KV3.1b is localized to somatic and axonal membranes of specific populations of CNS neurons. J Neurosci 15:4298-4314.

Zagha E, Lang EJ, Rudy B (2008) Kv3.3 channels at the Purkinje cell soma are necessary for generation of the classical complex spike waveform. J Neurosci 28:1291-1300.

Zhang W, Linden DJ (2003) The other side of the engram: experience-driven changes in neuronal intrinsic excitability. Nat Rev Neurosci 4:885-900.

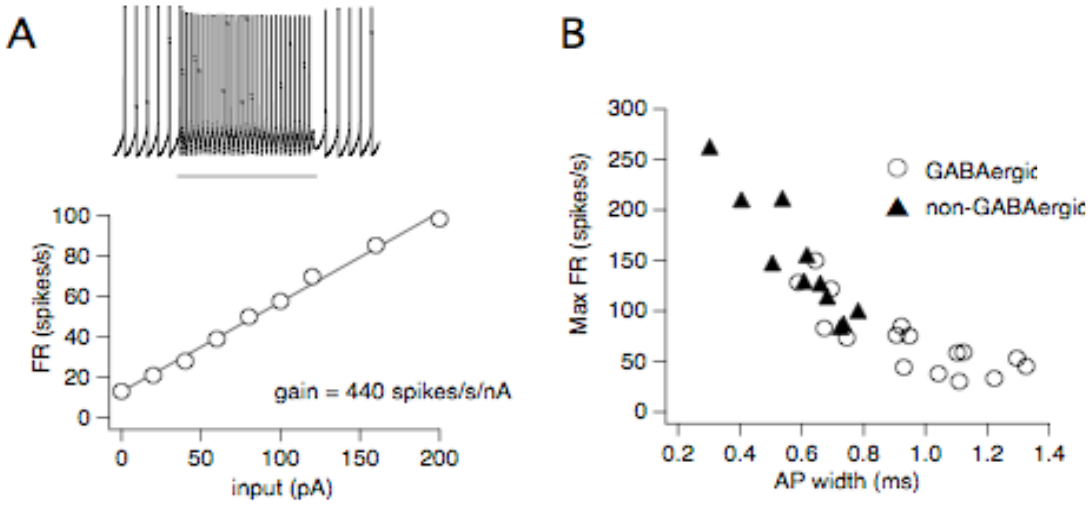

Fig. 5.1: Intrinsic firing properties are preserved in acutely dissociated MVN neurons. **A.** (*Top*) Recording of action potentials from a spontaneously firing neuron, driven to fire 30 Hz with 40 pA of DC current injection for 1 s. (*Bottom*) Average firing rates over 1 s in response to current injections of increasing intensities. The input-output firing rate graph shows the linearity characteristic of MVN neurons, referred to as neuronal gain. The maximum firing rate of this neurons was 100 pA with a gain of 440 spikes/s/nA. **B.** Plot of maximum firing rate vs. action potential width (measured at half height) for the population of GABAergic and non-GABAergic neurons. Most GABAergic neurons had wider action potentials (> 0.8 ms) and lower maximum firing rates (< 70 Hz) than non-GABAergic neurons, but the two populations showed some overlap.

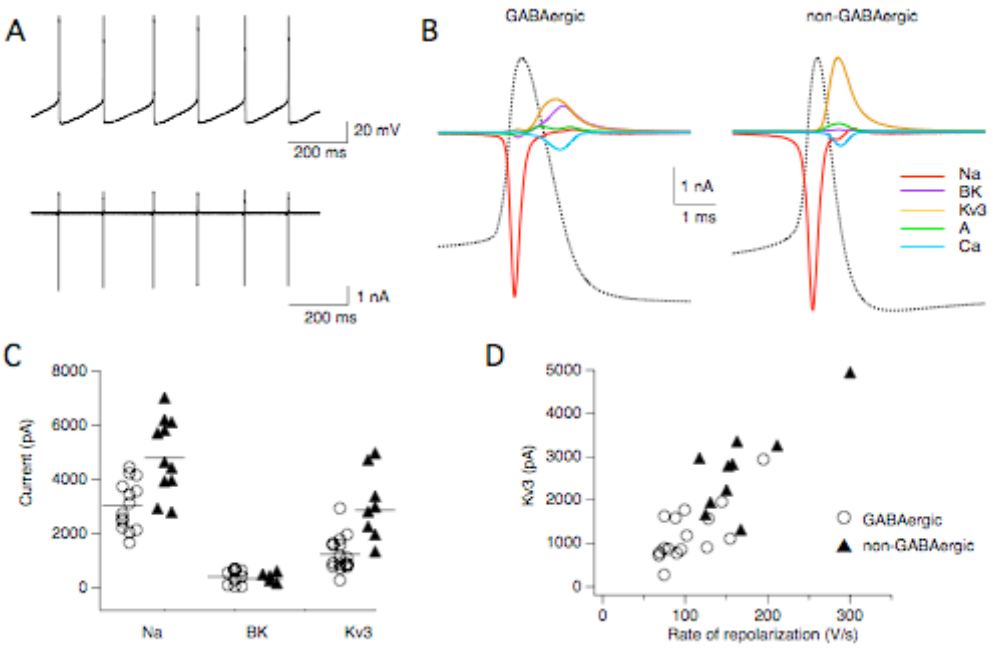

Fig. 5.2: Ionic currents activated during firing in MVN neurons. **A.** Spontaneous action potentials recorded from an MVN neuron (*top*) that were used as a voltage stimulus to measure the ionic currents active during firing (*bottom*). **B.** Pharmacologically identified ionic currents contributing to action potentials in representative GABAergic and non-GABAergic neurons. Currents were averaged across action potentials in a train. Average action potential waveforms are shown (dotted line). **C.** Peak amplitudes of Na, BK, and Kv3 currents measured during firing for the population of GABAergic and non-GABAergic neurons. Averages are indicated with lines **D.** Scatter plot showing the correlation between the amplitude of Kv3 during repolarization and rate of action potential repolarization ($r^2 = 0.74$).

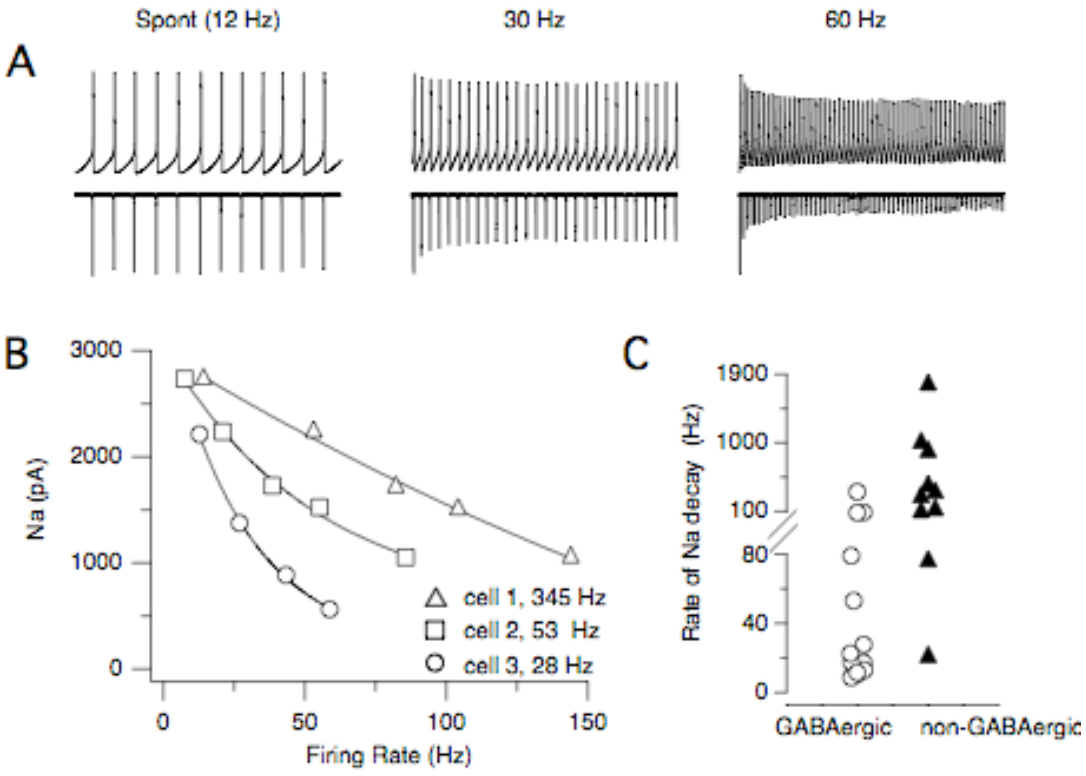

Fig. 5.3: Na current amplitudes decline exponentially over a neuron's firing range. **A.** Action potentials recorded at increasing frequencies from a GABAergic neuron which were used as voltage stimuli to measure the TTX-sensitive Na currents shown below. **B.** Change in average peak amplitude of transient Na currents during steady-state firing in 3 representative neurons across their firing range. Na current amplitudes were similar at spontaneous firing rates but declined at different rates. Neurons could not sustain firing once Na current amplitudes dropped below 0.5 – 1.5 nA. Cell 1: GABAergic neuron with a maximum firing rate of 60 Hz. Cell 2: GABAergic neuron with a maximum firing rate of 86 Hz. Cell 3: Non-GABAergic neuron with a maximum firing rate of 144 Hz. Rates of Na current decay are shown. **C.** Rates of Na current decay for the population of GABAergic and non-GABAergic neurons.

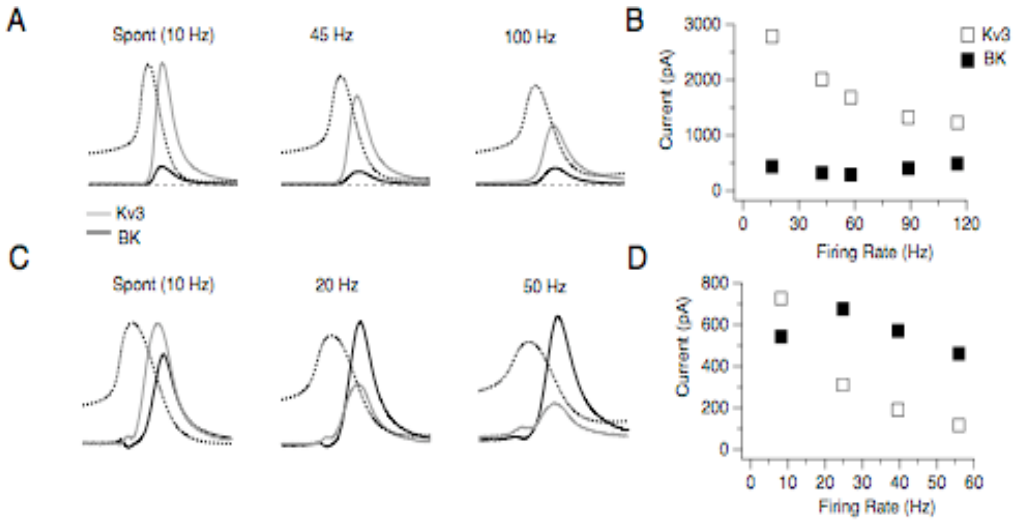

Fig. 5.4: Balance of BK and Kv3 currents during action potential repolarization **A.** Average Kv3 (grey) and BK (black) currents measured during steady-state firing at 10 Hz, 45 Hz, and 100 Hz in a representative non-GABAergic neuron. Action potential waveforms are shown (dotted lines). **B.** Peak amplitude of BK and Kv3 currents at each firing rate tested in same neuron in A. **C.** Average Kv3 (grey) and BK (black) currents measured during steady-state firing at 10 Hz, 20 Hz, and 45 Hz in a representative GABAergic neuron. Action potential waveforms are shown (dotted lines). **D.** Peak amplitude of BK and Kv3 currents at each firing rate tested in same neuron in C.

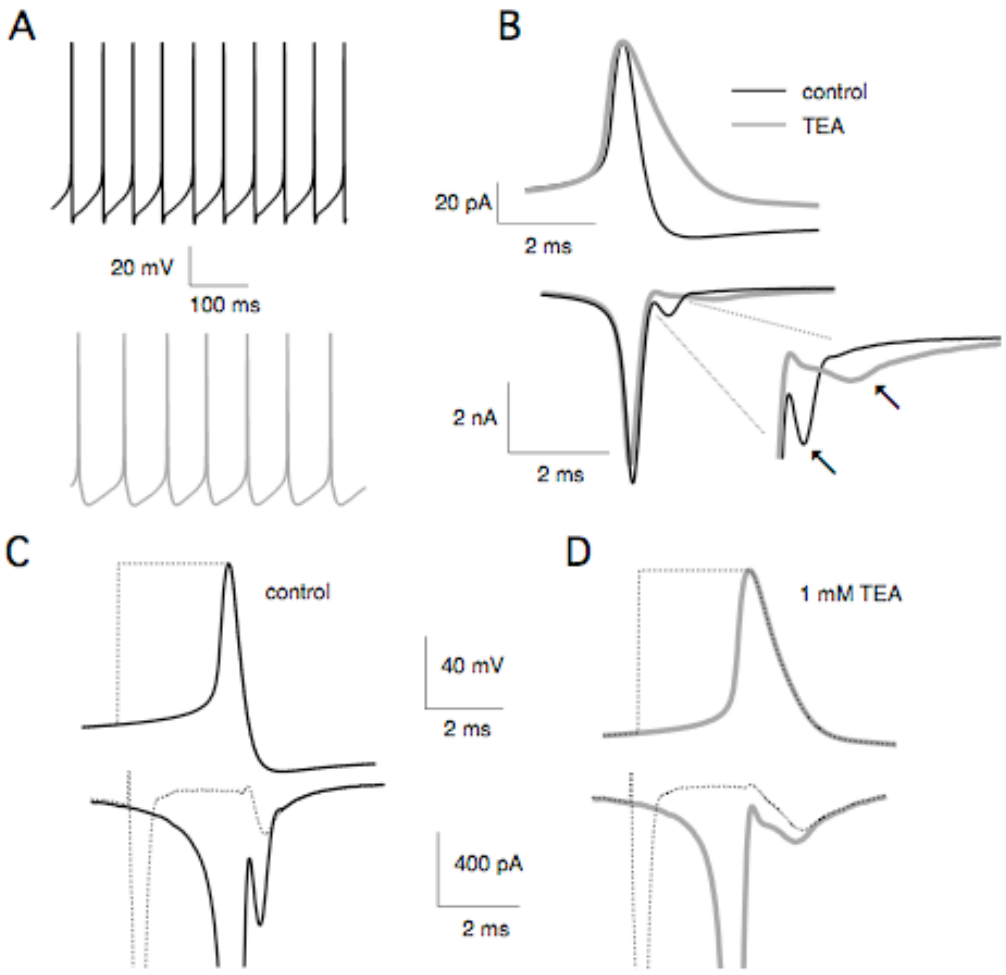

Fig. 5.5: Novel mechanism of Na current protection by Kv3 currents in non-GABAergic neurons. **A.** Trains of action potentials recorded at spontaneous firing rates in control ACSF (20 Hz, *black*) and after application of 1 mM TEA (14 Hz, *grey*). **B.** Average action potential waveforms from A, and average transient Na currents. *Inset*: Expanded view showing Na currents during action potential repolarization. Arrows indicate changes in the amplitude and kinetics of protected Na current after application of 1 mM TEA. **C.** Average Na currents in response to the action potential waveform in ACSF (black) and the corresponding hybrid spike waveform (dashed line), which held neurons at peak action potential voltage for 3 ms. **D.** Average Na currents in response to the action potential waveform in 1 mM TEA (grey) and the corresponding hybrid spike waveform (dashed line). Note the changes in the amplitude and kinetics of protected Na current during the hybrid spike in control in control but not 1 mM TEA conditions.

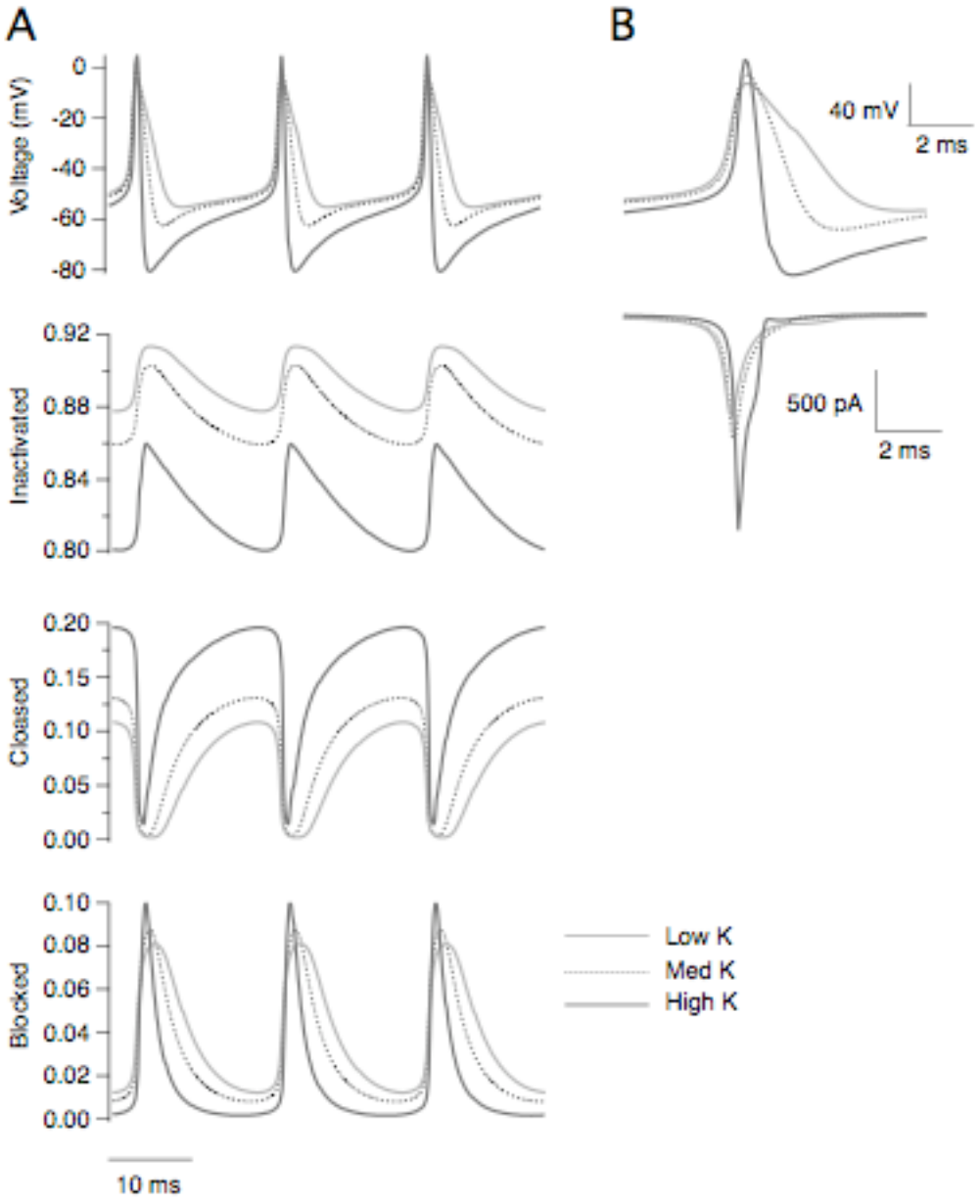

Fig. 5.6: Computer simulation of Na current during firing in MVN neurons. **A.** (*From top to bottom*) Action potentials at 60 Hz with different levels of Kv3 conductance (G_{max} = 0.0003 S/cm^2, light grey; 0.0010667 S/cm^2, dashed; 0.01 S/cm^2, dark grey). Traces are aligned to the peak of the 2nd action potential. Action potential widths are 0.6 ms, 1.3 ms, and 2.3 ms. Bottom graphs represent inactive-state closed-state and open-state probabilities of Na channel under different conditions of Kv3.
B. Simulated action potential waveforms on an expanded time scale and calculated Na currents under different conditions of Kv3.

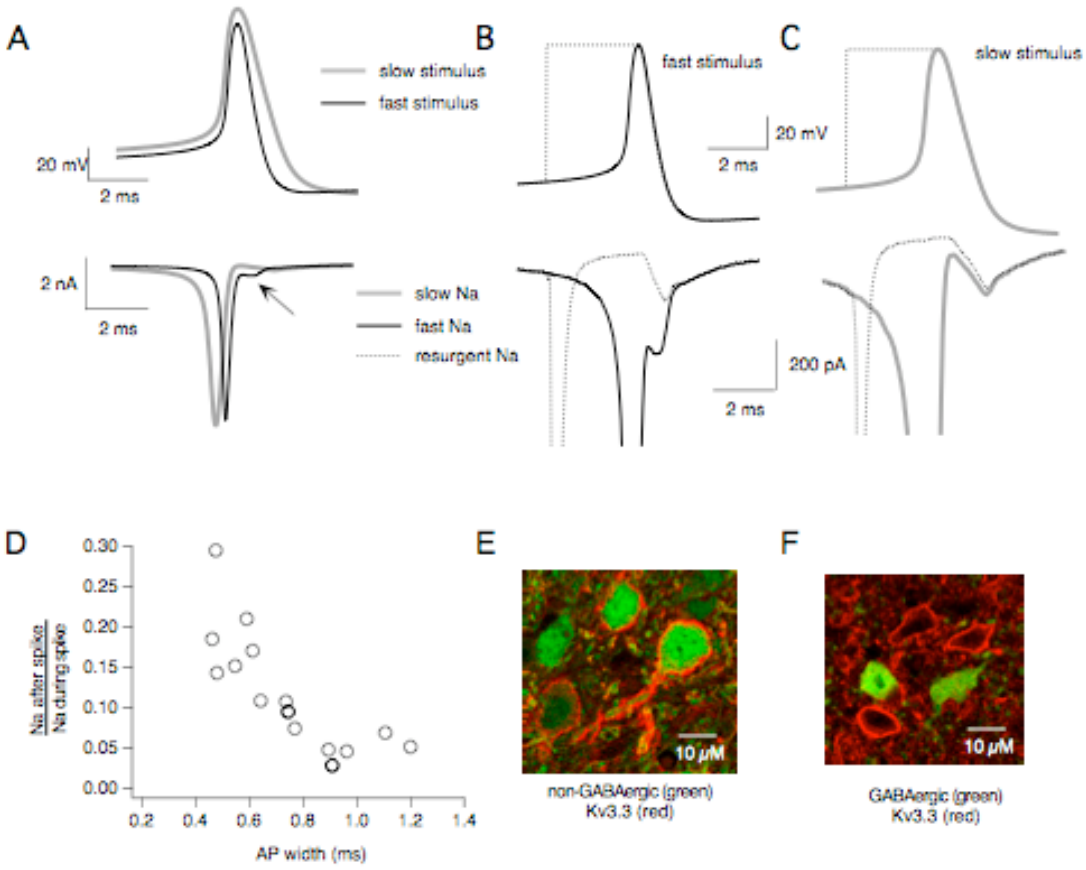

Fig. 5.7: Mechanism and extent of Na current protection vary across MVN neurons **A.** (*Top*) Voltage stimuli used to test the effect of rate of membrane repolarization on Na current protection across cells. Stimuli represent the average waveform over a 5 s train of action potentials recorded from a GABAergic (grey, slow stimulus) and a non-GABAergic neuron (black, fast stimulus). APw = 1.1 ms, slow stimulus; APw = 0.74 ms, fast stimulus. (*Bottom*) Representative Na currents elicited in a neuron in response to fast and slow stimuli, average across all spikes in the train. Arrow demonstrates the difference in kinetics and amplitude of protected Na current observed during action potential repolarization. **B.** Same stimuli and Na currents as in A, but overlayed with hybrid stimuli and Na current responses used to isolate resurgent current (dotted lines). Traces are for fast stimulus **C.** Same as B but for slow stimulus. **D.** Graph showing the amplitude of the protected current as a function of action potential width. In each cell, the peak amplitude of the protected Na current was normalized by the peak amplitude of the transient Na current during the action potential for comparison across neurons. The amount of Na current protection started increasing as a function of AP width for widths < 0.8 ms ($r^2 = 0.59$). **E.** Section from a YFP-16 mouse (green), stained with Kv3.3 (red). **F.** Section from a GIN mouse (green), stained with Kv3.3 (red).

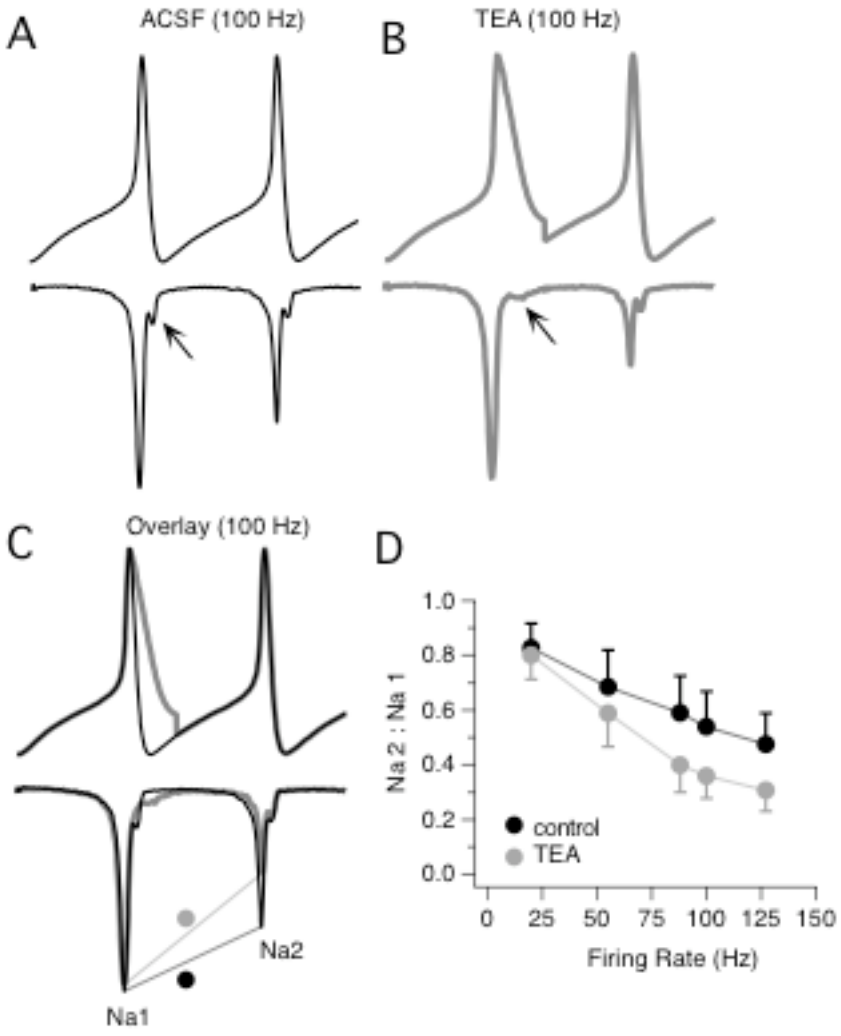

Fig. 5.8: Kv3-mediated protection enhances Na current availability at high firinig rates. **A.** (*Top*) Voltage clamp stimulus created from a pair of action potentials in ACSF, recorded from a neuron firing 100 Hz. APw = 0.65 ms. (*Bottom*) Na current responses to action potentials, recorded in a different neuron. **B.** Same as A but the repolarization phase of the 1st action potential was substituted with the repolarization phase from an action potential recorded in 1 mM TEA, when the neuron was firing its maximum rate in this condition, 69 Hz. APw = 1.4 ms. Na currents in A and B are from the same neuron. Arrows indicate the change in Na current protection when fast repolarization was present vs. when it was absent. **C.** Overlay of A and B. Lines represent change in peak Na current amplitude between the 1st and 2nd action potentials. **D.** Average ratios of Na current amplitudes between 1st and 2nd action potentials at each frequency tested in n = 9 neurons. Error bars represent sd.

VI. Conclusion

In the previous chapters I have described how ionic currents in medial vestibular nucleus (MVN) neurons shape the intrinsic firing properties of identified cell types in the vestibular circuit. This work presents the first direct measurements of the major Na and K currents expressed in MVN neurons and analyzes how they operate as functional units during firing to generate a broad spectrum of intrinsic properties. These studies address the broader question of how neuronal excitability is calibrated through a combination of genetic and functional regulation of ionic currents to generate a stable network with adaptive capabilities. In the MVN, Na currents are similar across neurons, withbiophysical properties tuned to promote reliable firing with high temporal precision, but outward K currents exhibit a higher degree of specialization. The amplitude of the total outward K current is similar between distinct classes of MVN neurons, but it is composed of different ratios of the same 4 major outward currents, coordinated to create a different balance of currents between distinct classes of neurons. During firing, these differences in K currents are amplified by their kinetic and voltage-dependent properties, influencing the functional availability of Na currents which diversifies firing properties of neurons in the circuit.

The ionic basis of temporal precision in MVN neurons

The vestibular system rapidly converts sensory information about head and image motion into temporally and spatially precise eye movements which requires specific tuning of the synaptic and intrinsic properties of neurons in the

circuit (du Lac and Lisberger, 1995). MVN neurons fire spontaneously, allowing them to immediately encode both excitatory and inhibitory inputs as bidirectional modulations in firing rate. They reliably fire action potentials at high rates, endowing them with temporal precision on the order of several milliseconds (Sekirnjak and du Lac, 2002; Smith et al., 2002; Bagnall et al., 2007).

Recordings of the ionic currents from MVN neurons reveal how they are genetically tuned for this function by the biophysical properties of their Na channels and expression of Kv3 channel subunits. Variability in temporal precision across neurons is achieved through graded differences in Kv3 currents that lead to different mechanisms of Na current protection across neurons. This has potentially broad implications for fast firing neurons across the brain that express Na and Kv3 channels similar to those found in MVN neurons. These include neurons in the cerebellum and deep cerebellar nuclei, fast-spiking interneurons in the cortex, brainstem auditory neurons, and neurons in basal ganglia such as the globus pallidus and subthalamic nucleus neurons (Perney et al., 1992; Martina and Jonas, 1997; Martina et al., 1998; Bevan and Wilson, 1999; Raman and Bean, 1999; Raman et al., 2000; Do and Bean, 2003; Leao et al., 2005; Mercer et al., 2007).

In Purkinje cell in the cerebellum, Kv3 currents influence Na current availability by changing their resurgent kinetics (Akemann and Knopfel, 2006; Zagha et al., 2008), but the extent of variability of this mechanism across neurons was not investigated. Variability in Kv3 currents across MVN neurons most likely arises through different levels of channel expression across neurons of the

same cell type (Gittis and du Lac, 2007), but differences across cell types may result from differences in the expression of channel subunits, particularly Kv3.3 which is expressed in non-GABAergic neurons but not GABAergic neurons in the MVN. In the globus pallidus, the kinetics of Kv3 currents are tuned by the expression of Kv3.4 subunits that form heteromeric channels with Kv3.1 subunits (Baranauskas et al., 2003). In the auditory brainstem, temporal precision is tuned by graded differences in Kv3 channel phosphorylation (Song et al., 2005). These results demonstrate a wealth of cellular mechanisms available for the tuning of a neuron's temporal precision and further experiments will be required to determine which of these mechanisms are global and which are specific to different systems.

The ionic basis of linearity in MVN neurons

Changes in the firing rate of MVN neurons are linear in response to sensory inputs due to the properties of the synaptic connections from the vestibular nerve (Bagnall et. al., in preparation) and linear transformation of inputs into firing rates, mediated by the intrinsic properties of the neurons themselves (du Lac and Lisberger, 1995; Smith et al., 2002). A fundamental question for network dynamics is how a combination of non-linear ionic currents can give rise to linear cellular properties. Insights into this problem will come through the study of how individual ionic currents in a neuron cooperate as a functional unit.

MVN neurons express a combination of purely voltage-gated channels (Na, Kv3), voltage-gated channels with some calcium sensitivity (BK), and purely

Ca-sensitive channels (SK). The rising and falling phases of an action potential are governed by the coordinated activity of Na, Kv3, and BK currents. The time at which a neuron fires the next action potential is determined by both Na current availability and the presence of currents in the inter-spike interval that oppose membrane depolarization. These inter-spike interval currents are likely to consist of a combination of calcium-sensitive BK and SK currents (Serafin et al., 1991; Johnston et al., 1994; Smith et al., 2002; Nelson et al., 2003; Nelson et al., 2005).

In MVN neurons, intracellular Ca levels are linearly related to neuronal activity (du Lac, unpublished observations). Recordings from acutely dissociated neurons demonstrate the presence of calcium-sensitive currents during the inter-spike interval (likely SK) whose amplitudes change linearly with firing rate and influence Na current availability before an action potential (Gittis, unpublished observations). This regulation of Na currents by a Ca-sensitive outward current could be the basis of linear input-output signal transformations in MVN neurons. During action potentials, the amplitude of Kv3 currents, and to a lesser extent BK currents, are coordinated with the amplitudes of Na currents by their voltage-dependent properties. This creates a system in which the rate of action potentials is sensitive to changes in inputs, but action potential generation is robust across a broad firing range.

Stability and plasticity in the vestibular system

The expression of ionic currents varies continuously in MVN neurons to generate a broad spectrum of firing properties (Gittis and du Lac, 2007), but cell

types in the MVN cluster in distinct regions of this parameter space (Sekirnjak et al., 2003; Sekirnjak and du Lac, 2006; Bagnall et al., 2007). This suggests that within a cell type, a certain amount of ionic diversity is acceptable and perhaps even beneficial, but this diversity obeys specific limits in different cell types. The factors that determine these limits and how they are enforced remain open questions, but studies from the lobster somatogastric ganglion may yield some insights. Work from this system has demonstrated that the expression level of any particular current varies nearly 2 to 4 fold across neurons, but that this variability can be limited by the coordinated expression of multiple ionic currents (Turrigiano et al., 1995; MacLean et al., 2005; Schulz et al., 2006).

Recordings from MVN neurons reveal that functional regulation of ionic currents may contribute to establishing these boarders as well. Both GABAergic and non-GABAergic MVN neurons express Na, BK, and Kv3 currents, but the relative ratio of Kv3 and BK currents during firing determines whether Na currents are protected by a resurgent mechanism or by a more rapid, Kv3-mediated form of protection. In most non-GABAergic neurons, Kv3 currents are sufficiently large to protect Na currents from inactivation, providing these neurons with a high level of temporal precision. In most GABAergic neurons, however, Kv3 currents fall below a critical level and the mechanism of Na current protection switches to the resurgent mechanism which restricts the maximum level of temporal precision.

The ability of neurons to maintain relatively stable outputs over wide variability in current expression is important for network stability, but poses a

theoretical problem for generating adaptive changes with subtle modifications to a single current (Goldman et al., 2001). The results of Goldman et al. suggest that neurons occupy an 'activity space' which is robust to changes in the amplitudes of some currents, but sensitive to changes in others. Different neurons within a population can lie in different regions of this parameter space, making some more susceptible to plasticity than others. It is tempting to apply this model to the vestibular system to explain how system-wide insults (ex. labyrinthectomy) can have differential effects on neuronal activity (Beraneck et al., 2003; Beraneck et al., 2004). An understanding of which ionic currents contribute to neuronal firing properties in different cell types may lead to a better understanding of these observations. For example, BK currents are important targets of plasticity that increase a neuron's intrinsic excitability in response to reductions in intracellular calcium levels (Nelson et al., 2003) and this mechanism of plasticity may be engaged during early recovery from labyrinthectomy (Nelson et al., unpublished). Given the greater relative importance of BK currents in GABAergic neurons than in non-GABAergic neurons during firing, this form of plasticity may specifically affect the GABAergic interneurons in the vestibular circuit. This ability for cell type-specific plasticity in the system would allow for targeted adaptive changes to adjust network output without rearranging the basic architecture.

References

Akemann W, Knopfel T (2006) Interaction of Kv3 potassium channels and resurgent sodium current influences the rate of spontaneous firing of Purkinje neurons. J Neurosci 26:4602-4612.

Bagnall MW, Stevens RJ, du Lac S (2007) Transgenic mouse lines subdivide medial vestibular nucleus neurons into discrete, neurochemically distinct populations. J Neurosci 27:2318-2330.

Baranauskas G, Tkatch T, Nagata K, Yeh JZ, Surmeier DJ (2003) Kv3.4 subunits enhance the repolarizing efficiency of Kv3.1 channels in fast-spiking neurons. Nat Neurosci 6:258-266.

Beraneck M, Idoux E, Uno A, Vidal PP, Moore LE, Vibert N (2004) Unilateral labyrinthectomy modifies the membrane properties of contralesional vestibular neurons. J Neurophysiol 92:1668-1684.

Beraneck M, Hachemaoui M, Idoux E, Ris L, Uno A, Godaux E, Vidal PP, Moore LE, Vibert N (2003) Long-term plasticity of ipsilesional medial vestibular nucleus neurons after unilateral labyrinthectomy. J Neurophysiol 90:184-203.

Bevan MD, Wilson CJ (1999) Mechanisms underlying spontaneous oscillation and rhythmic firing in rat subthalamic neurons. J Neurosci 19:7617-7628.

Do MT, Bean BP (2003) Subthreshold sodium currents and pacemaking of subthalamic neurons: modulation by slow inactivation. Neuron 39:109-120.

du Lac S, Lisberger SG (1995) Cellular processing of temporal information in medial vestibular nucleus neurons. J Neurosci 15:8000-8010.

Gittis AH, du Lac S (2007) Firing properties of GABAergic versus non-GABAergic vestibular nucleus neurons conferred by a differential balance of potassium currents. J Neurophysiol 97:3986-3996.

Goldman MS, Golowasch J, Marder E, Abbott LF (2001) Global structure, robustness, and modulation of neuronal models. J Neurosci 21:5229-5238.

Johnston AR, MacLeod NK, Dutia MB (1994) Ionic conductances contributing to spike repolarization and after-potentials in rat medial vestibular nucleus neurones. J Physiol 481 (Pt 1):61-77.

Leao RM, Kushmerick C, Pinaud R, Renden R, Li GL, Taschenberger H, Spirou G, Levinson SR, von Gersdorff H (2005) Presynaptic Na+ channels: locus,

development, and recovery from inactivation at a high-fidelity synapse. J Neurosci 25:3724-3738.

MacLean JN, Zhang Y, Goeritz ML, Casey R, Oliva R, Guckenheimer J, Harris-Warrick RM (2005) Activity-independent coregulation of IA and Ih in rhythmically active neurons. J Neurophysiol 94:3601-3617.

Martina M, Jonas P (1997) Functional differences in Na+ channel gating between fast-spiking interneurones and principal neurones of rat hippocampus. J Physiol 505 (Pt 3):593-603.

Martina M, Schultz JH, Ehmke H, Monyer H, Jonas P (1998) Functional and molecular differences between voltage-gated K+ channels of fast-spiking interneurons and pyramidal neurons of rat hippocampus. J Neurosci 18:8111-8125.

Mercer JN, Chan CS, Tkatch T, Held J, Surmeier DJ (2007) Nav1.6 sodium channels are critical to pacemaking and fast spiking in globus pallidus neurons. J Neurosci 27:13552-13566.

Nelson AB, Gittis AH, du Lac S (2005) Decreases in CaMKII activity trigger persistent potentiation of intrinsic excitability in spontaneously firing vestibular nucleus neurons. Neuron 46:623-631.

Nelson AB, Krispel CM, Sekirnjak C, du Lac S (2003) Long-lasting increases in intrinsic excitability triggered by inhibition. Neuron 40:609-620.

Perney TM, Marshall J, Martin KA, Hockfield S, Kaczmarek LK (1992) Expression of the mRNAs for the Kv3.1 potassium channel gene in the adult and developing rat brain. J Neurophysiol 68:756-766.

Raman IM, Bean BP (1999) Ionic currents underlying spontaneous action potentials in isolated cerebellar Purkinje neurons. J Neurosci 19:1663-1674.

Raman IM, Gustafson AE, Padgett D (2000) Ionic currents and spontaneous firing in neurons isolated from the cerebellar nuclei. J Neurosci 20:9004-9016.

Schulz DJ, Goaillard JM, Marder E (2006) Variable channel expression in identified single and electrically coupled neurons in different animals. Nat Neurosci 9:356-362.

Sekirnjak C, du Lac S (2002) Intrinsic firing dynamics of vestibular nucleus neurons. J Neurosci 22:2083-2095.

Sekirnjak C, du Lac S (2006) Physiological and anatomical properties of mouse medial vestibular nucleus neurons projecting to the oculomotor nucleus. J Neurophysiol.

Sekirnjak C, Vissel B, Bollinger J, Faulstich M, du Lac S (2003) Purkinje cell synapses target physiologically unique brainstem neurons. J Neurosci 23:6392-6398.

Serafin M, de Waele C, Khateb A, Vidal PP, Muhlethaler M (1991) Medial vestibular nucleus in the guinea-pig. II. Ionic basis of the intrinsic membrane properties in brainstem slices. Exp Brain Res 84:426-433.

Smith MR, Nelson AB, Du Lac S (2002) Regulation of firing response gain by calcium-dependent mechanisms in vestibular nucleus neurons. J Neurophysiol 87:2031-2042.

Song P, Yang Y, Barnes-Davies M, Bhattacharjee A, Hamann M, Forsythe ID, Oliver DL, Kaczmarek LK (2005) Acoustic environment determines phosphorylation state of the Kv3.1 potassium channel in auditory neurons. Nat Neurosci 8:1335-1342.

Turrigiano G, LeMasson G, Marder E (1995) Selective regulation of current densities underlies spontaneous changes in the activity of cultured neurons. J Neurosci 15:3640-3652.

Zagha E, Lang EJ, Rudy B (2008) Kv3.3 channels at the Purkinje cell soma are necessary for generation of the classical complex spike waveform. J Neurosci 28:1291-1300.